PHYSICS TODAY

September 2021 • volume 74, number 9

A publication of the American Institute of Physics

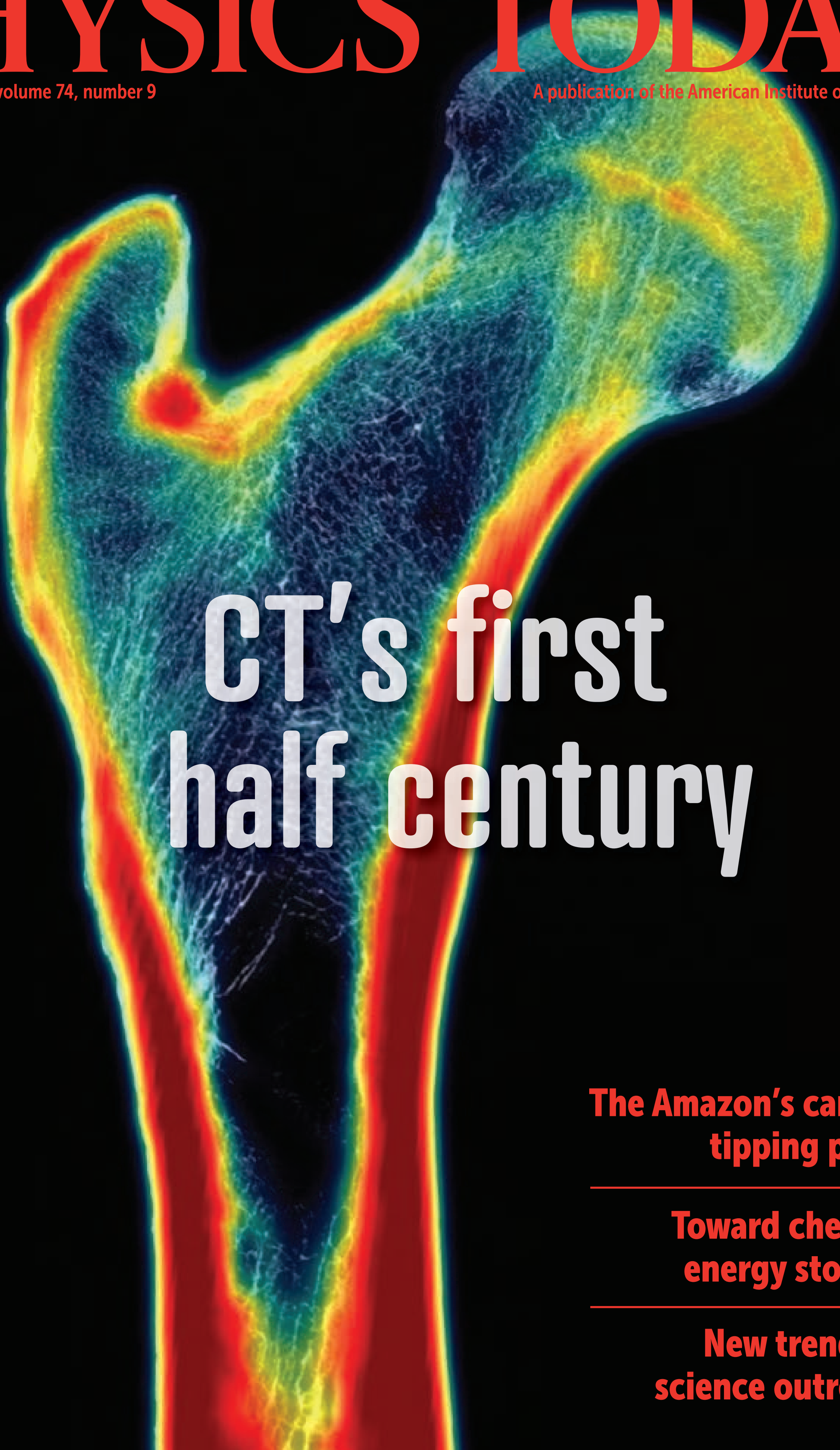

CT's first half century

The Amazon's carbon tipping point

Toward cheaper energy storage

New trends in science outreach

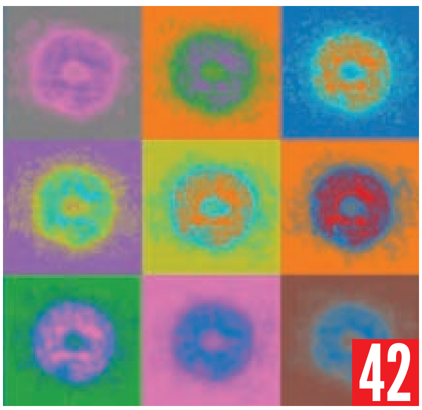

PHYSICS TODAY

September 2021 | volume 74 number 9

FEATURES

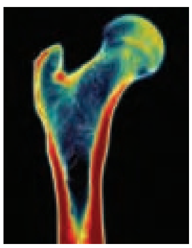

ON THE COVER: The longest bone in the human body, the femur connects to the pelvis at the hip joint. This high-resolution computed tomography (CT) scan of the bone reveals its inner microstructure. The colors denote the mineral volume fraction, which provides a spatial measure of strength and can be used to identify individuals at risk of osteoporotic fracture. For an account of CT's evolution and advances, turn to the article by John Boone and Cynthia McCollough on **page 34**. (Image courtesy of Lance Frazer/Southwest Research Institute.)

Recently on PHYSICS TODAY ONLINE

www.physicstoday.org

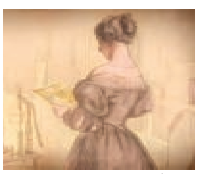

CARLYN IVERSON/NOAA

Eunice Newton Foote

A 19th-century scientist and inventor, Foote demonstrated the heat-absorbing properties of carbon dioxide and water vapor three years before John Tyndall discovered the greenhouse effect. Only in the past decade has her prescient prediction of global warming received its due.

physicstoday.org/Sep2021a

DAMIEN JEMISON/LLNL

Laser fusion

Scientists at the National Ignition Facility in California recently announced that they produced a fusion reaction that yielded more energy than was absorbed by the fuel to initiate the reaction. PHYSICS TODAY's David Kramer analyzes the laser fusion milestone and puts it into historical perspective.

physicstoday.org/Sep2021b

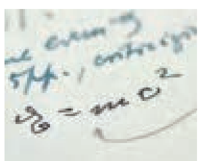

RR AUCTION

Einstein's handwriting

Earlier this year one of Albert Einstein's handwritten letters featuring the famous $E = mc^2$ sold for more than $1.2 million at auction. PHYSICS TODAY's Ryan Dahn looks at Einstein's preferred type of German-language cursive writing, which he likely adopted for practical and political reasons.

physicstoday.org/Sep2021c

PHYSICS TODAY (ISSN 0031-9228, coden PHTOAD) volume 74, number 9. Published monthly by the American Institute of Physics, 1305 Walt Whitman Rd, Suite 300, Melville, NY 11747-4300. Periodicals postage paid at Huntington Station, NY, and at additional mailing offices. POSTMASTER: Send address changes to PHYSICS TODAY, American Institute of Physics, 1305 Walt Whitman Rd, Suite 300, Melville, NY 11747-4300. Views expressed in PHYSICS TODAY and on its website are those of the authors and not necessarily those of AIP or any of its member societies.

PHYSICS TODAY

www.physicstoday.org

DEPARTMENTS

SUBSCRIPTION QUESTIONS? +1 800 344-6902 | +1 516 576-2270 | **ptsubs@aip.org**

Address
American Center for Physics
One Physics Ellipse
College Park, MD 20740-3842
+1 301 209-3100
pteditors@aip.org

PhysicsToday **@physicstoday**

FROM THE EDITOR

Space barons

Charles Day

My first encounter with what would become Richard Branson's business empire was in 1981. BBC DJ John Peel played a track, "Act of Affection," from the Wailing Souls' new album *Fire House Rock*. I liked the song. Skeptical that I'd find the LP in my local record store, I bought it from Branson's mail-order company, Virgin Records.

I hadn't thought much about Branson and his businesses until this past summer. On 11 July he and five others flew aboard Virgin Galactic *Unity 22* to the edge of space. Nine days later, former Amazon CEO Jeff Bezos made his own trip to the edge of space with three others aboard his company Blue Origin's *New Shepard*.

Although Branson founded Virgin Galactic to make money taking wealthy tourists into space, he sounds genuinely proud of the hundreds of jobs for astronautical engineers and others that Virgin Galactic and its partner companies have created. Blue Origin also wants to be paid to take people and cargoes into space, yet Bezos's space quest sounds visionary and altruistic. To quote a 2016 interview with him in *Insider*: "When it comes to space, I see it as my job to build infrastructure the hard way—I'm using my resources to put in place heavy-lifting infrastructure so the next generation of people can have a dynamic, entrepreneurial explosion into space. . . . I want thousands of entrepreneurs doing amazing things in space, and to do that we need to dramatically lower the cost of access to space."

Reactions to the rival space barons among the people I follow on Twitter and Facebook were uniformly negative. How could Branson and Bezos spend so much money to send themselves into space? Surely, there are more deserving causes. What about mitigating climate change, abolishing poverty, or eliminating tropical diseases?

The indignation brought to mind my friend Patrick McCray's feature article "The contentious role of a national observatory" (PHYSICS TODAY, October 2003, page 55). Whereas in most rich countries, governments fund big astronomy facilities, in the US, many of the largest telescopes have been funded by rich benefactors.

Real estate investor James Lick (1796–1876) left money in his will to the University of California to build what would become the Lick Observatory. Railroad financier Charles Yerkes (1837–1905) paid for the University of Chicago's Yerkes Observatory. The foundation established by oil magnate John D. Rockefeller (1839–1937) paid for Caltech's Palomar Observatory. More recently, the foundation established by Intel cofounder Gordon Moore (born in 1929) committed $200 million to help pay for the construction of the Thirty Meter Telescope (TMT), a project led by Caltech and the University of California.

In his article, McCray recounted how the privileged access of a few elite universities to the biggest telescopes retarded the development of equivalently powerful national facilities that could serve astronomers at all US universities. The conflict persists. Although the TMT and its rival, the Giant Magellan Telescope (GMT), each have international partners, the two projects are essentially private, not national.

Equity of access aside, is it a bad thing when rich people fund science? Without the largesse of Lick, Yerkes, Rockefeller, and their philanthropic successors, the big telescopes they funded might not have been built at all. Arguably, by not funding a TMT- or GMT-sized telescope, which each have a roughly $1 billion price tag, NSF could afford the equally expensive Laser Interferometer Gravitational-Wave Observatory.

Lick, Yerkes, and Rockefeller are numbered among the robber barons of the Gilded Age. Among the most ruthless and successful of them all was railroad magnate Jay Gould (1836–92). Unlike the trio of telescope builders, today Gould is known, if at all, only for his unscrupulous business practices and vast wealth.

Compared with funding a giant telescope, taking a joyride in space seems frivolous, which might account for the negative reaction I found on social media to Branson's and Bezos's ventures. Perhaps compounding the image problem, science fiction abounds in sinister space corporations, such as Tyrell in *Blade Runner*, Weyland-Yutani in the *Alien* movies, Tessier-Ashpool in *Neuromancer*, and Mao-Kwikowski Mercantile in *The Expanse*.

Still, our sun will eventually turn into a red giant and incinerate life on Earth. To survive, humanity will need a new, distant haven that only spacecraft can reach. In so far as commercial space travel will make that possible, we should commend it however grudgingly. PT

How a fake Kepler portrait became iconic

Textbooks and popular writings introduce portraits of historical personalities to illustrate the human side of science. Usually they get it right. Albert Einstein did stick out his tongue to reporters, Marie Curie really did dress in black, and J. Robert Oppenheimer wore a porkpie hat. But for the past few decades, one of the founders of modern physics and astronomy has been routinely portrayed erroneously. Since this year marks the 450th anniversary of Johannes Kepler's birth, it is timely and necessary to point out an egregious example of unwittingly propagated misinformation.

As this issue of PHYSICS TODAY goes to press, the top left painting below is the first image returned in a Google search of "Kepler portrait," and it's accompanied by a striking array of variations and re-creations. Prior to 6 August, it was the lead image on Kepler's Wikipedia page. For users in select countries, Google replaced its logo on 27 December 2013, Kepler's 442nd birthday, with a doodle that incorporated the portrait.

The portrait is in the possession of a Benedictine monastery in Kremsmünster, Austria. The earliest mention of the painting we have found is in the 1877 book *Geschichte der Astronomie* (*History of Astronomy*) by Rudolf Wolf. According to Wolf, the descendants of Kepler's siblings sold the painting to the abbot of the Kremsmünster monastery[1] in 1864. Ludwig Günther recounted a similar story in the introduction to his 1898 German translation of Kepler's *Somnium* (*The Dream*), stating that "according to the notes I received from Father Hugo Schmid, the monastery librarian there, the painting belonged to a notary [named] Gruner, who sold it in 1864 to the current abbot of the monastery, [Augustin] Reslhuber."[2] (All translations of German are ours.) Neither Wolf nor Günther identifies the artist who painted the portrait.

The painting is an oil on oak (35.5 cm × 44.5 cm) with no signature or attribution. There is only the Latin phrase *Aetatis Suae 39, 1610* (At the age of 39, 1610) in the upper right corner (which is usually omitted in reproductions). In a 1930 Festschrift published in honor of the 300th anniversary of Kepler's death, Ernst Zinner notes that the painting was sold to the abbey for 200 gulden and that Gruner was from Weil der Stadt (Kepler's birthplace, in what is now southwestern Germany).[3] Zinner summarizes Wolf's and Günther's descriptions, calls the painting an "alleged portrait," and notably includes the opinion of Seraphin Maurer, who examined the painting in the 1920s. Maurer, the curator and conservator at the Picture Gallery of the Vienna Academy of Fine Arts, stated the following:

> The overall impression of the picture is good, namely, it corresponds with [that] of a picture from the 17th century. However, upon closer inspection, the technical treatment (brushwork) shows that the painter had no understanding of natural forms but could only mechanically reproduce someone else's [work], which is clearly evident to the specialist. Furthermore, the colors have not yet taken on a glaze-like appearance, which is always the case with pictures from that time. There are no visible signs of aging such as cracks, so I presume that the picture was probably created around 1800 ([or] a little earlier or later). Likewise, the oak panel used [by the artist] has a finish that does not conform with the usual type from around 1600. These are the main factors that enable me to state that the picture is a copy. (reference 3, page 339)

Even before reading Zinner's article, we had long suspected that the painting could not be from earlier than the 19th

A COMPARISON OF PORTRAITS. Fake Johannes Kepler portrait (top left). Allegedly from 1610, this painting by an unknown artist is more likely from the 19th century. If it is based on anything, it likely derived from a portrait of Michael Mästlin. **Michael Mästlin portrait** (top right). A black-and-white photograph of an original from 1619 sometimes attributed to Conrad Melberger. The portrait, at the University of Tübingen, was flagged by Ernst Zinner as a possible source for the fake.[3] **Kepler portrait** (bottom left). An engraving based on a portrait of Kepler from 1620. The portrait was given to the Strasbourg University Library in 1627. (Courtesy of the Smithsonian Libraries and Archives.) **Presumed Kepler portrait** (bottom right). Attributed since 1973 to Hans von Aachen.[4,5] It is from around the same year inscribed on the fake portrait, likely 1612. (All four images are in the public domain.)

century for stylistic reasons, and we were quite pleased to find that Zinner and his informants reached the same conclusions.

It's likely that the painting is not even a painting of Kepler but, as Zinner suggested in 1930, a 19th-century forgery based loosely on a portrait of Kepler's teacher and mentor Michael Mästlin (top right). That image depicts Mästlin in the ruffled collar and academic gown typically worn by professors of that period. The alleged Kepler portrait held by the Kremsmünster monastery shows Kepler in a similar academic outfit, but that does not accord with what Kepler wears in other portraits that incontrovertibly depict him: a commemorative medallion from his wedding in 1597 and an official portrait from 1620 (bottom left). In those, Kepler wears a lace collar, which is more appropriate as he was neither an academic at the time nor a nobleman. Moreover, the Latin inscription in the alleged portrait could have been added by anyone knowing Kepler's birth date.

The bottom right painting is another presumed portrait of Kepler, from around 1610, that since 1973 has been attributed to Hans von Aachen, one of the favorite painters of Holy Roman Emperor Rudolf II and a contemporary of Kepler in Prague.[4,5] The top left and bottom right portraits cannot be simultaneous representations of the same person. Although the identifications are still disputed, at least in the case of the von Aachen the artist is known and the painting is original. Finally, another painting identified as Kepler, known as the Linz portrait, is dated to 1620. The artist is unknown, but it does bear resemblance to the depiction on the frontispiece of Kepler's *Rudolphine Tables* (1627).[6]

So how did the fake Kepler portrait spread? Except for Wolf's and Günther's mentions, we cannot find any examples of the portrait attributed as being Kepler before 2005. That's the year the portrait first appeared on Wikipedia, and thereafter it became ubiquitous. For example, it appears in a European Space Agency press release from 2011 (explicitly citing Wikipedia), the European Southern Observatory attached it to an article from 2016, and NASA used it in its Solar System Exploration educational materials in 2017. This past April the image appeared on the cover of *Giornale di Fisica*, an Italian magazine for secondary-school physics teachers.

Although this matter may just seem like a trivial byway, images fix in the mind. Kepler deserves better.

References

1. R. Wolf, *Geschichte der Astronomie* (*History of Astronomy*), R. Oldenbourg (1877), p. 308, n. 4.
2. L. Günther, *Keplers Traum vom Mond* (*Kepler's Dream of the Moon*), B. G. Teubner (1898), p. xx.
3. E. Zinner, *Ber. Naturwiss. Ver. Regensbg.* **19**, 337 (1928/1930).
4. O. Gingerich, *Trans. Int. Astron. Union* **15A**, 639 (1973), p. 642.
5. T. D. Kaufmann, *The School of Prague: Painting at the Court of Rudolf II*, U. Chicago Press (1988); D. Jansová, "Kapitoly z dějin sběratelství na Kolowratském zámku v Rychnově nad Kněžnou" ("Chapters from the history of collecting at Kolowrat Castle in Rychnov nad Kněžnou"), bachelor's thesis, Palacký University Olomouc (2014).
6. See H.-J. Albinus, D. Suckrau, *Math. Intell.* **43**(1), 64 (2021).

Steven N. Shore
(steven.neil.shore@unipi.it)
University of Pisa
Pisa, Italy
Václav Pavlík
(vpavlik@iu.edu)
Indiana University
Bloomington

Hydrogen as an aviation fuel

Powering airplanes by hydrogen, as reported on by David Kramer in the December 2020 issue of PHYSICS TODAY (page 27), is a nice theoretical idea that brings little practical benefit.

Apart from the difficulties of handling hydrogen as a cryogenic liquid or a gas at very high pressure, the most serious problem with hydrogen as an aviation fuel isn't the weight of the tanks containing it but rather its low density, even as a liquid. Consider the Toyota Mirai, an electric car powered by a hydrogen fuel cell: The hydrogen is stored as a gas in polycarbonate tanks at 700 bar, twice the pressure proposed for the hydrogen-powered aircraft. The 2021 Mirai can hold 5.6 kg of hydrogen, but that's just 6% of the combined mass of the fuel and the fuel tanks. For tanks of conventional aviation fuel—kerosene or aviation gasoline (avgas)—the mass is mostly fuel, not tank structure.

The energy per unit volume of liquid hydrogen is 24% that of avgas or kerosene; that of hydrogen at 350 bar, only about 8%. Light aircraft use only a small part of the wing to store fuel. The combination of fuel cell and electric motor has approximately twice the efficiency of an internal combustion engine, though, so only half as much energy needs to be stored.

The situation is very different for long-range, turbine-powered aircraft used for intercontinental travel. The whole wing serves as a fuel tank, and fuel can account for 45% of a plane's allowed maximum takeoff mass. Even for the high-bypass-ratio turbofans found on a commercial aircraft, a substantial part of the high-altitude cruise thrust comes from the turbine core, not the fan, so driving the fan with a fuel-cell-powered electric motor effectively makes the aircraft more like a slower turboprop. The low density of hydrogen, even as a liquid, means that the aircraft doesn't have the space for the fuel needed for an intercontinental journey.

A flight of 500 nautical miles (900 km) takes about 1.25 hours. If the aim is to minimize carbon dioxide emissions from travel, then for flights of less than that distance—for which hydrogen is viable, though not necessarily practical—it would be better to just take the train!

Peter Rez
(peter.rez@asu.edu)
Arizona State University
Tempe

Correction

July 2021, page 24—Steel Made via Emissions-Less Technologies (SMELT) was incorrectly identified as a program of the Advanced Research Projects Agency–Energy. SMELT is in fact a "request for information," seeking public input that could potentially lead to a future program. PT

The Amazon is reaching its carbon tipping point

The tropical forest can no longer be counted on to help clean up humanity's environmental mess.

FIGURE 1. DELIBERATE BURNING to make way for agriculture destroys thousands of square kilometers of the Amazon rainforest every year, mostly in the more populated east. The fires themselves are considerable sources of carbon emissions, and the deforestation also upsets the carbon balance of the remaining forest through its effect on the local climate. (Photo by guentermanaus/Shutterstock.com.)

Greta Thunberg, the Swedish environmental activist, points out in her social media profiles that she was "born at 375 ppm"—a reference to the atmospheric concentration of carbon dioxide at the time of her birth in January 2003. By January 2021, that concentration had reached 415 ppm. The 40 ppm increase means that the atmosphere's carbon content rose by 85 billion tons over those 18 years.

As destructive as that increase has been, as evidenced by the increasing incidence of severe weather all over the world, it could have been a lot worse. Anthropogenic carbon emissions average roughly 10 billion tons a year, which is twice as much over 18 years as the amount that ended up in the atmosphere.

Where did the rest of it go? Half of it dissolved in the ocean—where it's doing its own damage by acidifying marine waters, but at least it's not warming the whole climate. The rest was taken up by land ecosystems, with tropical forests such as the Amazon thought to be doing an outsize share of the work.

But forests' role as carbon sinks is not inevitable. Trees and other plants absorb carbon during photosynthesis, but they also release it again when they die and decay. Over the long term, those processes must be in near equilibrium. Humankind has been fortunate, so far, that forests have responded to rising atmospheric CO_2 levels by taking in more carbon than they release, thereby shielding us from the full impact of our emissions.

That protective effect may already be waning, concludes a research team led by Luciana Gatti of Brazil's National Institute for Space Research in São José dos Campos.[1] Just in the past decade, a large portion of the southeastern Amazon appears to have flipped from carbon sink to carbon source—even after the researchers discount the substantial carbon emissions from the many fires that are deliberately set to clear the land (as shown in figure 1) for cattle ranching and other agriculture.

Airborne

It's not easy to measure how much carbon is flowing into or out of a forest the size of the Amazon. More than two decades ago, Gatti and her colleagues noticed a scale gap in the understanding of carbon fluxes: Most studies focused on either extremely small scales (tracking the growth and carbon content of individual trees, for example) or extremely large ones (inferring the net carbon balance of all the world's land ecosystems put together by estimating the fluxes through the atmosphere and ocean).

To bridge the gap, they took a clever but laborious approach. Starting in December 2000, they hired a light aircraft to repeatedly fly above the small northern Brazilian city of Santarém and collect flasks of the air that was wafting over the Amazon.[2] The samples carried a record of all the trace gases emitted or absorbed by the parts of the forest they traversed: If a parcel of air passed through a carbon source, it would pick up more CO_2 than the atmospheric average; if it passed through a carbon sink, it would have less. Because the Brazilian trade winds blow reliably from east to west, with a variable north–south component, the Santarém samples probed a region of the northeast Amazon making up some 10% of the forest's area.

As the results came in, two things stood out. The first was how large the forest's CO_2 emissions were: The air above Santarém consistently contained more CO_2, not less, than the fresh Atlantic air entering the Amazon from the east. "It was much more than we expected," says

Gatti, "and the community was skeptical at first." The excess carbon was coming from deliberately set fires: Cutting and burning of the Amazon, although unlawful, is common. (See PHYSICS TODAY, May 2004, page 24.) To separate the fire emissions from the ecosystem's carbon flux, the researchers tracked the samples' concentrations of carbon monoxide—released in combustion but not in biological processes—along with their CO_2 content.

The second striking observation was the variability of the numbers. Fire emissions showed a seasonal pattern, as trees were cut during the region's wet season from January to June and burned during the dry season from July to December. The ecosystem's carbon flux also varied a lot from season to season and from year to year. "It was clear that we needed long-term measurements to really understand what was going on," says Gatti.

It was also clear that understanding the whole Amazon would entail sampling beyond just Santarém. The vast forest is regionally heterogeneous: The east is more populated than the west, so deforestation and fires are concentrated there. The eastern Amazon is also dry for half the year, with the dry-season months averaging not much more than 50 mm of rainfall, whereas monthly rainfall in the western Amazon seldom dips below 100 mm. Those differences could easily affect the regions' carbon balance.

Spreading out

In 2010 the researchers began a new project to take their measurements Amazon-wide. Twice a month they'd collect air samples from above not one but four sites around the Brazilian Amazon. In addition to Santarém in the northeast, the sites included Rio Branco in the southwest and Alta Floresta in the southeast—both population centers with plenty of air commerce and easy access.

Sampling from the northwestern Amazon proved far more of a challenge. Few commercial airports serve the sparsely populated, impoverished area, and few local pilots were available to collect and transport the samples. Initially, from 2010 until 2012, the researchers contracted with a one-airplane company in the town of Tabatinga. That relationship came to an end when the plane crashed. In 2013, they restarted sampling in the city of Tefé, a few hundred miles away, and they've been collecting samples from there ever since.

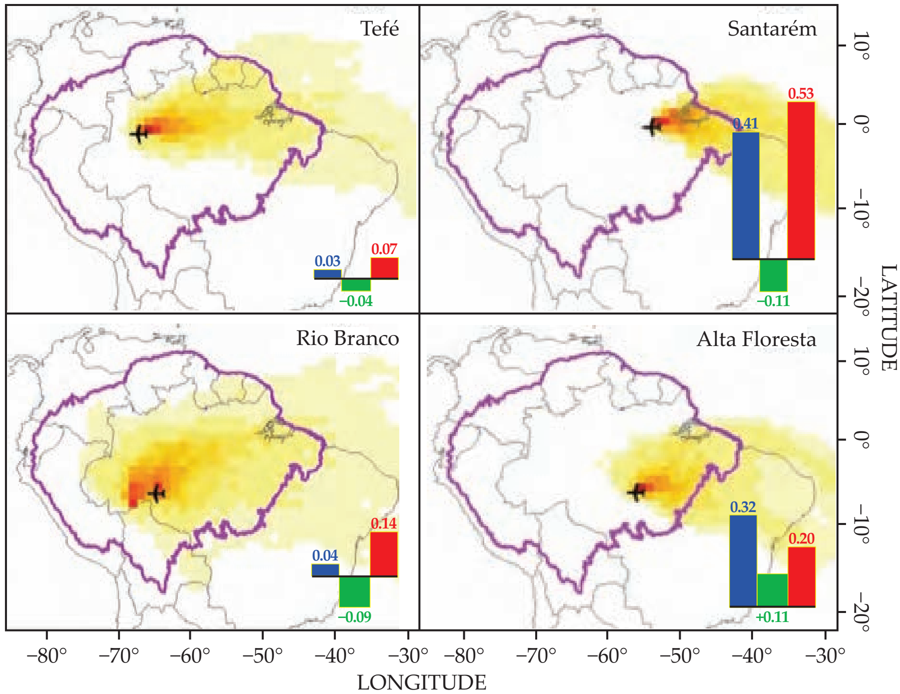

FIGURE 2. AMAZONIAN AIR Carries a record of all the atmospheric gases absorbed or emitted at points upwind of the sampling site. Based on an analysis of wind patterns from 2010 through 2018, the shaded areas on the maps show the average regions of influence for four sites throughout the Amazon. The bar charts show the carbon fluxes for each region in units of tons of carbon per square kilometer per day: Total carbon emission is shown in blue, carbon emitted by fires in red, and carbon exchange by the ecosystem in green. In the region around Alta Floresta in the southeast, even the ecosystem is now a net carbon source, not a sink. (Adapted from ref. 1.)

The project's first paper, published in 2014 and covering data from 2010 and 2011, highlighted the Amazon's year-to-year variability.[3] Whereas 2010 was a major drought year in Brazil, 2011 was relatively wet. Fires in both years caused significant carbon emissions—but in 2011 the emissions were roughly compensated by the ecosystem's carbon sink, whereas in 2010 the ecosystem absorbed almost nothing. When the forest dried out, its capacity to absorb carbon was hindered.

The current paper[1] analyzes the samples collected from January 2010 through December 2018. During that time, the researchers periodically reran a model of wind trajectories to assess what parts of the Amazon their samples were probing. Those average regions of influence are shown in figure 2. (Tabatinga isn't shown, but its region of influence is similar to Tefé's.)

The bar charts in the figure show the carbon fluxes for each region averaged over the nine-year period: net carbon balance (blue), as measured by the samples' CO_2 concentrations; fire emissions (red), as inferred from the samples' CO; and the ecosystem flux (green), which is the difference between the two. As the measurements show, the western Amazon (Tefé and Rio Branco) is nearly carbon neutral: The ecosystem absorbs most of the carbon that the fires emit. In the eastern Amazon (Santarém and Alta Floresta), fire emissions are more significant. And not only are they not balanced out by the ecosystem absorptions, but the ecosystem around Alta Floresta is itself a net carbon emitter.

Out to dry

That alarming result appears to be a new development. At the beginning of the study period—perhaps even in the drought year of 2010—the researchers' measurements indicated that the Alta Floresta–area ecosystem was probably a net absorber of carbon. But the trend since then has been progressively in the direction of net carbon emission.

Why the change, and could the rest of the Amazon follow suit? Part of the explanation may lie in the southeast Amazon's physical geography. Despite its overall wetness, the region is unusually devoid of large lakes and rivers, so it relies heavily on evapotranspiration from trees and other plants to supply the atmosphere with moisture that falls again as rain. When part of the area is deforested, the remaining forest is deprived of rainfall, and its health suffers.

Evapotranspiration is also important for regulating temperature: The energy of converting water into vapor helps cool the forest, so the loss of a moisture source makes the region hotter. Compared with other parts of the world, tropical forests don't usually experience wide temperature swings, so their organisms are adapted to narrow temperature ranges (see PHYSICS TODAY, September 2019, page 16). Even a small amount of warming can threaten species' ability to thrive. Dry-season temperatures in the southeast Amazon have already risen by a whopping 2.5 °C in just the past four decades.

The changing climate, the researchers conclude, creates a feedback cycle. As the forest becomes hotter and drier, organisms die off, and the ecosystem grows less resilient and less able to keep itself cool and moist in years to come. All the while, it's emitting more and more carbon than it can absorb.

The southeast Amazon is especially vulnerable due to its paucity of water sources, but all parts of the Amazon are trending toward higher temperatures and drier dry seasons. "Every quantity in every region has been linear for 40 years," says Gatti, "except for the temperature change in the southeast, which is accelerating. Other regions could start accelerating too, because all the processes are interconnected."

The researchers' current analysis extends only through 2018, so it doesn't cover the effects of the devastating 2019 wildfires or the ongoing COVID-19 pandemic. But apart from some disruptions—one of the pilots they were working with died of COVID-19—they've kept collecting samples and are continuing to analyze them. "We can't stop," says Gatti. "The Amazon is changing very quickly, and going on with these measurements is very important."

Johanna Miller

References

1. L. V. Gatti et al., *Nature* **595**, 388 (2021).
2. J. B. Miller et al., *Geophys. Res. Lett.* **34**, L10809 (2007); L. V. Gatti et al., *Tellus, Ser. B* **62**, 581 (2010).
3. L. V. Gatti et al., *Nature* **506**, 76 (2014).

An unconventional superconductor isn't so odd after all

NMR measurements and previously published specific-heat data rule out earlier claims of strontium ruthenate's spin-triplet superconductivity.

As electrons move through a Bardeen-Cooper-Schrieffer (BCS) superconductor, they attract positive charges in the lattice, and the subsequent deformation leads to an attractive interaction between time-reversed electron states. Below some critical transition temperature T_c, that electron–phonon interaction forms Cooper pairs of electrons with *s*-wave symmetry, and their collective behavior constitutes a macroscopic quantum state of matter. That is, the electrons stay paired and flow through a superconductor without any resistance. (See the article by War-

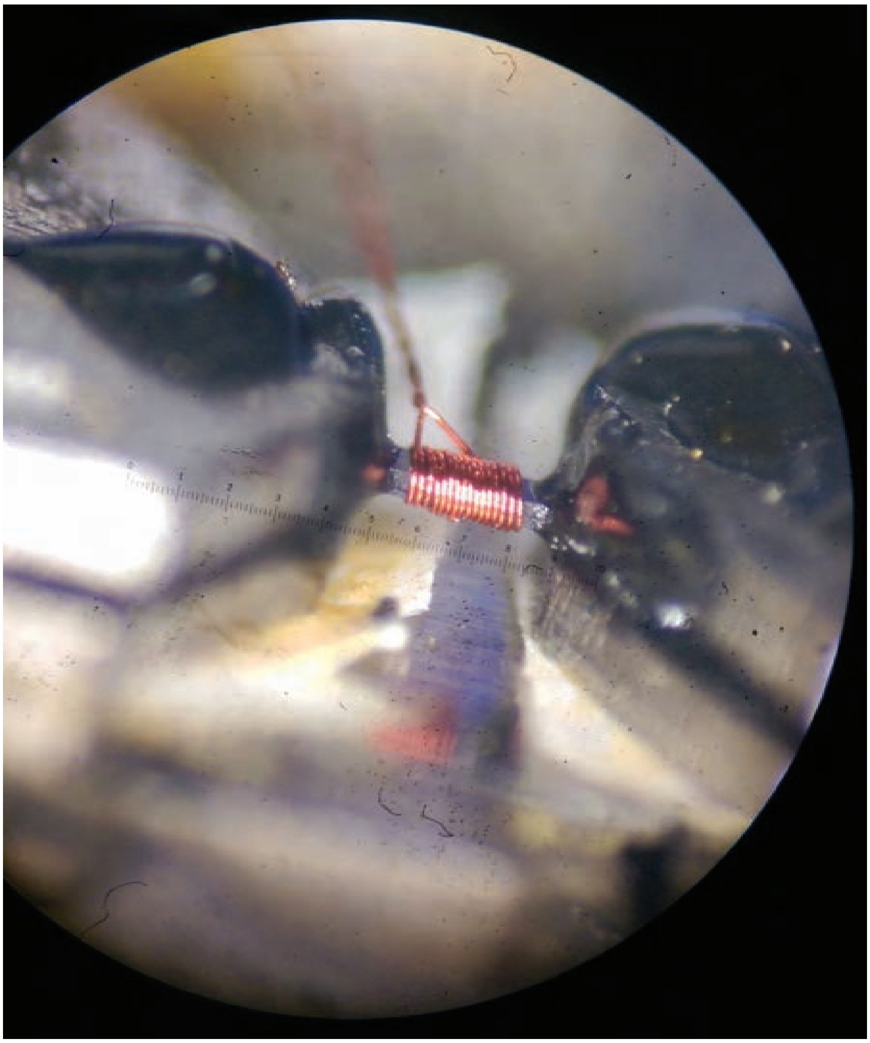

FIGURE 1. STRONTIUM RUTHENATE is superconducting below a critical transition temperature of 1.5 K. Researchers explored its unconventional superconducting state by wrapping a crystalline sample in an NMR coil and observing its response to a magnetic field. The results showed no detectable magnetic response from the superconducting condensate. That finding rules out previously postulated theories of odd-parity superconductivity in which paired electrons have the same spin. (Courtesy of Andrej Pustogow.)

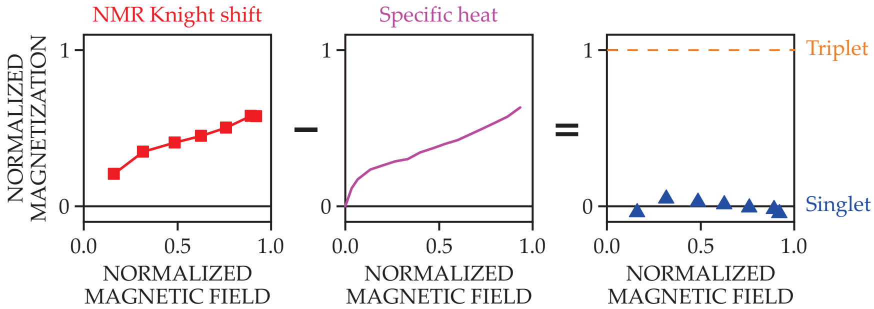

FIGURE 2. ELECTRON-SPIN SUSCEPTIBILITY in strontium ruthenate (SRO) can be inferred from the material's response to a magnetic field, normalized to the upper critical field, and measurable by the NMR Knight shift of oxygen-17 atoms in SRO's superconducting state. The field-dependent magnetization measured by the Knight shift (red squares and line) doesn't differ from that induced by nonsuperconducting quasiparticles, as inferred from specific-heat measurements in the system (purple line). The lack of difference means that the electron pairs (blue triangles) in the superconducting SRO condensate don't contribute detectable magnetization. SRO, therefore, has an even-parity, or spin-singlet, state—rather than the long-thought odd-parity, or spin-triplet, state. (Figure by Andrej Pustogow.)

ren Pickett and Mikhail Eremets, PHYSICS TODAY, May 2019, page 52.)

In 1994 researchers discovered that below a T_c of 1.5 K, strontium ruthenate (Sr_2RuO_4, or SRO) is superconducting.[1] Although its layered perovskite structure is similar to that of high-T_c, cuprate-based unconventional superconductors that don't strictly follow BCS theory, SRO has several important differences. For example, unlike cuprates, SRO is conducting and superconducting in its stoichiometric form and therefore doesn't require any dopants to be added to its structure. That clean form provides an ideal framework through which to study the emergence of unconventional superconductivity. (See the article by Yoshiteru Maeno, Maurice Rice, and Manfred Sigrist, PHYSICS TODAY, January 2001, page 42.)

A year after the discovery, researchers proposed that the similarity between SRO and superfluid helium-3 may favor an electron pairing in SRO with *p*-wave symmetry.[2] Conventional *s*-wave or unconventional *d*-wave superconductors are inversion symmetric, and their paired electrons must have opposite spins, known as even parity. But a superconductor with *p*-wave symmetry would have electron pairs with the same spin, or odd parity. In such spin-triplet pairing, an electron's spin can exist with one of three values of the quantum spin component. If SRO had such a pairing, it could be manipulated by a magnetic field, which would potentially be useful in spintronics and quantum computing.

Since then, researchers have reported experimental evidence consistent with *p*-wave symmetry in SRO, including time-reversal symmetry breaking (see PHYSICS TODAY, December 2006, page 23) and half-quantum vortices (see PHYSICS TODAY, March 2011, page 17). The findings have been the accepted explanation of SRO's exotic properties for about 20 years and have tantalized physicists with the promise of revealing new insights in unconventional superconductivity.

But in 2019 a paper by then-postdocs Andrej Pustogow and Yongkang Luo and their adviser Stuart Brown of UCLA questioned the prevailing *p*-wave explanation.[3] They analyzed a superconducting SRO crystal subjected to variable stress, and the results ruled out one of the several possible odd-parity states of SRO. Now a new paper by UCLA graduate student Aaron Chronister, Pustogow, Brown, and their collaborators has provided convincing evidence that excludes all odd-parity superconductivity in SRO. Their results are consistent with an unconventional even-parity state.[4]

A long experiment

As Brown recounts, he and his collaborators' investigations were strongly motivated by a 2017 result from Andrew Mackenzie's team at the Max Planck Institute for Chemical Physics of Solids in Dresden, Germany. That experiment suggested that the uniaxial strain applied to an SRO crystal that raised the T_c from 1.5 to 3.5 K could indicate an odd-parity to even-parity transition of the superconducting state.[5]

"To us," says Brown, "this meant that the superconducting state is profoundly affected by this stress, and it opened up an opportunity to revisit the SRO order-parameter question and any possible stress-induced phase change but in a vastly broadened parameter space."

To measure the electron pairing of SRO, Chronister and Pustogow held a magnetic field in a fixed orientation parallel to the sample's ruthenium oxide layers and then varied its strength. The spin susceptibility can be inferred from the Knight shift, a measurement of the NMR frequency shift of the oxygen-17 atoms in the superconducting material. Figure 1 shows the crystalline SRO sample with an NMR coil wrapped around it.

Such an experiment has its challenges. In particular, superconductivity in SRO or any other material is lost at a magnetic field strength higher than the so-called upper critical field B_{c2}. SRO's small B_{c2} of 1.5 T limits the signal intensity and spectral resolution of the NMR measurements. The signal intensity is further weakened by the need to regulate the RF eddy current that arises from the NMR pulse. Without RF regulation, the SRO crystal could be exposed to significant temperature fluctuations.

Mackenzie helped improve the signal intensity by acquiring oxygen that was highly enriched in oxygen-17 from Eric Bauer at Los Alamos National Laboratory. The researchers added it to the SRO samples for the experiments and Knight-shift measurements. Even with that improvement, though, the experiments still took weeks to complete, and meaningful analyses required the team to average the results from thousands of individual NMR spectra.

Then in March 2020, the coronavirus lockdown limited how often the researchers could conduct work in the lab. "We made the best out of the time that we could use," Pustogow says. He recalls thinking, "If we can only come in twice a week, we'll do the long experiment that doesn't need a lot of housekeeping. And it can line up with the coronavirus rules."

Nail in the coffin

The 2019 results[3] contradicted earlier findings and assumptions. To determine the cause of the discrepancies, Chronister and colleagues analyzed the RF-heating effect from the NMR pulses. At the high T_c of cuprate superconductors, RF heating isn't substantial enough to raise the temperature above T_c. But at the low T_c of SRO, they found that the excess heat was sufficient to nudge SRO from its superconducting state into a normal-conducting one. The UCLA team surmised that the earlier evidence of SRO's odd-parity state came from measurements that were collected in the normal state, rather than the sought-after superconducting state.

Convincing new evidence that extended beyond the 2019 finding came when the researchers compared two different measurements of the superconducting condensate's magnetization: their own Knight-shift data and previously acquired observations of the specific heat of a high-quality SRO crystal. Specific heat in that system is sensitive only to quasiparticles that are produced in the superconducting state. As figure 2 illustrates, the researchers found no difference when they subtracted the specific-heat data from their Knight-shift magnetization results.

The agreement between the Knight-shift and specific-heat measurements means that the electrons forming Cooper pairs in the superconducting state of SRO do not contribute detectable spin polarization to the overall magnetization. The pairing state must therefore be even parity.

The road to resolution

Even though the results disagree with the prevailing interpretation of SRO that physicists have had for more than two decades, they are consistent with the emergence of unconventional superconductivity from a well-described Fermi liquid. By starting from perturbative electron–electron collisions, theorists have shown that at low temperatures, resistivity in a Fermi liquid increases as T^2, and experimentalists have observed that power-law resistivity in SRO.

Although the odd-parity state has been overturned by the results of Chronister and colleagues, determining how to interpret the spin-singlet state of SRO in conjunction with other recent experimental results remains a challenge. Another method to study the electron pairing in SRO and other superconducting materials is muon-spin spectroscopy. The technique implants spin-polarized muons into a material and then records the interaction of the muon's magnetic moment with its surroundings.

Vadim Grinenko and Shreenanda Ghosh at Dresden University of Technology in Germany and their collaborators published a paper earlier this year using that method on single-crystalline SRO samples. They reported a small magnetic buildup, which by definition breaks time-reversal symmetry. A uniaxial stress broke the sample symmetry and resulted in a two-component order parameter: a spin-singlet superconducting state followed by one that was interpreted as a chiral state, perhaps with *d*-wave symmetry. (See "An unconventional superconductor undergoes two transitions," PHYSICS TODAY online, 22 March 2021.)

Physicists are also using ultrasound measurements to study SRO. According to Ginzburg–Landau theory, discontinuities in the elastic constant at the superconducting transition reflect electron pairing. Recent results found such a discontinuity in the shear elastic constant of SRO as the temperature was increased across the superconducting transition.[6] Like the muon-spin results, the observation is consistent with a two-component order parameter.

Spin states compatible with the recent reports of time-reversal symmetry breaking, ultrasound discontinuities, and spin-singlet pairing are possible. Verifying which particular spin state, however, will require more research. Brown and his colleagues are currently examining the effects of exposing superconducting SRO to especially high stress.

Alex Lopatka

References

1. Y. Maeno et al., *Nature* **372**, 532 (1994).
2. T. M. Rice, M. Sigrist, *J. Phys.: Condens. Matter* **7**, L643 (1995); G. Baskaran, *Physica B* **223–224**, 490 (1996).
3. A. Pustogow et al., *Nature* **574**, 72 (2019).
4. A. Chronister et al., *Proc. Natl. Acad. Sci. USA* **118**, e2025313118 (2021).
5. A. Steppke et al., *Science* **355**, eaaf9398 (2017).
6. S. Benhabib et al., *Nat. Phys.* **17**, 194 (2021); S. Ghosh et al., *Nat. Phys.* **17**, 199 (2021).

A simple magnetic field configuration could trigger solar eruptions

A sheared magnetic loop in the Sun's corona can give rise to a thinning sheet of electrical current, magnetic reconnection, and tension forces strong enough to hurl material into space.

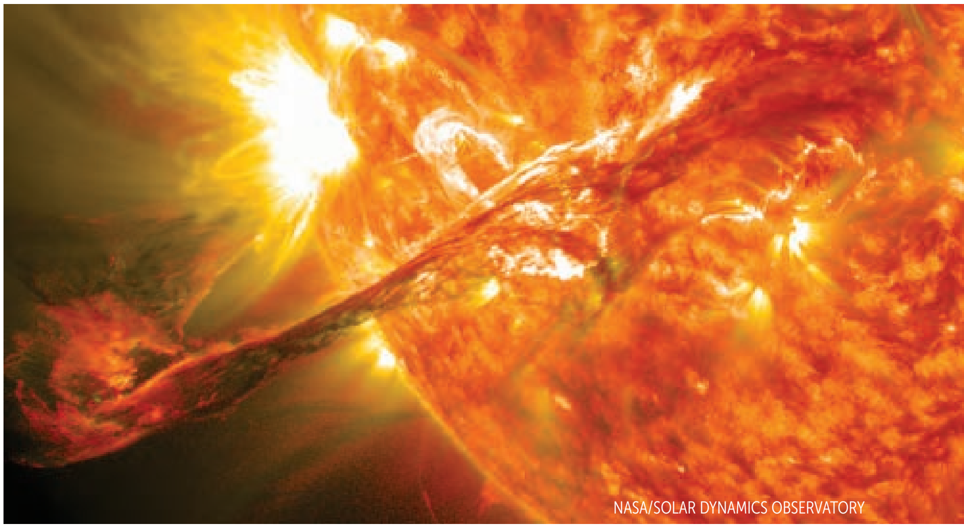

FIGURE 1. CORONAL MASS EJECTIONS occasionally erupt from the Sun's surface and launch a hot stream of energetic plasma out into space. The one captured here by the Atmospheric Imaging Assembly on NASA's *Solar Dynamics Observatory* erupted on 31 August 2012 and traveled at 1450 km/s.

Richard Carrington made the first record of a solar flare in 1859 from his observatory outside London. Although it wasn't clear at the time, research since then has shown that such eruptions can have an enormous impact on Earth's space neighborhood. The tons of plasma spewed into space may breach Earth's protective magnetic field and eventually emerge as auroras and geomagnetic storms.

Combined observations and theory have led physicists since Carrington to understand that solar eruptions, including flares and coronal mass ejections such as the one shown in figure 1, are powered by magnetic fields in the Sun's corona.

A remaining challenge is pinpointing a specific mechanism that triggers those eruptions. As a precondition for eruption, many models invoke complex magnetic field structures such as twisted ropes of flux to create an instability that drives an eruption, but astronomers have rarely observed such topologies in the preeruption corona.

Now Chaowei Jiang at the Harbin Institute of Technology's campus in Shenzhen, China, and colleagues have demonstrated through three-dimensional simulations that magnetic field lines that are arranged in a simple looped configuration near sunspots are sufficient to initiate a solar eruption.[1]

Tangled up in plasma

In the 1960s, solar physicists converged on an explanation for how small solar flares form. They postulated that the magnetic field lines that permeate the Sun's plasma atmosphere interact with one another in a process called magnetic reconnection (see Physics Today, September 2013, page 12). When oppositely directed field lines approach each other, they can break and reconnect in a lower-energy configuration. The field lines are bent tightly immediately after reconnection. Then they abruptly straighten and release energy, much like the snapping of a rubber band.

Because the plasma conducts electricity, the field lines cannot move with respect to the plasma in which they are embedded. As a result, when the field lines move, so does the plasma. The straightening field lines then launch jets of charged particles in opposite directions away from the reconnection locus, as illustrated in figure 2. (See the article by Forrest Mozer and Philip Pritchett, Physics Today, June 2010, page 34.) That process generates the kinetic energy in a solar eruption.

But that picture does not explain what initiates the reconnection process. The Sun's corona remains quiescent as long as two magnetic forces in the plasma are balanced. The magnetic pressure-gradient force generally points outward, while the magnetic tension force generally points inward and confines an eruption. A fundamental question that therefore remains—and also is a central point of controversy—is how the preeruption force balance is abruptly destroyed.

A theory proposed in the 1980s suggested that a single bipolar loop of magnetic flux, pinned at either end to sunspots on the solar surface, could disrupt the stability of the corona and lead to an eruption. Portions of the loop would squeeze together slowly and rearrange quickly in a way that initiated magnetic reconnection.[2] Increased outward magnetic pressure would then cause the entire configuration to expand and disrupt the equilibrium. The field lines would twist around each other as the eruption progressed.

Simulations in two dimensions have provided support for that simple configuration's ability to generate enough energy to disrupt the corona's stability.[3] Because it's so difficult to observe the details of the Sun's corona, 3D simulations are vital to providing evidence in support of theoretical models. However, scientists have struggled to get such simulations to reproduce the phenomenon. The simple field-line configuration model had "never been proven to initiate, alone, an eruption in any 3D simulation," according to Guillaume Aulanier at the Plasma Physics Laboratory in Paris.[4]

Instead, many of the current 3D simulations favored by the solar-physics community today rely on the preexistence of a twisted flux rope or other multipolar field-line topologies that are more complex than simple bipolar loops. Tightly twisted lines of a flux rope create an ideal instability in the plasma and disrupt the magnetic force balance. That disruption then drives rapid magnetic reconnection.

Twisted plasma loops are indeed visible in observations of coronal mass ejections—but only after the eruption is underway. Those observations have fueled debate over whether complex flux topologies exist before the eruption or are

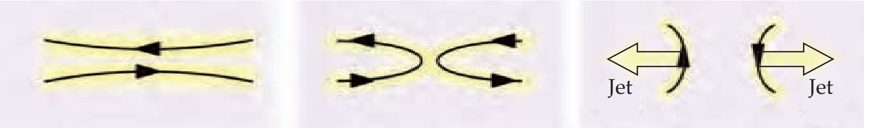

FIGURE 2. MAGNETIC RECONNECTION occurs in a plasma when oppositely directed field lines approach each other (left). Immediately after reconnection, the newly configured field lines are tightly bent (center). As the field lines abruptly straighten, they transfer magnetic energy into oppositely directed particle jets (right). When magnetic reconnection happens in the Sun's corona, the kinetic energy it generates may drive an eruption. (Adapted from PHYSICS TODAY, October 2001, page 16.)

formed during it.[5] Solving that puzzle could provide clues to the mechanism that initiates the eruption.

Shearing and twisting

Revisiting the simple field-line configuration proposed decades ago, Jiang and his colleagues now show in 3D that an eruption may proceed without any complex preeruption field-line structure. Using China's National Supercomputing Center in Tianjin, the researchers designed a magnetohydrodynamic simulation driven by slow rotational flow of the plasma at the Sun's surface.

They found that horseshoe-like loops of flux ballooned outward while remaining connected to the solar surface. The horseshoe's pinned sides sheared against one another, forming a sheet of electrical current. As the current sheet became thinner, the field lines pushed toward each other and then abruptly rearranged themselves. That reconnection converted magnetic energy to kinetic energy and drove the eruption, as illustrated in figure 3. A rope of magnetic flux—the multicolored circular structure that becomes increasingly twisted over time—appeared only after the eruption had initiated and thus dispelled the notion that it was a necessary preexisting condition.

Closer analysis of the forces experienced by each field line in the erupting flux revealed the real culprit: Strong curvature in the newly reconnected field lines created a slingshot effect that resulted in extremely strong magnetic tension forces directed away from the Sun. Those forces provided an efficient means of driving particles and radiation into space and showed that the eruptions were driven from below by the reconnection jet (see figure 2).

Key to the simulation's success was its high numerical accuracy and resolution. Jiang and colleagues accomplished that goal by building height-dependent gravitational acceleration and grid-dependent numerical resistivity into the code. The result was a highly conducting plasma on par with the ones used in laboratory experiments.

The researchers also imposed boundary conditions to ensure that an untwisted loop remained pinned at the solar surface long enough for a current sheet to form. But the simulation needed high accuracy to maintain the field-line-pinning condition so it could create a current sheet in the plasma's evolution before the eruption. Earlier 3D simulations failed to reach the requisite accuracy. If the field lines' connection points slipped at all, the simulation resulted in energy loss that prohibited the current sheet from forming. "It is only by fulfilling such a stringent requirement that the fast, turbulent reconnection can arise and impulsively convert the magnetic energy into an explosion," says Jiang.

Regardless of the precise magnetic configuration, the researchers argue, the key mechanism remains the same. A thin current sheet forms slowly in the central part of the field and then rapid magnetic reconnection triggers and drives the explosion via a jet from below.

"The model that this work supports has been around since the 1980s," says Peter Wyper at Durham University. "But only as a conjectured cartoon. No simulations until now have got it to work, so other mechanisms have become favored instead. This work suggests that it may play a more crucial role after all."

Already, observations provide support for Jiang's simulations. The morphology of the simulations is consistent with eruptions captured by NASA's *Solar Dynamics Observatory*. Additionally, many observations of the preeruption corona show thin, hot structures that could be a proxy for the slowly formed current sheet before eruption. The finding could lead to a universal model of solar eruptions and provide better understanding of how the phenomenon influences space weather.

Rachel Berkowitz

References

1. C. Jiang et al., *Nat. Astron.* (2021), doi:10.1038/s41550-021-01414-z.
2. R. L. Moore, B. J. Labonte, *Symp. Int. Astron. Union* **91**, 207 (1980).
3. T. Amari et al., *Astron. Astrophys.* **306**, 913 (1996).
4. G. Aulanier, *Proc. Int. Astron. Union* **8**(S300), 184 (2013).
5. S. Patsourakos et al., *Space Sci. Rev.* **216**, 131 (2020).

PT

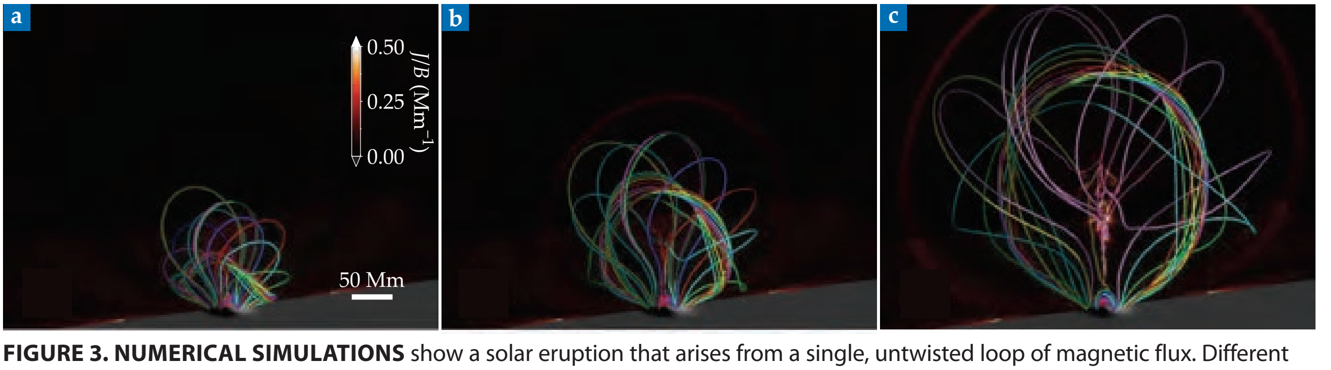

FIGURE 3. NUMERICAL SIMULATIONS show a solar eruption that arises from a single, untwisted loop of magnetic flux. Different colors distinguish individual magnetic field lines. The red halo-like rings indicate the electric current density. **(a, b)** Field lines become twisted around each other, leading to the rope structure that appears as outer lines forming loops around the inner ones. **(c)** The turbulent region at the configuration's core drives runaway reconnection. (Image courtesy of Chaowei Jiang.)

Better ways to store energy are needed to attain Biden's carbon-free grid

Experts say lithium-ion batteries will be overtaken for grid-scale energy-storage applications by other battery technologies and nonchemical storage.

ENERGY VAULT

AN ARTIST'S RENDERING of Energy Vault's grid-scale energy-storage system adjacent to an array of solar cells. Inside the building, a bank of freight elevators move composite blocks up and down to store and generate power.

When the sun is shining, solar power in California is so abundant that the price for electricity from photovoltaics sometimes falls to zero. Indeed, California at times has had to pay its neighbors to take some of its surplus solar energy. But what if that energy could be stored for nighttime use, or for days or weeks when cloudy periods curtail production?

The problem of storing massive amounts of electricity becomes increasingly urgent as more and more intermittent renewable electricity is delivered to the power grid. About 13% of total US electricity supply, excluding hydroelectric power, comes from renewable sources, according to the Energy Information Administration. Even at that modest level, "the grid is 40 seconds from blackout all the time," says Robert Abboud, CEO of Beacon Power, which produces flywheels for short-term energy storage. "The only way we stay sane is to balance the grid all the time between generation and demand. If we don't do it correctly, it just falls down."

Barring a renaissance in nuclear power, a breakthrough in fusion, or dramatic reductions in the cost of carbon capture and storage, meeting the Biden administration's aggressive goal of a carbon-free electricity supply by 2035 will require a mainly renewable energy system. Storage remains too expensive for massive amounts of renewables to compete against legacy electricity sources such as coal and natural gas. Recognizing that reality, the Department of Energy in January 2020 announced a goal to lower by 90% the levelized cost of storage on an electricity grid by 2030, to around 5 cents per kilowatt-hour (¢/kWh). Levelized cost is defined as the nationwide average of capital and operating costs summed over the lifetime of the asset.

Similarly aggressive cost-reduction targets have been achieved for solar and wind energy, notes Daniel Kammen, who heads the Renewable and Appropriate Energy Laboratory at the University of California, Berkeley (see PHYSICS TODAY, June 2021, page 27). Kammen codeveloped a two-factor model that correctly predicted the plunge in solar costs that has occurred during the last four years. Using that model as a basis, he says the US is already ahead of DOE's storage price target and likely will get there by 2025. "We think that with the 1¢/kWh to 3¢/kWh that solar is already at, we'll have baseload renewable power systems that are much cheaper to install and operate than it is to operate existing fossil-fuel plants," he says.

DOE has included $1.16 billion in its fiscal year 2022 budget request for R&D on all forms of energy storage, more than doubling the $400 million it's spending this year. That proposed outlay indicates the priority that the agency attaches to storage, says Eric Hsieh, director of grid systems and components in DOE's Office of Electricity.

Water and chemistry

Pumped hydroelectric storage has been employed by electric utilities for more than a century, and today it still accounts for about 95% of all grid-scale capacity. Electricity generated during low-demand periods is used to pump water from one reservoir to another at a higher elevation. When demand is high, water is released through turbine generators to the lower pool. Although efficient and suitable for long-term storage, pumped hydro is severely restricted in its further deployment by availability of suitable locations, multibillion-dollar capital costs, and environmental concerns.

More recently deployed technologies provide short- and medium-duration energy-storage needs. Capacitors and flywheels address the short term. Beacon Power's flywheels, for example, can boost power nearly instantaneously to provide load-leveling services—such as voltage and frequency regulation—to PJM, the nation's largest regional transmission organization. Although flywheels can't provide long-term storage yet, Abboud says that will come soon with the development of higher-strength carbon-fiber materials and magnetic bearings made with high-temperature superconductors, both of which will dramatically increase the rate of spin and mitigate energy lost by friction.

For storage of two to six hours, lithium-ion batteries dominate. Tesla, the leading supplier of grid-scale batteries, surpassed

3 GWh of deployments in 2020 alone. In California, where investor-owned utilities are required by law to provide a total of 1325 MW of power capacity by 2024, PG&E, the state's largest utility, has already contracted for more than 1400 MW of lithium-ion deployments by 2023, nearly triple its 535 MW share of the state mandate. One of those projects, located at an electric substation in Monterey County, will be among the largest utility-owned lithium-ion projects in the world when it becomes operational later this year with a capacity of 182 MW. Consisting of 256 Tesla Megapack battery units, the facility will be capable of dispatching a total of up to 730 MW of energy over four hours. It will enhance grid reliability by addressing capacity deficiencies resulting from increased local energy demand, according to the company. It will also provide energy and load-leveling services to the electricity markets served by the California Independent System Operator.

But lithium-ion's economics and physical properties limit its storage duration to eight hours of discharge. "If you take a lithium-ion system, charge it, and leave it for three months, it will self-discharge," says Vincent Sprenkle, technical group manager for the Electrochemical Materials and Systems Group at Pacific Northwest National Laboratory (PNNL).

The energy storage company BoxPower has built several solar-powered microgrids of up to 250 KW with lithium-ion batteries to service PG&E customers in remote, wildfire-endangered locations. Those systems require backup generation from propane. "Battery storage is currently the limiting factor," says CEO Angelo Campus. "In order to get to a truly 100% renewable solution, you have to start thinking about multiday or even seasonal range."

Lithium is less than abundant, and the cobalt used in some batteries is even more scarce. (See Physics Today, December 2019, page 20.) The battery's solvent electrolyte is flammable, as was illustrated by the fire at a Tesla Megapack grid-scale storage site near Melbourne, Australia, in late July. The solvents could also create a hazard in the event of a leak.

Most industry experts agree that lithium-ion batteries' cost floor is too high, says Hsieh. The most promising battery technologies for long-term applications can decouple power from energy capacity, he says. In such battery types, energy-storage capacity can be increased by adding to the volume of electrolytes stored in the tanks. The battery's electrochemical cells can be electrically connected in series or parallel to determine the power. (See the article by Héctor D. Abruña, Yasuyuki Kiya, and Jay C. Henderson, Physics Today, December 2008, page 43.) Within that category, redox flow batteries appear to be the leading candidates. Flow batteries consist of tanks of aqueous chemical redox pairs—electroactive compounds that can reversibly undergo reduction and oxidation—that flow through a fuel-cell-like device to generate electricity.

PG&E

TESLA MEGAPACK lithium-ion batteries located at a PG&E substation in Northern California. When completed later this year, the facility will be capable of dispatching energy to the grid at the rate of 182 MW for up to four hours.

Redox flow-battery chemistries can vary, but the most common pair is vanadium–vanadium, in which that element's four valence states are utilized. "[Flow batteries] have a nice body of scientific inertia behind them," Hsieh says. "Most of the people working on them think there is a viable pathway to achieve very low costs." Organic electrolytes that could further reduce flow batteries' cost are being developed, says Wei Wang, director of PNNL's Energy Storage Materials Initiative.

Unlike lithium-ion technology, aqueous-electrolyte batteries use abundant, nontoxic materials, says Esther Takeuchi, a materials scientist at Stony Brook University and Brookhaven National Laboratory. She notes that R&D investments in large-scale storage batteries have paled in comparison to the attention that's been devoted to lithium-ion for electric vehicles and consumer electronics. Although energy densities and voltages of aqueous cells are lower than those of lithium-ion cells, they might be 20% of the price. Takeuchi and her colleagues have been investigating an aqueous-electrolyte stationary battery with a zinc anode and manganese oxide cathode.

Because of the pumps, tanks, and power electronics they require, however, flow batteries have a "not insignificant cost floor," says Hsieh. Costs will come down as the manufacturing process is optimized, says Sprenkle. Flow batteries are less efficient (70–85% in the case of vanadium) than lithium-ion (90–95%), so marginal improvements in efficiency should have a big impact on lowering their levelized cost.

DOE is taking another look at the more-than-century-old lead–acid battery for grid-storage applications, says Hsieh. Today's lead–acid cells discharge only 20–30% of their theoretical potential, and research on basic material properties is addressing how much more of that capacity could be used. "You could take advantage of a well-developed fully closed recycling-life-cycle supply chain in the US to get more performance out of an existing technology," he says. Lead–acid's lifetime of around two years needs improvement to compete against lithium-ion's seven years, notes Sprenkle.

DOE has research programs underway on other battery chemistries, including sodium ion and sodium metal. "Batteries making it into the market is a long slog," says Takeuchi. "But things are changing quickly. One change is our ability to probe batteries effectively to really understand the mechanisms. That's one of the things we can do so well at Brookhaven. It takes years off the front end of R&D." Improved computational power also is speeding up the development process. "Historically batteries were developed in a very Edisonian" trial-and-error way, she notes.

Heat, gravity, hydrogen

Nonchemical storage options include hydrogen, gravity- and thermal-based systems, and compressed air. "The real wild cards are the completely new technologies," says Hsieh. "Every week I hear about a different type of thermal storage: storing heat in fluids or in concrete blocks, or in carbon-fiber blocks, with various ways of converting heat back into electricity." Those systems are attractive in part because their base materials are so cheap. Only a couple of them should be needed to meet DOE's cost-reduction goal, he notes.

Some concentrated solar arrays today focus solar energy onto a molten-salt medium during the day, storing the heat to generate electricity in the evening or during cloudy weather (see PHYSICS TODAY, June 2021, page 27).

As electric vehicles become more prevalent, their collective batteries can become a grid-scale storage medium, says Kammen. "Every grid-enabled [equipped for bidirectional charging] F-150 truck and Tesla could be part of a roving fleet of storage."

Some schemes are conceptually simple—others not as much. Swiss-based Energy Vault's technology of raising and lowering 35-ton blocks made of dirt and polymer can store energy for just 60% of lithium ion's levelized cost, according to a 2020 report from the forecasting firm BloombergNEF. The company predicts that by 2025 that number will drop to 51%, which would make Energy Vault's storage system the least expensive among a dozen new alternatives ranked by Bloomberg. Other ventures included WattJoule's redox flow battery; Ambri's liquid-metal battery, composed of a liquid calcium-alloy anode, a molten-salt electrolyte, and a cathode of solid particles of antimony; a cryogenic air-storage system from Highview Power; and Siemens Gamesa's thermal storage system, in which rocks are heated resistively and the stored energy is then discharged by steam turbine.

Energy Vault CEO Robert Piconi says the company has redesigned its product since its first grid-connected commercial deployment in Switzerland last year. In that system, computer-controlled cranes mounted atop each other stacked and unstacked the blocks. The redesign came in response to customer demand for higher power and shorter-duration storage. The new model employs freight elevators instead of cranes to raise and lower the blocks inside structures that resemble 30-story office buildings. Piconi says the company has eight orders across four continents totaling 1.2 GWh. One contract, with the renewable energy giant Enel Green Power, also calls for Energy Vault to recycle worn-out fiberglass wind-turbine blades into its storage blocks.

The Canadian company Hydrostor offers a fossil-fuel-free system where compressed air is stored in purpose-built underground caverns. A closed-loop water reservoir maintains the system at a near-constant pressure throughout the charge–discharge cycle. The heat generated from compression is extracted and stored. As the cooled air enters the cavern, it displaces the water, pumping it to the surface. During discharge, hydrostatic pressure forces the air to the surface, where the stored heat expands it to drive a turbine.

Hydrostor's first commercial plant, located in Goderich, Ontario, has been in operation since 2019, providing up to 10 MWh of peaking capacity to the grid operator. A number of other projects, in Australia, Chile, the US, and Canada, are in various stages of development.

Analyses performed at PNNL have shown that compressed-air pressurization of an underground cavern is one of the most cost-effective storage solutions, says Sprenkle. But it's not necessarily a green technology. And Hsieh notes that compressed-air storage is geographically limited.

Hydrogen produced through water electrolysis using surplus renewable energy can be a long-term energy-storage medium, though costs remain a challenge, says Hsieh.

David Kramer

Replacing high-risk radioactive materials remains a challenge

The medical industry is substituting x-ray sources for cesium-based blood irradiators. Other industries are also exploring alternative technologies.

NNSA

MEMBERS OF DOE'S Radiological Assistance Program survey the inside of the University of Washington's Harborview Research and Training Building in Seattle after a sealed cesium-137 source was breached in May 2019. Such radiation exposure could be avoided by replacing cesium-based blood irradiators with new x-ray technology.

A radioactive iridium-192 source capable of causing permanent injury within minutes of exposure went missing in late July, according to the US Nuclear Regulatory Commission (NRC). Prime NDT Services—a business based in Strasburg, Ohio, that uses nondestructive testing methods to evaluate the integrity of oil and gas pipelines—shipped the ^{192}Ir source from Ohio to Michigan on 12 July. Eight days later the carrier informed the company of the disappearance. Dozens of similar incidents around the US have been reported to the NRC this year.

The risks of accidental radioactive contamination and deliberate dispersal by terrorists have prompted governments worldwide to fund the search for substitutes for commercial radioisotope technology. After the 9/11 terrorist attacks in 2001, Congress tasked the National Research Council with reviewing technologies that rely on high-risk materials and recommending nonradioactive replacements that couldn't be readily weaponized.

The report, released in 2008, found that a handful of radionuclides make up the majority of high-risk sources in the US and suggested that cesium chloride sources, in particular, should be replaced. A follow-up report released in June of this year by the National Academies of Sciences, Engineering, and Medicine (NASEM) renews the call to decrease the reliance on radioactive materials.

But over the past 12 years, the US medical field, science research enterprise, and industry have increased their use of radioactive sources by 30%, according to regulatory commission data.

Targeting cesium chloride

The 2021 NASEM report focuses on the riskiest radiation sources. Blood-irradiator devices, for example, contain cesium chloride and other materials that the International Atomic Energy Agency (IAEA) defines as category 1 sources. They can cause death or permanent injury, even if someone is exposed to grams of material for just a few minutes. Category 2 sources include the americium-241 and beryllium mixture found in logging tools for oil exploration and radiometric-instrument calibration. They typically require an exposure time of hours to cause severe health conditions.

Common smoke detectors use ^{241}Am to ionize air molecules; an interruption of the resulting current indicates the presence of smoke. They're a category 5 radiation source, which the IAEA ranks as unlikely to cause any injury.

Devices with cesium-137 are commonly used in research and in the medical industry. For example, to prevent graft-versus-host disease and other transfusion-based illnesses, medical facilities routinely expose blood to ionizing radiation, which kills white blood cells. The ^{137}Cs is traditionally bonded to chloride. The resulting crystalline powder is easily handled and stored, but its high water solubility makes it easy to disperse and even capable of diffusing through concrete.

The US Department of Energy's National Nuclear Security Administration has funded numerous efforts to replace cesium chloride blood irradiators. One promising technology uses x rays to deliver ionizing radiation to blood, and several companies now offer commercial units to the medical industry. According to a 2018 report by the nonprofit Nuclear Threat Initiative (NTI) in Washington, DC, the costs of three devices approved by the Food and Drug Administration range from $200 000 to $270 000.

In 2016 Emory University Hospital in Atlanta, Georgia, purchased an x-ray blood irradiator and retired its radiological one. Mount Sinai hospital in New York City followed suit in 2019, replacing all of its cesium blood irradiators. Georgia-based manufacturer Rad Source Technologies has sold devices to hospitals in the US and Saudi Arabia. Thomas Kroc, the committee cochair of the recent NASEM report, says that "the 2008 academies report did talk about the promise of x-ray technology. It has taken until now for it to really mature to the point where it's starting to emerge on the market."

A few national health systems have started or completed the switch. In the wake of the 2011 Fukushima Daiichi reactor accident, Japan began phasing out the use of cesium blood irradiators; 75% of the country's units have now been replaced with x-ray ones. By 2016 France and Norway had supplanted all their cesium blood irradiators with x-ray ones.

Cobalt-60

Another common, high-risk radioisotope is cobalt-60, which is most often used to sterilize medical devices and to kill insects, fungi, and bacteria in food processing. It's effective because the panoramic irradiator that holds the source is typically housed in a shielded room and shoots 1.17 and 1.33 MeV gamma rays at items on a conveyor belt. According to the 2021 NASEM report, the US has about 72 000 category 1 and 2 ^{60}Co sources and roughly 3200 category 1 and 2 ^{137}Cs sources.

Suresh Pillai, who studies molecular microbiology and food safety at Texas A&M University, says "to the best of my knowledge, there are no new cobalt-60 facilities being commissioned in the US." DOE has funded R&D for electron-beam sterilization technology and other replacements for ^{60}Co.

"The facts on the ground show that especially in medical device and food processing, nonradioactive machine sources are growing," says Pillai. Still, electron-beam makers face regulatory hurdles and an uphill battle against industry inertia. Operators of ^{60}Co sources and device manufacturers have a 50-year head start, and Pillai says there are not enough electron-beam suppliers. Switching from gamma-ray sterilization to electron-beam technology requires that the materials be boxed in different packaging, which is expensive and involves a significant reorganization of sterilization supply chains.

In India, blood and low-dose research irradiators that rely on ^{60}Co, which has a 5-year half-life, are being replaced by devices employing ^{137}Cs, which has a 30-year half-life. Although proponents argue that the longer half-life of ^{137}Cs translates to fewer handling and transportation operations and thus may be less risky, it's still a category 1 source. India's strategy relies on vitrified ^{137}Cs, which lacks the water solubility of the isotope's more common powdered form.

In a June 2020 paper from the Observer Research Foundation, a think tank based in New Delhi, India, Rajeswari Pillai Rajagopalan says that "while India has made a strong case for cesium-137, it could be useful for India to explore other replacements that might not present the same dangers as cesium-137."

MORE R&D is needed to lower the cost of less risky, nonradioactive alternatives to the gamma-ray-based logging tools that the oil and gas industry uses to measure the density and porosity of rock formations. (Photo by iStock.com/sasacvetkovic33.)

In addition to technological innovation, issues associated with the supply of ^{60}Co may be helping to drive the adoption of replacements. In 2014 the amount of ^{60}Co on the global market slumped after a joint Russian–British business venture collapsed. The shutdown of an Argentinian reactor in 2016 for refurbishment further strained the global supply.

In an October 2020 presentation to the NASEM report committee, Nordion—a health science company based in Ottawa, Canada, that is a primary supplier of ^{60}Co sources—said the supply of ^{60}Co is now 5% below demand.

Well logging

Although the bulk of ^{137}Cs sources are found in the medical industry, the oil industry uses the radioisotope too. Drillers, equipped with a ^{137}Cs source housed in a data-logging tool, detect and measure the density of the surrounding rock to determine its capability for holding hydrocarbons. A second detector measures and corrects for naturally occurring radiation.

Another tool common in petroleum exploration contains an americium–beryllium source and emits neutrons in the borehole of a well to estimate the ground's porosity. The porosity characterizes the well's economic feasibility by quantifying the ease with which hydrocarbons will flow through the rock reservoir to the well. (For more on the physical techniques used in oil exploration, see the article by Brian Clark and Robert Kleinberg, PHYSICS TODAY, April 2002, page 48.)

The IAEA has established protocols for the storage, transport, and use of radioactive sources in hydrocarbon exploration. Still, radioactive logging sources have been stolen—including in India in 1993 and in Argentina in 2009. Others have gone missing. In 2003 the americium–beryllium source of an oil company in Nigeria disappeared for several months before turning up in Germany.

The most surefire way to mitigate such risk would be to use an alternative, nonradioactive technology for petroleum exploration. One substitute device detects scattered x rays to measure a rock formation's density and porosity. But its accuracy is not as high as a ^{137}Cs logger, the data it collects require correction, and it isn't as widely available as radioactive devices.

The oil industry favors radioactive well-logging tools because of their stable radiation output, relatively low cost, and small footprint: They can operate in a tight, high-temperature space without an additional, bulky power supply. "If you've got something that still has 10 years of service life left and the alternative is not significantly less expensive, then there's going to be very little push to give up that service life," says committee cochair Kroc.

Ioanna Iliopulos, a senior consultant at NTI, says the oil industry is extremely competitive. "There are a few big companies and a lot of mom-and-pop shops, and expanding funding for alternative technologies has not been a priority due to narrow profit margins."

One size doesn't fit all

Health-care providers and researchers, particularly in some low-income countries in Africa, need financial support to purchase nonradioactive devices. They also lack qualified operators for the instruments and reliable, uninterrupted power supplies.

Cultural and social concerns also influence whether radioactive materials get replaced. Hubert Foy, a committee member of the 2021 NASEM report, is the founding director of and senior research scientist at the African Centre for Science and International Security in Accra, Ghana. He says it's important to ensure buy-in from users and the community. "I've seen that the technology is not being fully utilized within the developing-country community," he says. "I would have loved to see in the academies report an assessment of the infrastructure and cultural implications of the adoption and use of alternative technology."

Laura Holgate, a vice president at NTI, says, "More can be done about the regulatory setting and environment so that those who do make the change have a benefit." She says that leadership from the White House could spur a government–industry partnership, where government agencies, nuclear regulators, and business leaders could talk in a noncompetitive environment about the alternative technologies and how to overcome the challenges to adopting them.

For radioactive sources without a ready alternative, Holgate says, "you really need to have security levels consistent and commensurate with the threat to human health and the economic, operational, and societal impacts." Strong security measures, such as having cameras, providing access control, and always having two people execute critical procedures, are far from universal, she adds.

Jennifer Elster, a research scientist at Pacific Northwest National Laboratory, notes that "avoiding the security costs and end-of-life costs associated with removal and disposal of radioactive material is likely to be a strong incentive in considering alternative technologies."

Enhanced security, however, doesn't necessarily protect against an insider adversary. "One of the things that is of rising concern to NTI and others is the growth of domestic extremism, not just in the US but abroad," says Holgate. "There have been statements by extremist groups about ambitions to build dirty bombs."

Edwin Lyman, director of nuclear power safety at the Union of Concerned Scientists in its Washington, DC, office, is less convinced of the danger. "I've been a dirty bomb skeptic for a long time. This concern was elevated in part to distract attention from the more serious issue of the potential for nuclear terrorism from the theft of materials that could be used in a nuclear bomb. Nonetheless, radiological materials can pose serious risks, and it is a worthwhile goal to seek safer substitutes where feasible."

Holgate, Iliopulos, and Lyman agree that the IAEA categorization could be improved. A source's risk is determined by the amount of radioactivity it emits within a given exposure duration. But that classification has limitations. The possibility of a terrorist stealing radioactive materials may have a low probability, for example, but the prospect's high socioeconomic consequences makes some radioactive sources, such as ^{137}Cs, more dangerous than the IAEA presumes.

The 2021 NASEM report calls for the IAEA and the US NRC to rethink materials categorization to include probabilistic health effects, such as increased long-term cancer risk, and the economic and social effects of a radiological dispersal event. Lyman approves of the recommendation but says it's challenging: "The problem with these hard-to-quantify threats is that you can't mobilize public opinion and policymakers unless something terrible happens."

Despite the challenge, Lyman says, "every vulnerable source that's replaced or removed and every gram of plutonium that's secured is incremental progress, and it builds up over the years."

Alex Lopatka PT

Improving science education: *It's not rocket science* IT'S HARDER!

Fernanda Urrutia of the Gemini Observatory in Chile works with children on an experiment with colored filters. The activity was developed by the University of California, Berkeley's Lawrence Hall of Science through its Great Explorations in Math and Science program. (Image courtesy of International Gemini Observatory/NOIRLab/NSF/AURA/M. Paredes.)

Stephen Pompea is an observatory scientist emeritus at NSF's NOIRLab in Tucson, Arizona, and a visiting professor at Leiden University in the Netherlands. **Pedro Russo** is an assistant professor at Leiden Observatory and in the department of science communication and society at Leiden University.

Stephen M. Pompea and Pedro Russo

Scientists can help by partnering with museums, out-of-school programs, schools, organizations that develop instructional materials, or other educational projects.

Our subtitle paraphrases a frequent statement from George "Pinky" Nelson, an astronomy researcher who spent 11 years as a NASA astronaut and flew on three space missions, including the first one after the *Challenger* accident. In the decades after his stint at NASA, he expanded his career and straddled the fields of science research, engineering, and science education—he served, among other roles, as a professor of physics at Western Washington University and as director of the American Association for the Advancement of Science's Project 2061, a long-term R&D initiative focused on improving science education. Nelson's informed perspective highlights the difficulty of enhancing the science education system.[1]

Efforts to improve science literacy and science education have faced many challenges in recent decades. In the US, for example, the No Child Left Behind Act of 2001 emphasized a high-stakes testing program that eroded teacher and school autonomy and thus weakened and stalled long overdue changes in science education practices. That trend may change as physicists increasingly recognize the importance and value of their own and their organizations' engagement in educational activities. By participating, they will gain personal satisfaction and strengthen their organizations' bonds to their communities. What's more, those activities can fulfill the "broader impacts" criteria required by NSF and other funders or can meet institutional obligations to disseminate knowledge of scientific methods and results.

In this article we highlight some trends that are encouraging physicists to join ongoing efforts to improve science teaching and learning worldwide. Although not new, those trends are again gaining attention and interest from scientists and their organizations. The efforts center on a broad systems-based approach that recognizes the complexity of the science education ecosystem. With a foundation of the best research-based pedagogies, physicists can step into partnership roles in schools, outside-of-school programs, international events, and other activities designed to improve science literacy.

Using best practices

Our knowledge of the challenges of educational transformation comes from decades of experience designing, implementing, and evaluating innovative science education projects. We have collaborated with new and experienced teachers, museum educators, educational researchers, and educational development teams to reach audiences from preschool children to older adults. We have also worked with diverse science, engineering, and education professional societies and with governments and nongovernmental organizations worldwide. In our work with scientists at national laboratories, universities, and industrial research facilities, we have learned many lessons on how we can be more effective in our educational efforts and have applied them to our work.

From our experience working in the education arena, we know that physicists have had the most success and enjoyment when they have been well prepared about their audience and its needs. Many scientists are unfamiliar with the best practices for teaching and learning at preschools, primary and secondary schools, afterschool clubs, and museums. Fortunately, high-quality free resources are available that summarize the extensive research on learning in diverse settings.[2]

To streamline the process for scientists who are getting involved for the first time or who want to increase their level of involvement, we recently completed a review of the research on best practices for supporting and interacting with the part of the science education ecosystem that encompasses preschool to high school learners.[3] Although our review is specific to astronomy, most of the suggestions apply to all fields of science and engineering education. We highlight throughout this article a few of those best practices most useful for scientists.

Starting young

Working with undergraduate and graduate students is easier and more familiar to many scientists than working with younger

students. Older students already have mathematical and scientific foundations to build on and have opted into science classes. Teaching them has been compared to shooting an arrow and then placing the target at the landing site just before the arrow hits. Hitting the bullseye is still satisfying but raises the question of how much influence a teacher has on an older student. Introducing science to children at younger ages is challenging but can greatly expand their science perspective during their highly formative and less predictable early development.

In the early 1960s, Jerome Bruner at Harvard University initiated many of the science education reform efforts of current importance. His focus was on early learning and a so-called spiral curriculum, wherein subjects are explored in more detail each year rather than being "saved" for a specific age range—for example, chemistry in 10th grade and physics in 11th grade. Bruner strongly believed that any science concept can be adapted for any age level. For the youngest students, actively engaging with science activities and demonstrations will be more effective than being given verbal or mathematical explanations, which may work for older students. Bruner pointed out that people learn to ride a bike by doing it, not by looking at a picture book or an instruction sheet.

Robert Karplus, in his mid-1960s work at the University of California, Berkeley's Lawrence Hall of Science, also offered a method to improve the elementary school science curriculum. He left his career in theoretical quantum electrodynamics research because he believed that working with younger learners would be as challenging and rewarding as his university research and teaching. Karplus developed and championed a learning-cycle model that has proven effective for learners of all ages. His cycle posited that learning happened in three phases—exploration, invention, and discovery—that could be cycled through repeatedly. His main legacy is the emphasis on hands-on experiences over textbook-centered learning. Karplus's learning-cycle model, which has been modified by many others since, reflects a deep understanding of the scientific investigation process and allows for rigorous student engagement in science exploration, learning, and applications.[4]

Elementary school teachers typically focus on imparting basic foundational skills in reading, writing, and mathematics. Although they understand the best teaching approaches, including those derived from Bruner and Karplus, applying their skills to teaching science is difficult because of pressure to concentrate on other subject areas. Many elementary school teachers also lack confidence in their knowledge of science topics and how to effectively integrate science and their core subjects.

Scientists can work with teachers to overcome those difficulties by engaging with such teacher–scientist partnerships as the NSF Graduate Fellows in K–12 Education and the Astronomical Society of the Pacific's Family ASTRO and Project ASTRO programs.[5] Scientists know the science, and teachers know how children learn. Both can gain from a deeper understanding of how younger students learn science. Guided by educators aware of students' science misconceptions and naive theories, a class can explore science concepts more successfully. And for scientists, working with elementary teachers is highly rewarding and constructive.

Roles in schools

Scientists have more to offer schools than classroom presentations and demonstrations in person or by video. Traditionally, scientists have taken on school roles based on their assessments of what a class or school lacks, often from their own childhood experiences or from short-term involvement in their child's school. A better approach is for scientists to work with teachers and find the best ways to address the most pressing classroom concerns. The scientists are then responsive to and respectful of the needs of the teaching professionals working every day in the educational arena.

Science teachers often express a need for more training in online teaching methods, access to high-quality interactive-learning materials, and more information about current science discoveries and techniques. They also are interested in having a scientist on call who can explain concepts and terms, help them find appropriate activities and demonstrations, and support and encourage them as part of their professional support system. Most elementary- and secondary-level science teachers say they have an inadequate educational background to effectively teach the physical sciences. That need for more professional preparation and support has been persistent for decades; from our perspective, it seems to become more acute every decade.

One way to meet teachers' needs is to become what's known as a science ambassador. In that role, scientists serve as a liaison between the science and education communities. They help teachers find educational materials and equipment and connect them to a university or research community. An ambassador must understand how the formal education system works: how educators are trained, what demands they deal with, and how students learn science concepts at each age level.[6] Professional societies, such as the American Astronomical Society, offer ambassador training at conferences.

Active science in the classroom

Scientists are often surprised to discover that many school science classes devote little or no time to students actually doing science. We, too, have found that it is increasingly rare for

FIGURE 1. COMPUTER-BASED TOOLS are available at the Teen Astronomy Café at the Vera C. Rubin Observatory in Tucson, Arizona. Students use them for analyzing large data sets. The café also offers science talks and informal discussions with graduate students and postdocs, and coffee and food are available. Because of the COVID-19 pandemic, the café is now freely available online at www.teenastronomycafe.org. (Image courtesy of NOIRLab/NSF/AURA.)

elementary-age learners to perform even simple physical science experiments, despite those activities' proven effectiveness in getting them excited about the subject.[7] Instead, classes at all levels often consist of learning science vocabulary, memorizing the scientific method, and reading or talking about science principles or laws or about scientists.

In effect, classes emphasize science preparation calisthenics at the expense of allowing students to play the science game. The result is science classes that are boring and pedantic, a detrimental combination. As Robert Yager, former head of both the National Association for Research in Science Teaching and the National Science Teaching Association, pointed out in a 1988 essay, doing science is immensely more interesting:

> Unfortunately, however, our students rarely get to play—rarely get to do real science, to investigate a problem that they have identified, to formulate possible explanations, to devise tests for individual explanations. Instead, school science means 13 years of learning the rules of the game, practicing verification-type labs, learning the accepted explanations developed by others, and the special vocabulary and the procedures others have devised and used.[8]

In our experience, gifted students are often the ones most frustrated by not having a chance to participate in science questioning and exploring. One highly gifted student we know almost dropped out of junior high school after being labeled by his science teacher as difficult and disruptive. What had he done? He had challenged the teacher by asking for evidence that Earth goes around the Sun. Scientists welcome and applaud such questions and challenges rather than being threatened by them. That student is now a distinguished engineer at IBM. Science participation, not dogmatic memorization, powers science enthusiasm.

Free-choice education

When choosing science education roles, physicists often gravitate toward schools and classrooms. But other opportunities are available in afterschool and out-of-school programs. Those informal, free-choice settings include afterschool clubs, natural history and science museums, planetariums, libraries, hands-on science and technology centers, and visitor centers at research facilities. Other options are street fairs, county and tribal fairs, community events, summer camps, science cafés, science festivals, talks in restaurants and pubs, and any other place that gathers a potentially science-interested audience.[9]

Examples of the many available activities for scientists at those venues include helping design a museum exhibit, creating a science program for a children's discovery center, and giving a talk at a local library.[10] Scientists are especially effective in informal settings, such as pub and restaurant science nights, teen science cafés, and science festivals, when they encourage their audience to actively participate.[11] (See figures 1 and 2 for examples of two such events.)

Making a talk shorter and less formal and leaving significant time for discussion, debate, and wide-ranging questions can improve audience interest, engagement, and satisfaction. Similar to other fields, the informal education field has a strong research basis behind its pedagogy. It is specialized and sophisticated, and it offers diverse and expanding roles for informal education professionals.[12]

Building science capital

Many innovative science education programs are built on a concept called science capital, a term from the 2013 influential UK science education policy report *ASPIRES: Young People's Science and Career Aspirations, Age 10–14*. Science capital refers to the sum of all science-related knowledge, attitudes, experiences, and resources that individuals build up, including the science they know and learn, what they think about science, and their daily engagement with science and science-interested people. A capital-based perspective of the educational ecosystem encourages partnerships that offer children the opportunity to learn about STEM (science, technology, engineering, and math) in school and other settings and that encourage systemic change to create a support system for learners.[13]

Creative approaches to reach or serve new communities have been successfully implemented worldwide, often with scientists as key team members. For example, scientists have contributed to programs that encourage design and visual thinking in science. Such programs—called STEAM for their combination of the STEM fields and art—can inspire children with artistic interests and visual thinking skills to pursue science and technology-related careers.

Laura Carsten Conner, an associate professor of science education at the University of Alaska Fairbanks, and her collaborators have studied how girls view science and the value of art–science connections in building their science identities. Her research formed the basis of the programs Colors of Nature and Fostering STEAM, which combine art and science and were developed by a team of physical and biological scientists, visual artists, informal science educators, and educational researchers. The programs include science cafés that host interactive events with scientists, training for education professionals on integrating art and science into lessons about nature's colors, and two-week summer academies for girls to explore color with scientific tools such as spectrometers and light and scanning electron microscopes (see figure 3).

Carsten Conner's projects have demonstrated the importance and value of building science capital as a core approach to innovative science education. Art–science connections can reach new audiences and offer an encouraging environment for students to start building up that capital.[14]

International and global programs

Many scientists have told us that singular experiences, such as looking through a kaleidoscope, seeing the Moon magnified, observing with an IR camera, playing with a gravity well, or watching the magnetic levitation of a superconductor, were life-altering events. Many want to know how they can share those powerful experiences.

One way scientists have connected with others has been by taking part in ambitious worldwide educational projects, many centered around United Nations–initiated international years that publicize a particular science or the anniversary of an important scientific event. Some examples are the International Year of Astronomy 2009 (IYA2009) to celebrate the 400th anniversary of Galileo Galilei using his astronomical telescope; the International Year of Light and Light-Based Technologies 2015 (IYL2015); the 100th anniversary of the International Astronomical Union (IAU100), which took place in 2019; and the International Year of Sound 2020–2021 (see the December 2020 issue of PHYSICS TODAY). Those international-year designations are ubiquitous and can motivate scientists to create projects that reach new audiences. Although the time-limited and somewhat ad hoc nature of the events could be a detriment, in practice the novelty and urgency inspire ambitious new ideas and approaches.

International projects are largely led by scientist volunteers who rely on the sponsoring organizations to encourage the participation of their scientist members. For example, the IYL2015 team comprised scientists and engineers from the Optical Society, SPIE, the American Physical Society, the European Physical Society, and other partners outside the US.

To succeed educationally, an international-year program needs strong leadership and planning. Securing the official worldwide designations often requires three to five years of advance planning. Each project in the program will be more successful if it has a bold, focused goal and a diverse team of scientists and educators to plan and implement it.

For example, for the well-received IAU100, led by Ewine van Dishoeck of Leiden University, scientists partnered with educators to create many worldwide education projects. One of them, the Einstein Schools Programme, offered online resources for students to learn about the varied effects of gravity and was adopted by more than 200 schools worldwide (see figure 4).

FIGURE 2. COMMUNITY-BASED educational events such as Astronomy Day or National Astronomy Week are effective ways to bring science activities to wide audiences. During this 2019 activity at the Prince Kuhio Plaza shopping mall in Hilo, Hawaii, a staff member from the Gemini Observatory investigates colored filters with a student. At the annual event, the observatory connects to the community and learns more about its educational needs. (Image courtesy of International Gemini Observatory/NOIRLab/NSF/AURA/J. Pollard.)

Another particularly successful set of projects[15] was developed for IYA2009. From Earth to the Universe created exhibitions of astronomical images from various telescopes that were translated into 40 languages and used in 70 countries and a thousand locations, including parks, libraries, subway stations, and airports. Overall, 10 million people saw them. The Galileo Teacher Training Program, which was initiated with volunteer help in 75 countries, created the largest international network for astronomy teacher training workshops.

Also a product of IYA2009, the Galileoscope student telescope kit[16] was created by three US scientists supported by a team of individuals and organizations, including the American Astronomical Society. The team lamented the lack of high-quality but inexpensive telescopes for kids and decided to fix the problem. With some institutional support and partnering but no initial funding, they designed, manufactured, and distributed a quarter of a million new high-quality telescope kits with accompanying educational materials to 110 countries. The Galileoscope is still in production, and its educational materials are free and widely available.

In our experience, scientists bring great value to such projects because of their willingness to share their intense passion about science.

Scientist–educator hybrids

As scientist–educator hybrids ourselves, we've noticed that more scientists each year are choosing to pursue and integrate both roles into their careers. The share that each person gives each role varies with their interests, skills, and career stage. Many scientists have gone beyond educational volunteering and have become full-time education and community engagement professionals. Others enjoy helping, designing, or implementing new programs as part of education and community engagement teams with the support of their university, research lab, medical center, or company.

Scientists on educational development teams fill an important and perhaps unique role by modeling educational materials and projects after the process of scientific investigation. For example, in 1992 Craig Blurton of the NASA Classroom of the Future in West Virginia directed and supervised many bleeding-edge educational software projects in the fields of astronomy, planetary science, biology, and environmental science. He brought scientists from across the country who shared a passion for both research and education to work with his educational researchers and multimedia developers. Together they created realistic and immersive simulations that allowed students to do science as part of teams exploring cutting-edge science problems.

Among the results were the computer programs *Astronomy Village: Investigating the Universe*, geared to high school students and supported by NASA, and *Astronomy Village: Investigating the Solar System*, geared to middle school students and supported by NSF. The educational packages won many awards, including Best Microcomputer Software of the Year from *Technology and Learning* magazine. Students at the virtual Astronomy Village, shown in figure 5, work in teams on research projects with simulated instruments, space probes, and ground-based telescopes. They do laboratory and thought

FIGURE 3. ART-INCLINED STUDENTS at the Colors of Nature program use microscopes, cameras, and spectrometers to learn about fluorescence, animal vision, polarization, the spectral properties of pigments, light interference, and structural color. The program, which supports students, families, and educators interested in exploring the connections between art and science, hosted multiple summer academies for girls in Tucson, Arizona (shown here), and Fairbanks, Alaska. (Image courtesy of NOIRLab/NSF/AURA/S. Pompea.)

FIGURE 4. KIP THORNE (center) in 2019 meets the student team from Chile's University of La Serena and its NOIRLab project leaders who performed observations at the Cerro Tololo Inter-American Observatory during that July's total solar eclipse. The measurements re-created the famous century-old results that confirmed the bending of light predicted by general relativity. The project was part of the Einstein Schools Programme for the 100th anniversary of the International Astronomical Union, which facilitated creative projects worldwide for students to explore the role of gravity in astronomy. (Image courtesy of NOIRLab/CTIO/NSF/AURA/P. Marenfeld.)

experiments and use image processing to analyze real images and data from NASA, NSF, and NOAA. At the end they announce their results at a mock press conference and answer probing questions.

Those two programs capture the essence of collaborative science research and immerse students in authentic, cutting-edge topics, such as extrasolar planets, Earth-crossing objects, the search for life in our solar system, and supernovae searches. The packages were also among the first instructional materials for secondary school students that used the internet (Netscape 2.0 for the first Astronomy Village program!), email messages, and sophisticated image processing.

Another group of scientists and educators was led by astronomer Isabel Hawkins, who was director of the Center for Science Education at the Space Sciences Laboratory, University of California, Berkeley, from 1997 to 2008. They developed innovative instructional materials for the Great Explorations in Math and Science project. Their resulting nationally tested astronomy teacher guides draw from research-based teaching methods, including those of Karplus, and are easy to use even for teachers with limited math or science backgrounds.

Many hybrid scientist–educator teams have developed high-quality instructional materials that capture the essence of scientific exploration. Physicists interested in creating instructional materials can join similar development teams that have a track record of addressing the current needs of teachers and students.

Taking a long-term perspective

Physicists can appreciate the impact of forces acting over long periods of time. Addressing the persistent and seemingly intractable problems in the science education ecosystem requires an enduring effort and continued systemic change. Despite many notable educational achievements and innovations, in our opinion overall progress in science education has been erratic in the US and most other countries.

The quality of science education at all levels still varies widely. The fragmentation of US cities into multiple school districts and public, charter, and private schools all but guarantees inequities in resources, teaching, and learning. For most students, their postal address or ZIP code remains the best predictor of the short- and long-term educational achievements available to them.

Teachers lack access to high-quality instructional materials and training on how to use them. Labs for active learning and computer-based activities often fall into disrepair and disuse. Successful professional development programs for science teachers fade over time because of a lack of funding. New programs and organizations work to address those issues but make only small dents before they lose momentum or funding.

Research organizations that want to help improve education often end up collaborating with their local advantaged suburban schools rather than with needier schools that would benefit more from a partnership. Scientists and organizations can also fall into the trap of choosing projects that make them look good rather than have more educational merit. The more difficult task of establishing educational partnerships with di-

FIGURE 5. COMPUTER PROGRAMS let students simulate research in the planetary sciences with data from ground and space-based telescopes and interplanetary probes. In *Astronomy Village: Investigating the Solar System*, middle school students explore possible habitats for life throughout the solar system. They navigate from the home screen (left) to a simulated telescope with control panel (right), a virtual lab with instructions for on- and off-computer experiments, a simulated press conference where students answer probing questions, and more. The program uses research-based pedagogy merged with the typical research process, which includes ill-defined science problems that have no obvious right answers. (Image courtesy of NSF/Classroom of the Future, Wheeling Jesuit University.)

verse communities is replaced with the simpler short-term task that can generate good publicity.

The formal and informal science education systems need longer-term commitments from scientists and their organizations. In turn, those organizations must value, reward, and support the efforts of individual scientists. Neglected communities also require additional exploration, dialog, and time to develop an authentic partnership with a research organization and have their needs understood.

Next steps

Many scientists want to help improve the science education ecosystem. But buying magnets for a teacher is easy; training a new group of teachers each year about magnetism is much harder. The easy fixes have a limited effect. If you want to get involved, you will first need additional knowledge and experience to effectively improve science education locally, regionally, nationally, or internationally.

The investment that you make to understand the needs of your local community's educational system will provide a large return for you and the community. Partnering with educational institutions to pursue productive and efficient action together is also critical to help you avoid the frustration that occurs when you work in isolation.

So how can you start? Talk with a teacher or a youth club leader in an economically challenged area near you and partner with them long-term to meet their needs. Encourage your organization to devote its resources to address the broader needs of students and educators in struggling local communities. Answer this summons to service, and work together.

REFERENCES

1. "Former Astronaut George 'Pinky' Nelson Champions Science Literacy," e-interview, Education World (accessed 5 August 2021).
2. National Research Council, *How People Learn: Brain, Mind, Experience, and School: Expanded Edition*, National Academy Press (2000).
3. S. M. Pompea, P. Russo, *Annu. Rev. Astron. Astrophys.* **58**, 313 (2020).
4. J. M. Atkin, R. Karplus, *Sci. Teach.* **29**(5), 45 (1962).
5. J. A. Ufnar, M. Bolger, V. L. Shepherd, *J. High. Educ. Outreach Engagem.* **21**(3), 69 (2017); M. Bennett, A. Fraknoi, J. Richter, *Int. Astron. Union Colloq.* **162**, 249 (1998).
6. R. Driver et al., *Making Sense of Secondary Science: Research into Children's Ideas*, Routledge (2014).
7. National Academies of Sciences, Engineering, and Medicine, *How People Learn II: Learners, Contexts, and Cultures*, National Academies Press (2018).
8. R. E. Yager, *Sci. Teach.* **55**, 77 (1988).
9. National Research Council, *Surrounded by Science: Learning Science in Informal Environments*, National Academies Press (2010).
10. M. Storksdieck, C. Stylinski, D. Bailey, "Typology for Public Engagement with Science: A Conceptual Framework—Working Paper 2," Center for Research on Lifelong STEM Learning (2016).
11. E. L. Rice, B. W. Levine, *CAPjournal* **21**, 13 (December 2016); M. A. Mayhew, M. K. Hall, *Sci. Commun.* **34**, 546 (2012); B. Wiehe, *J. Sci. Commun.* **13**(4), C02 (2014).
12. K. Morrissey, J. E. Heimlich, D. Schatz, *Mus. Manag. Curatorsh.* (2020), doi:10.1080/09647775.2020.1803109.
13. D. Schatz, L. D. Dierking, *J. Mus. Educ.* **23**(2), 22 (1998).
14. L. D. Carsten Conner et al., *Connect. Sci. Learn.* **1** (October–December 2019).
15. P. Russo, C. Cesarsky, L. L. Christensen, *Proc. Int. Astron. Union* **5**, 559 (2009).
16. S. M. Pompea et al., *Proc. SPIE* **7738**, 773803 (2010). PT

Image courtesy of Hiroshi Moriya, MD, PhD, Ohara General Hospital, Japan.

Computed tomography turns 50

John M. Boone and
Cynthia H. McCollough

Modern high-performance CT scanners are unparalleled among three-dimensional imaging systems in data acquisition speed and spatial resolution.

John Boone is a professor of radiology and biomedical engineering at the University of California, Davis. **Cynthia McCollough** is the Brooks-Hollern Professor and a professor of medical physics and biomedical engineering at the Mayo Clinic in Rochester, Minnesota.

Computed tomography (CT) uses thousands of x-ray transmission measurements taken at different angles around a patient to produce three-dimensional cross-sectional images of the human body. That technology allows physicians to visualize their patients' internal anatomy, as shown in the opening image, and reveals the presence of acute and chronic diseases and the consequences of injury in remarkable detail. Prior to the integration of CT into clinical radiology, physicians relied on exploratory surgery to diagnose many serious patient symptoms. Thankfully, that's now a relic of the past.

CT had a curious birth. The Central Research Laboratories of the British music company EMI were well known for their development of stereophonic sound, broadcast television devices, and radar. Yet in the late 1960s, with financial support from the UK's Department of Health and Social Security, radar-operator-turned-electrical-engineer Godfrey Hounsfield developed the first x-ray CT scanner (see reference 1 and box 1). On 1 October 1971, radiologist James Ambrose performed the first patient CT scan[2] at Atkinson Morley Hospital in the UK.

Since that first clinical use, CT has grown ever more sophisticated and versatile. The early years of CT scanner advancements coincided with other technological developments. Those include improvements to precision machining, advanced bearing systems, solid-state x-ray detectors, lasers, semiconductor integration, and composite materials—all of which enabled faster and more precise CT hardware performance. Computers also continued to get faster, and more sophisticated computer algorithms led to improved image quality, which dramatically expanded the commercial CT market. The fields in which CT has been applied are remarkably diverse. Box 2 describes a few beyond the field of medicine.

More than 90 million medical CT examinations are now performed each year in the US. The pervasiveness reflects the value of the information that CT provides for both medical diagnosis and treatment planning. The large number is driven by physicians on the front lines of medicine, who order the exams, and not by radiologists, who interpret the CT scans prescribed by their referring physician colleagues.

CT imaging requires some 10^6–10^9 x-ray transmission measurements taken around the patient and at positions along the long (z) axis of the body for each reconstructed image. During data acquisition, an x-ray tube generates a relatively uniform beam of x rays with an incident number of photons S_0. The beam is collimated along the z-axis such that only a cross section of the patient is exposed. The x rays are exponentially attenuated by the patient's body and a smaller number of photons S is detected in each element of the detector array. Thus, in a known geometry, $S = S_0\, e^{-\mu t}$, where t is the thickness of the patient's tissues and μ is the sum of their linear attenuation coefficients along that beam trajectory. Those CT measurements are then transformed to projection values according to

$$P = \mu t = \ln\left\{\frac{S_o}{S_o e^{-\mu t}}\right\}. \quad (1)$$

The equation assumes a single x-ray energy. But the beam is actually polyenergetic; hence μ is considered an effective linear attenuation coefficient. The projection values P are the data that are used to reconstruct the CT images, and the logarithm linearizes P with respect to μ. That means the grayscale values in the image are physically dependent on μ. It also implies that the grayscale values in the CT images are not affected by the

BOX 1. COMPUTED TOMOGRAPHY AND THE NOBEL PRIZE

CT inventors Godfrey Hounsfield and Allan Cormack were awarded the Nobel Prize in Physiology or Medicine in 1979. That's an interesting distinction, given that neither researcher was a physiologist or physician. (Both were physical scientists—an engineer and physicist, respectively; for their Nobel lectures, see reference 12.) A South African physicist who worked in the US at the time the prize was awarded, Cormack investigated the mathematical principles[13,14] of tomographic imaging using a cobalt-60 radiation source in the early 1960s.

Working independently in the UK, Hounsfield developed CT hardware using an x-ray tube between 1967 and 1971. His scanner was used to make the first CT images in patients. An affable man, he became a celebrity in the radiology world, recognized as the humble engineer who changed the worldwide practice of medicine forever. The early CT community named the grayscale values in CT images "Hounsfield units" in his honor.

BOX 2. BIG AND SMALL SYSTEMS

Computed tomography (CT) systems extend far beyond medical applications, from small-specimen imaging systems to huge devices designed for nondestructive testing. At the small end of the spectrum, CT systems can produce images of tiny specimens, from gemstones to fruit flies, at pixel dimensions below 20 nm. At the other extreme, in 2009 government engineers constructed a CT scanner able to evaluate the structure of nuclear warheads, and an aerospace company built a two-story-tall system to scan aerospace components such as rocket assemblies and turbine blades for imperfections.

In more familiar applications, CT scanners are used at airports for scanning the interiors of checked bags. Most specimen and industrial scanners rotate the specimen, rather than the x-ray tube and detector array. That imaging geometry greatly simplifies the mechanical design of the system. For human scanning, however, the x-ray tube and detector array, not the patient, are rotated.

entrance exposure levels S_0. Thus, unlike in film-based radiography, images are never over- or underexposed.

Medical CT imaging uses x-ray energies of about 30 to 150 keV. At those photon energies, Compton scattering dominates x-ray interactions in tissue. Compton scattering depends on electron density ρ_e as

$$\rho_e \approx \rho\, N_0 \frac{Z}{A}, \qquad (2)$$

where ρ is the mass density, N_0 is Avogadro's number, Z is the atomic number, and A the atomic mass number. It turns out that Z/A is the same (½) for the prevalent elements—carbon, oxygen, and nitrogen—that compose soft tissue. Hence, the CT image primarily shows a map of mass density, with some Z dependence due to the photoelectric x-ray interaction, which is more pronounced for higher Z elements, including bone (calcium), metal implants (titanium, tantalum, steel), and injected contrast agents (iodine).

Panel a of figure 1 illustrates the mechanical designs of an early CT system, in which overcoming the physics of inertia was a major challenge. The first scanner used an x-ray tube and an x-ray detector mounted opposite each other on a rigid but movable gantry—the framework into which the patient's head was placed. The first-generation, translate–rotate design mechanism was fundamentally limited by the large mass of the lead-shielded gantry, which had to accelerate and then decelerate for each projection measurement. Eighty measurements were acquired during translation of the x-ray tube and detector from one side of the patient to the other, after which the gantry rotated 1°. The tube and detector were then translated across the patient again and the gantry rotated another 1°. That was repeated until the gantry had rotated a total of 180°; the process acquired a total of 14 400 transmission measurements in about 4.5 minutes.

The transmission data were used to produce an 80 pixel × 80 pixel image representing the scanned cross section of the patient via a process known as image reconstruction. The image thickness was determined by the width—either 8 or 13 mm—of the collimated x-ray beam. To image a greater length of the body, the technologist repeated the entire process, one cross section at a time. A complete brain scan consisted of only six images, the acquisition of which took about 30 minutes, during

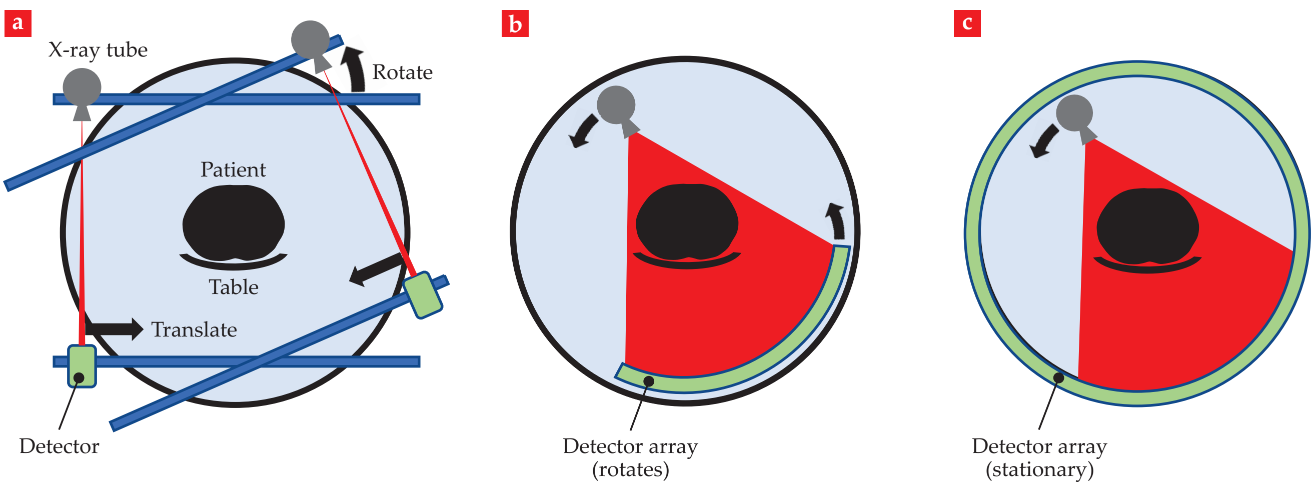

FIGURE 1. COMPUTED TOMOGRAPHY (CT) has evolved considerably since 1971. **(a)** In the translate–rotate geometry, the x-ray tube and detector were mounted opposite one another, with the patient's head placed between them. The tube and detector together translated across the width of the patient's head in one direction, after which the frame on which they were secured rotated by 1°; the tube and detector were then translated back across the patient's head in the other direction. Those processes were repeated until the device had rotated 180° around the patient. **(b)** In the rotate–rotate geometry, an array of detectors sits opposite an x-ray tube that emits a fan-shaped beam. Both the tube and the detectors rotate synchronously around the patient to acquire data. Producing significantly shorter scan times, the geometry is used in all commercial CT scanners today. **(c)** In the rotate–stationary geometry, the detector was a stationary, ring-shaped array and the fan-shaped x-ray beam rotated around the patient within the detector array. The expensive detector array, less dose-efficient geometry, and limited ability to block scattered radiation led to abandonment of this geometry. (Courtesy of John Boone/University of California, Davis.)

which the patient needed to hold perfectly still. Such long acquisition times initially limited the procedure to imaging of the head, because it could be immobilized.

Despite the long acquisition times, images from the first CT scanners created tremendous excitement among radiologists and other physicians, and their feedback encouraged corporations to invest heavily in the technology's development. Next-generation scanners incorporated a somewhat wider x-ray beam but used fundamentally the same acquisition process. Third-generation scanners, shown in panel b of figure 1, incorporated a curved detector array with an angular coverage of about 60°. The x-ray tube was mounted in a fixed position opposite the detector array, and together they rotated around the patient. That arrangement dramatically reduced acquisition times.

After one rotation's worth of data collection, either using a translate–rotate or rotate–rotate mechanism, the gantry's rotation was braked to prevent severing the cables that connected the gantry to the stationary frame. In the early 1990s, slip-ring technology was introduced to conduct power and signal to the rotating gantry, eliminating the need to stop gantry rotation and rewind the cables. The slip ring did more than allow the gantry to rotate continuously; it also allowed for helical, or spiral, scanning. In contrast to the sequential acquisition of data for one cross section of the body at a time—during which the patient table was stationary for x-ray exposure—in helical scanning the patient is moved through the rotating gantry while transmission measurements are taken. The result is a helical trajectory of the x-ray source around the patient, which completely eliminated the inertial constraints during the entire patient scan.

As scan times decreased, x-ray tubes needed to produce the same number of photons in a shorter time. The introduction of helical CT thus led to improvements in x-ray tube design to achieve the higher x-ray production rates. But the fundamental physics of heat conduction in the tube's vacuum environment remained a limitation. In the late 1990s, innovations in detector design helped to address limitations in tube power. Instead of using just one array of detectors, which covered only 10 mm along the patient, researchers developed scanners with multiple detector arrays along the z-axis. In 1999, scanners with sixteen 1.25 mm detector arrays became available, although only four data channels were available at first. Current systems exist with up to 320 detector arrays and data channels. With that expansion came an increase in the collimated x-ray beam width—from 10 mm to 160 mm. The 16-fold increase in solid angle allowed the x rays produced by the tube to be used 16 times more efficiently.

Having a greater number of thinner detector arrays also improved the spatial resolution along the z-axis of the patient. That resolution, about 5–10 mm using the outdated single-detector array systems of the 1970s through the 1990s, is now 0.5 mm or less. With that improvement, scanners could routinely make coronal and sagittal CT images, allowing physicians to visualize 3D data in 2D planes along the z-axis, as shown in figure 2. CT imaging is no longer referred to as a CAT scan, because it is no longer limited to the axial plane (the "A" stood for axial). Since the addition of helical scanning and multiple detector arrays, gantry rotation speeds have reached 240 rotations per minute. Acquisition times have gone from 4.5 minutes for one cross-sectional image in 1971 to about 5 seconds for an entire scan of the chest, abdomen, and pelvis, which can comprise over 500 images, each representing a 1 mm cross section of the patient. Thus, over 50 years, the scan time per image has decreased by a factor of more than 25 000.

From projection data to images

Figure 3 illustrates how projection data $P(x, \theta)$ can be used to reconstruct the CT image, a process called filtered back projection. The projection data are recorded in terms of distance along the detector array x and angular position around the patient θ, and those data are mathematically projected backward onto a digital matrix $I(x, y)$ using simple trigonometry. The process adds the projection value P to each pixel in the matrix along the path where $P(x, \theta)$ was acquired. As that procedure is repeated for all the data, the values of P reinforce each other at the location of more attenuating objects and build up a cross-sectional picture of the patient's anatomy.[3] Although this description is conceptually accurate, modern CT scanners use a diverging beam, whose x rays spread out in a fan. That geometry requires that data be rebinned onto a Cartesian coordinate system prior to back projection. A mathematical filtering process is also applied to the projection data prior to back projection.

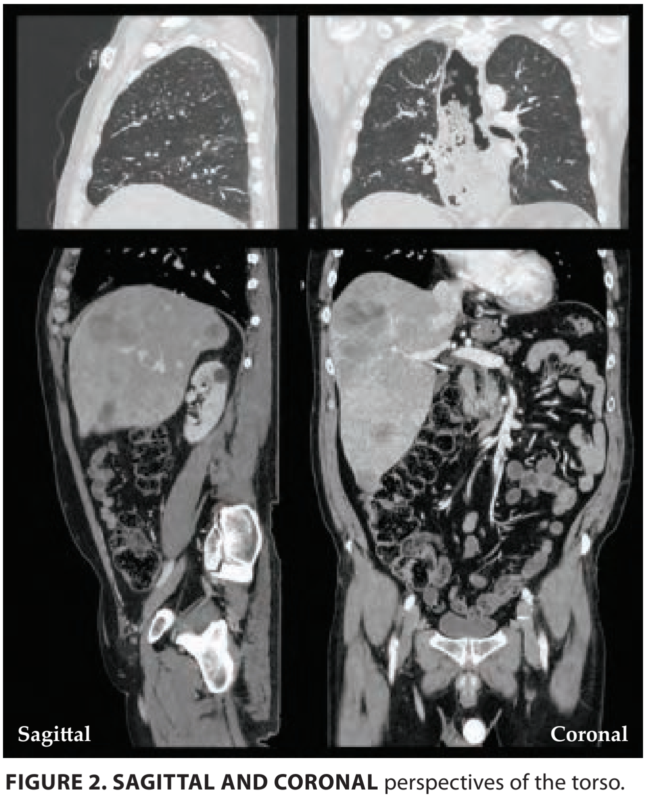

FIGURE 2. SAGITTAL AND CORONAL perspectives of the torso. Images of the thorax (top) and abdomen and pelvis (bottom) demonstrate the remarkable clarity with which computed tomography (CT) imaging can depict human anatomy. Excellent contrast between air, tissue, and bone makes CT scans of the lung essential for diagnosing many pulmonary disorders. A vascular contrast agent containing high-atomic-number iodine can be injected to enhance the contrast of soft tissues in the abdomen and pelvis and make blood vessels and cardiac chambers visible. (Courtesy of Canon Medical Systems, USA.)

A modern CT scanner may use 1000 angular projections θ and 1000 measurement x from each detector array for each of n detector arrays along the z-axis (with n ranging from 16 to 320). With multiple detector arrays, a CT scan can collect projection data at each angle and z-axis position, $P(x, \theta, z)$, such that the reconstructed images form a 3D data set, $I(x, y, z)$. As shown in figure 4, axial images $I(x, y)$ display the 3D data at a specific z location, coronal images $I(x, z)$ display the 3D data at a specific y location, and sagittal images $I(y, z)$ display the 3D data at a specific x location. The data can also be displayed using volume-rendering techniques.

Because of the increasing power of computers over the years, iterative reconstruction (IR) methods are now routinely available. They go beyond filtered back projection to include statistical considerations and a physical model of the CT system to produce images with lower statistical noise. And by reducing image noise during the reconstruction process, physicians can use lower radiation doses. But even with powerful computers, IR methods can still require minutes-to-hours of reconstruction time. That's unacceptable in a busy radiology department where patients may need immediate attention. Artificial intelligence techniques known as convolutional neural networks (CNNs) have recently become available and in many cases are replacing IR approaches. They are considerably faster to perform and can produce images with better spatial resolution and lower noise levels.

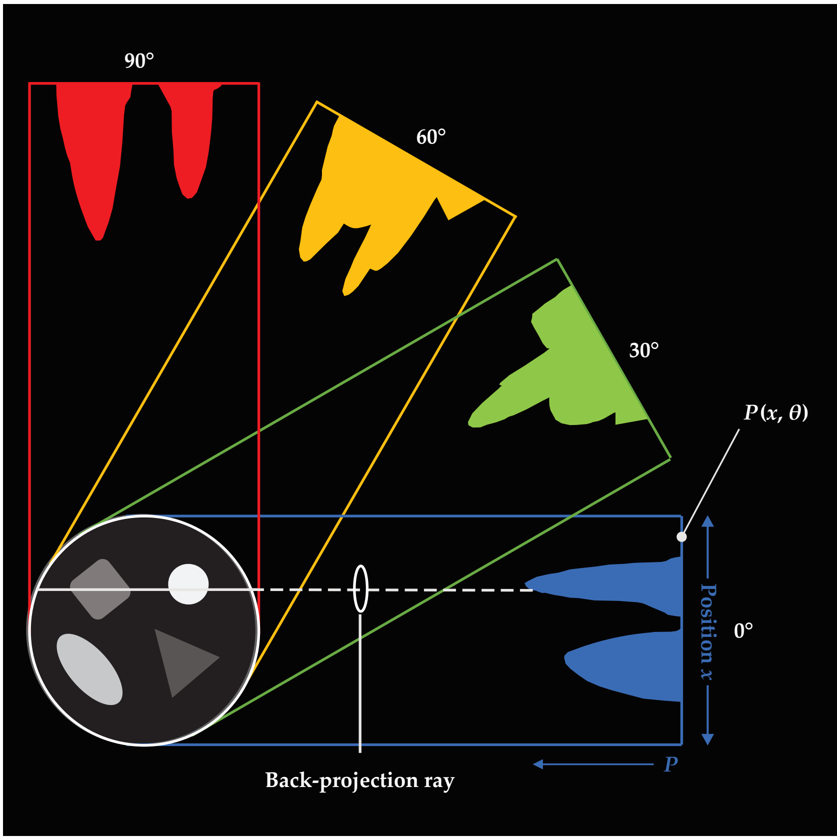

FIGURE 3. FILTERED BACK-PROJECTION RECONSTRUCTION. These projection data represent the total x-ray attenuation of an object along a path between the x-ray source and detector. To reconstruct the computed tomography (CT) image, the data are back projected along the direction in which they were acquired. The process uniformly distributes the measured attenuation along the line between the x-ray source and detector. The image shows four data sets at four different projection angles θ, but clinical systems typically acquire about a thousand angular projections, each comprising about a thousand individual data points along the width of the detector. After all the data are back projected, a cross-sectional representation of the scanned object emerges. The projection data sets are mathematically filtered prior to back projection to overcome the blurring inherent in that process. (Courtesy of John Boone/University of California, Davis.)

Quantitative imaging

Unlike other imaging modalities in a radiology department, CT scanners produce quantitatively meaningful grayscale images, in which the pixel values are related to μ, the linear attenuation coefficient of the imaged material. CT numbers are defined in terms of Hounsfield units (HU), in honor of the inventor of the first clinical CT scanner,

$$\mathrm{HU}_v = 1000\left\{\frac{\mu_v - \mu_\mathrm{w}}{\mu_\mathrm{w}}\right\}. \tag{3}$$

HU_v is the HU value of a given voxel v, μ_v is the linear attenuation coefficient of that voxel as determined by the CT reconstruction process, and μ_w is the linear attenuation coefficient of water. When a voxel contains only water, the CT number equals 0 HU, and when a voxel contains only air, it equals −1000 HU. The quantitative nature of the grayscale in CT images assists in making a correct medical diagnosis. For example, lesions in the lung tend to be benign when they are calcified, an effect that increases the CT number relative to cancerous lesions. Hence, lung nodules with very high CT numbers are typically benign. Other examples include the measurement of bone mineral density, which is broadly used as a predictor of fracture risk, and blood perfusion measurements, which can reveal reductions in blood flow to organs such as the brain and heart.

The physical dimensions measured in CT data sets are also quantitatively accurate. That's a result of the well-defined geometry required in CT, in which all transmission measurements are made along straight lines between the x-ray source and detector elements. Because of that geometry, radiation-based cancer treatments can be accurately planned and performed; biopsy needles can be accurately positioned; and linear, areal, and volumetric measurements can be accurately made. For example, the correct size for a stent to be placed in a patient's artery can be determined by the measurement of the diameter of the artery on the CT image. The volume of a tumor can be assessed by outlining its 3D boundaries, and a patient's response to radiation or drug therapy can be deduced by measuring changes in tumor volume over time.

Radiation levels

Imaging with CT provides an amazing look into a patient's body and can provide lifesaving diagnostic information, but it also involves exposing patients to ionizing radiation, which at high doses is known to produce alterations in DNA that can potentially lead to the development of cancer. Although the relatively low radiation dose levels used in CT can be assessed ac-

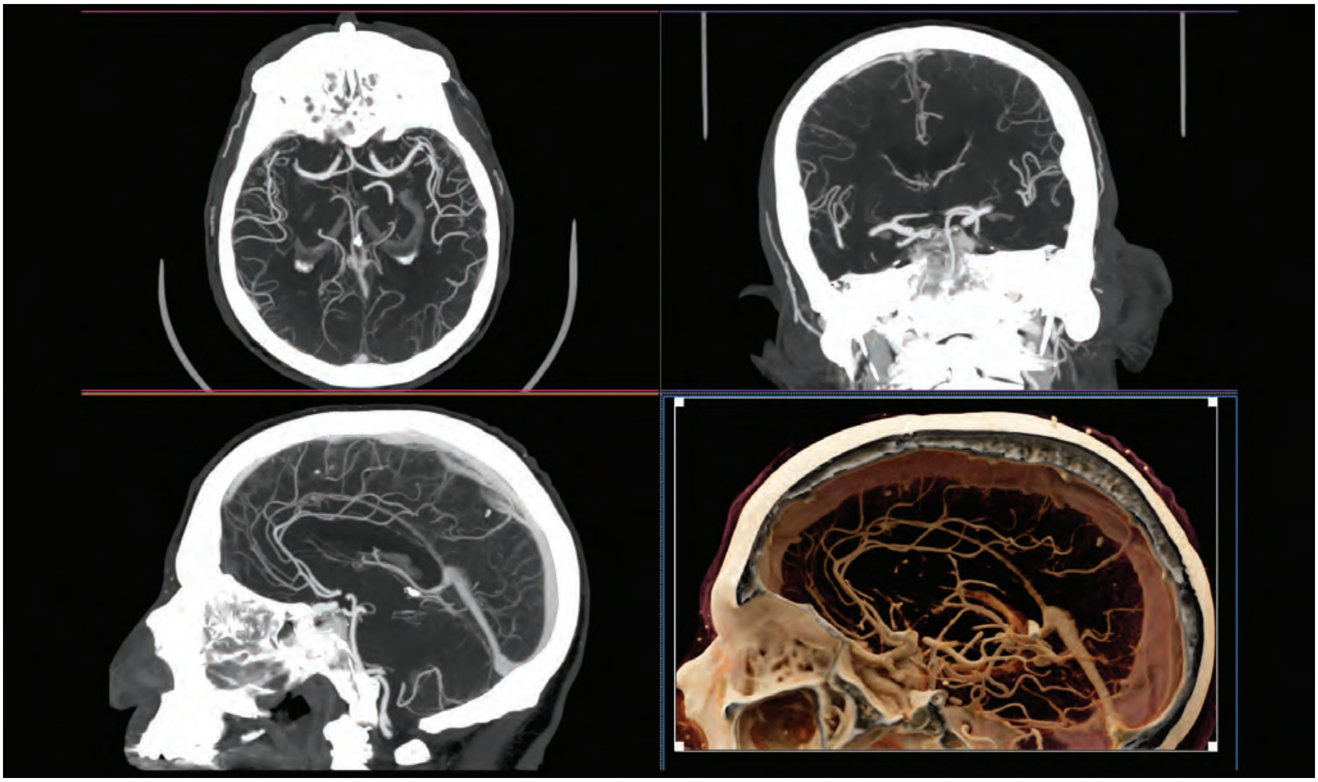

FIGURE 4. BLOOD VESSELS in the brain. Once referred to as CAT (computed axial tomography) scanners because the data were acquired and reconstructed in the axial plane, modern CT systems have submillimeter detector pixels along the *z*-axis of the patient. Those pixels enable high-resolution volumetric data acquisition and reconstruction. The three-dimensional data can be viewed as 2D images using axial (top left), coronal (top right), sagittal (bottom left), and volume-rendering techniques (bottom right). (Courtesy of Cynthia McCollough/Mayo Clinic.)

curately, the resulting risks are difficult to quantify. That's because radiation is a relatively weak carcinogen. Hence, epidemiological studies of individuals exposed to the low radiation doses are difficult to perform. They also vary in their conclusions because of numerous uncertainties and different model assumptions; some studies demonstrate a small health benefit, some show no effect, and some exhibit a small health detriment.

What's more, the effect of a known radiation dose depends upon many factors, including the distribution of dose to different tissues and organs; the timing of repeated exposures; and the patient's age, sex, race, genetics, and health status, all of which influence the radiobiological impact of an x-ray exposure.[4] For example, because children's cells are more actively reproducing than the cells of an adult, most organs and tissues of a child would have a higher risk of negative health effects than those of an adult exposed to the same amount of radiation. Fortunately, lower doses of radiation are needed to obtain diagnostic-quality CT images in children, because of their smaller size.

Despite the difficulty in predicting a patient's exact risk from a CT scan, the amount of radiation used for medical imaging is known to increase a person's risk of getting cancer by only a small amount compared with the baseline risk of developing cancer. For example, out of 1000 people, about 400 will develop cancer sometime in their lifetime. In contrast, of 1000 patients who receive a CT scan of their chest, abdomen, and pelvis, only one of them might develop cancer from the scan. That same CT scan, however, can provide information critical to the medical care of a patient who is ill or injured. In almost all situations where a physician recommends a CT exam, the potential benefit to the patient far outweighs any potential risk.

Still, radiation can be scary for some patients, and details of scientific studies and statistics can be hard to explain. One helpful approach is to describe potential risks in terms of effective dose.[3] For example, the effective dose from naturally occurring radiation sources, such as radon gas or cosmic rays, in Denver, Colorado, is about 5.2 mSv/year, whereas in San Francisco, it is 3.1 mSv/year. Moving to Denver from San Francisco therefore increases a person's background radiation exposure by about 2 mSv/year—the equivalent of one head CT scan per year. No one is likely to worry about an increased radiation dose of 2 mSv/year when considering a move to Denver, yet some patients hesitate when they are advised to get even one CT scan. That type of comparison may help patients and their families put the small amount of radiation from a CT scan into perspective. Even when a CT scan is negative, or normal, it can provide physicians with important information about where to turn next.

Clinical implications

The use of CT in caring for patients continues to increase because of its proven medical value in the hands of experienced radiologists. The clinical demand for CT is driven by the modern scanner's ability to produce exquisitely detailed images of patient anatomy, the wide availability of scanners, and the time required to perform most exams: 5–10 seconds. Recently, two manufacturers developed CT systems that can resolve objects as small as 125–150 microns.[5] The achievement promises further improvements in the imaging of bone, lung, and vascular tissues.

Because CT scans are so fast, image artifacts from patient motion are few, even for pediatric patients, making sedation no longer necessary in most cases. Although special electron-beam CT scanners were built for cardiac imaging in the past,[6] modern CT systems can routinely image the heart using cardiac-gating techniques.[3] Some CT scanners can also perform multi-energy imaging, in which projection data acquired at different x-ray effective energies can be processed to isolate specific materials,[7] such as the organic crystals that cause gout; identify different classes of kidney stones; and differentiate different types of arterial plaque. Relatively low-cost cone-beam CT scanners have also emerged in recent years for highly specialized clinical applications, such as breast,[8] orthopedic,[9] and dental imaging.[10]

The value of CT imaging to medicine and many other disciplines has exceeded even the high expectations of Hounsfield and other CT pioneers. Now, 50 years after its introduction to clinical medicine, CT is an essential tool of modern medicine—a stethoscope on steroids. Indeed, in a survey of leading US physicians, CT, along with magnetic resonance imaging, was ranked as the most important medical innovation of the 20th century.[11] To celebrate CT's birthday, millions of patients whose lives have been improved by its diagnostic and treatment-planning capabilities can raise a glass to a technology that makes the unseen visible. And the generations of CT scientists and physicians who have contributed to CT's technological development can enjoy a well-deserved pat on the back.

Conflict-of-interest statement: John Boone has received research funding from CT and CT-component manufacturers, including Varian Medical Systems, Siemens Medical Systems, Canon Medical Systems, TeleSecurity Sciences, and Imatrex. He is a stockholder and cofounder of Izotropic Imaging, which focuses on cone-beam breast CT. He has received patent royalties from his university-owned patents licensed by Samsung Electronics and Izotropic Imaging. Cynthia McCollough is the principal investigator of a research grant to Mayo Clinic from CT manufacturer Siemens Healthcare. She has received patent royalties from Mayo-owned patents licensed to Siemens Healthcare.

REFERENCES

1. G. N. Hounsfield, *Br. J. Radiol.* **46**, 1016 (1973).
2. J. Ambrose, *Br. J. Radiol.* **46**, 1023 (1973).
3. J. T. Bushberg et al., *The Essential Physics of Medical Imaging*, 4th ed., Wolters Kluwer Health (2020).
4. J. M. Boone et al., *Radiology* **265**, 544 (2012).
5. A. M. Hernandez et al., *Med. Phys.* **48**, 2760 (2021); S. Leng et al., *Radiographics* **39**, 729 (2019).
6. M. J. Lipton et al., *Radiology* **152**, 579 (1984).
7. T. R. C. Johnson, *AJR, Am. J. Roentgenol.* 199, S3 (2012).
8. J. M. Boone et al., *Radiology* **221**, 657 (2001).
9. Q. Cao et al., *Med. Phys.* **45**, 114 (2017).
10. W. C. Scarfe, A. G. Farman, P. Sukovic, *J. Can. Dent. Assoc.* **72**, 75 (2006).
11. V. R. Fuchs, H. C. Sox Jr, *Health Aff.* **20**, 30 (2001).
12. G. N. Hounsfield, "Computed medical imaging," Nobel lecture presented at Karolinksa Institute, Stockholm, 8 December 1979; A. M. Cormack, "Early two-dimensional reconstruction and recent topics stemming from it," Nobel lecture presented at Karolinksa Institute, Stockholm, 8 December 1979.
13. A. M. Cormack, *J. Appl. Phys.* **34**, 2722 (1963).
14. A. M. Cormack, *J. Appl. Phys.* **35**, 2908 (1964). PT

Ptychography:

A solution to the phase problem

First envisioned for elucidating crystalline structures, the technique is now used for high-resolution lensless imaging, wavefront sensing, and more.

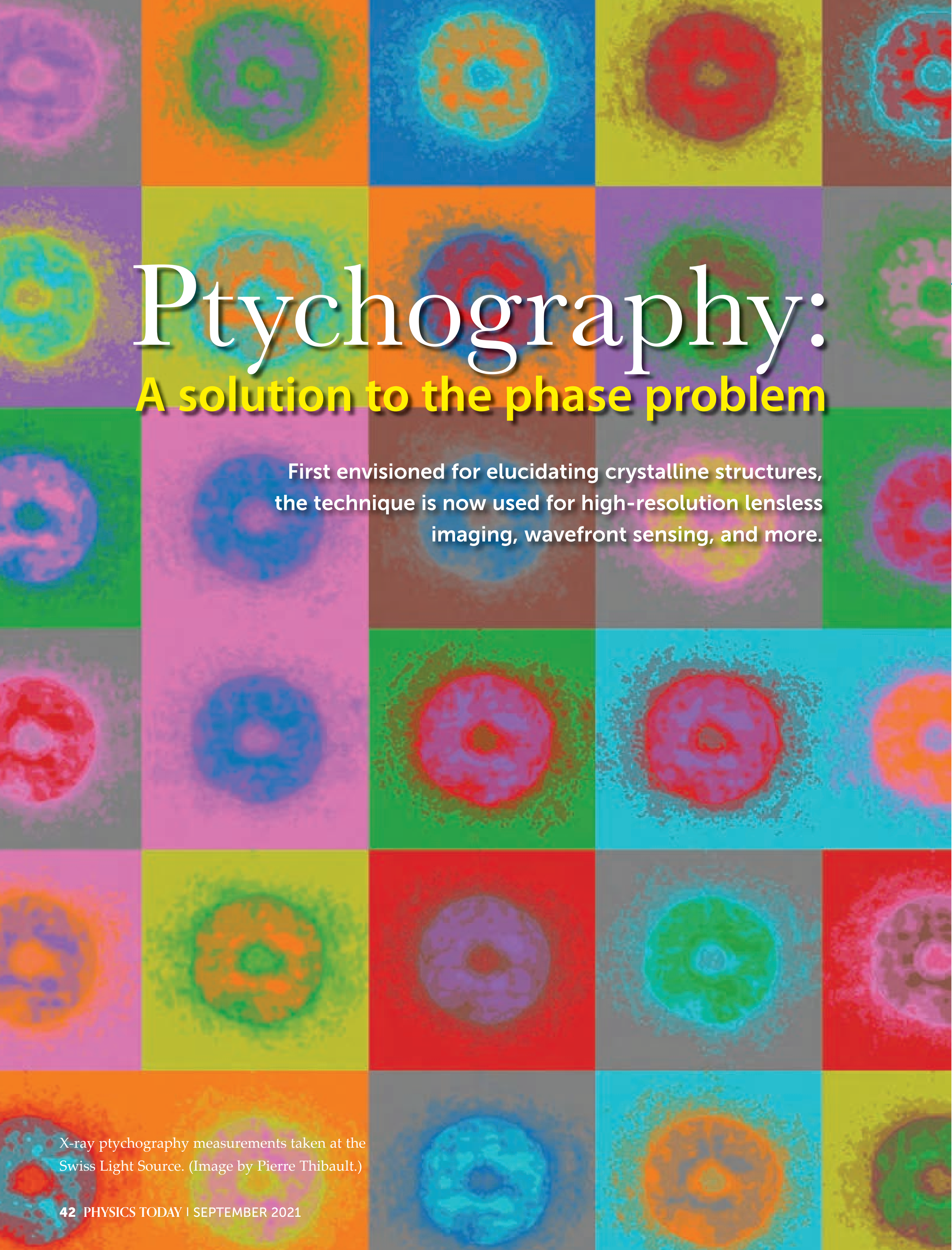

X-ray ptychography measurements taken at the Swiss Light Source. (Image by Pierre Thibault.)

Manuel Guizar-Sicairos works as a beamline scientist for the coherent small-angle x-ray scattering beamline at the Swiss Light Source, part of the Paul Scherrer Institute, in Villigen, Switzerland. He has developed algorithms and applications for x-ray ptychography and nanotomography since 2008. **Pierre Thibault** is a full professor at Italy's University of Trieste, where he works on the development of x-ray ptychography and other high-resolution, coherence-based imaging and tomography techniques.

Manuel Guizar-Sicairos and Pierre Thibault

Over the past 15 years, ptychography applications and methods have advanced significantly. Ptychography is a computational microscopy technique for acquiring images with resolutions beyond the limits imposed by beam diameter, optical aberration, and numerical aperture—NA, a measure of the range of incident angles an optical system can accept. Nowadays it encompasses various experimental techniques with visible light, UV light, x rays, and electrons. Emerging applications include, for example, accurate wavefront-aberration measurement for space telescopes.

A bit of history

Ptychography was introduced in 1969 in a three-part paper[1] by Walter Hoppe, an influential figure in the field of electron microscopy. (For more about the technique's name, see box 1.) But it gained little traction during his lifetime: In 1982 Hoppe described ptychography as one of his "nearly forgotten old ideas."[2] Only once computers gained sufficient memory and computing power, and after a few other technical difficulties were addressed, did ptychography gradually reemerge.

Hoppe's idea was to retrieve a crystal's structure by illuminating it with a tightly focused coherent electron beam and measuring the far-field intensity distribution. In the far-field limit, the scattered beam encodes the crystal's reciprocal-space structure, and periodic sharp points, called Bragg peaks, appear when a periodic structure is illuminated with a homogeneous coherent field. The complex-valued wave fields of those peaks are needed to reconstruct the real-space structure through Fourier synthesis. The magnitude of the wave fields can be obtained from the peaks' measured intensities, but the corresponding phases cannot be directly measured. The impossibility of directly measuring those phases, and the difficulty of retrieving them through indirect means, is known as the phase problem. (See, for example, the article by Keith Nugent, David Paganin, and Tim Gureyev, PHYSICS TODAY, August 2001, page 27.)

Ptychography was Hoppe's attempt at tackling the difficult task. In the regime where multiple-scattering effects are negligible, the transmitted wave field is proportional to the product of the beam's wave field and the crystal's transmissivity, which depends primarily on its electron density distribution. In reciprocal space, that product becomes the convolution of the crystal's reciprocal-space structure, consisting of narrow peaks, and the Fourier transform of the beam. Hoppe realized that if the beam was small enough—comparable to the lattice spacing—the width of its Fourier transform would be comparable to the spacing between the Bragg peaks, and the convolution would broaden those peaks enough that they would overlap and interfere with each other. Translating the beam by small steps then creates a beating pattern in the overlap region from which the phases of the peaks can be unambiguously extracted. Although Hoppe had written his 1969 series of papers mainly about solving crystal structures, he devoted the third part to applying the same principles to nonperiodic objects.

Ptychography has since evolved into a lensless microscopy technique in which image-forming optics are replaced by computational reconstructions. The resolutions of x-ray and electron microscopy techniques are limited by the need for well-corrected high-NA optics. Ptychography removes that limit; its resolution is, in principle, restricted by the maximum diffraction angle at which intensities can be measured with sufficient statistics. Additionally, the technique has loose requirements for the quality and size of the illuminating beam because the resolution is not limited by the illumination spot size or by wavefront aberrations in the focusing optics (see, for example, box 2). Those features make ptychography experimentally advantageous compared with scanning-probe microscopy and holography, both of which require a near-perfect illuminating beam that is as small as the resolution sought.

Ptychogram as a spectrogram

The input data for a ptychography reconstruction is a collection of intensity measurements referred to as a ptychogram (see figure 1). Ptychograms are strongly related to spectrograms, which are widely used as representations of a signal's frequency content. Spectrograms commonly represent a frequency spectrum's variation with time, much like a sheet of music. A one-dimensional sound is represented with a two-dimensional spectrogram, with one axis being time and the other

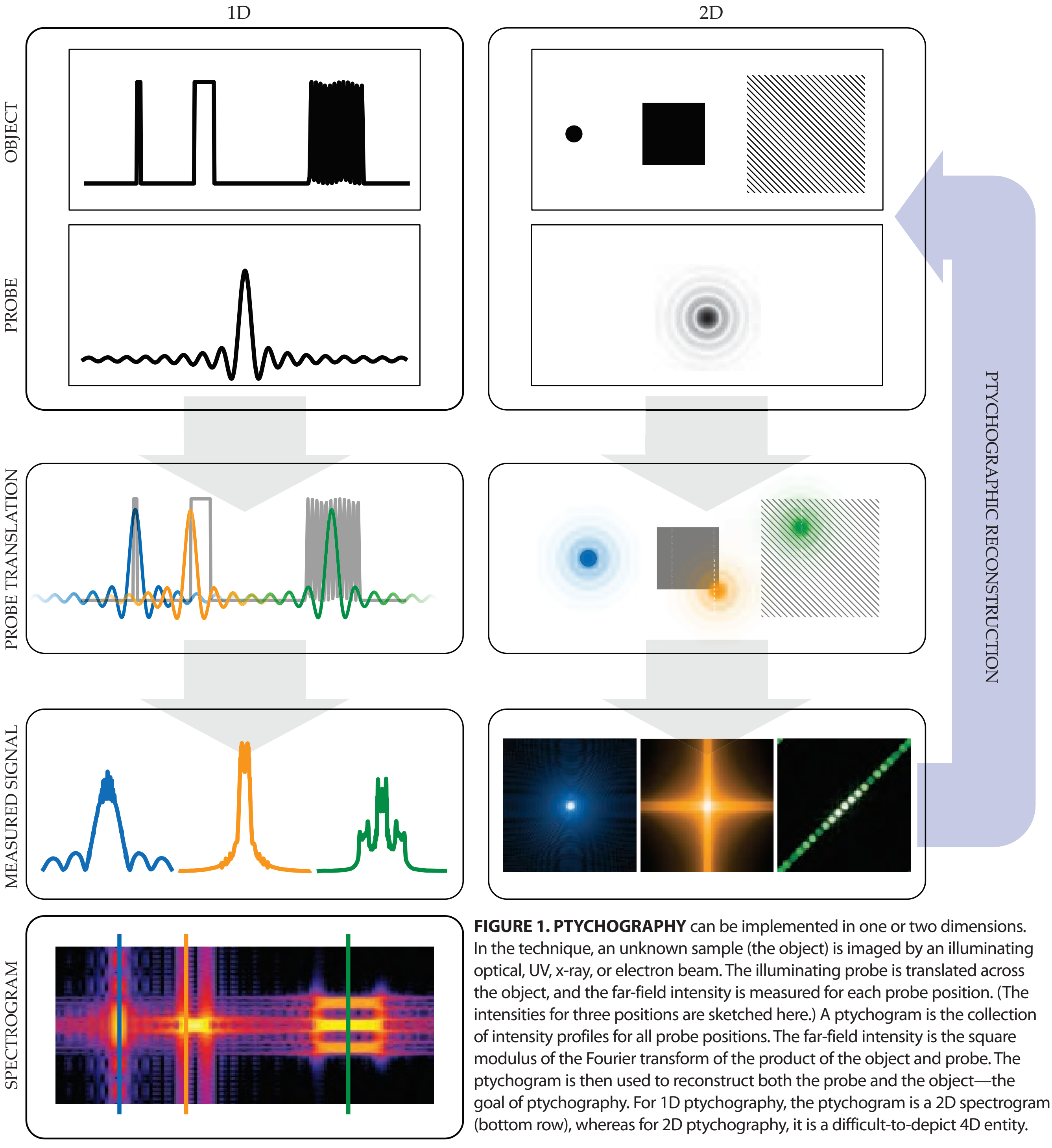

FIGURE 1. PTYCHOGRAPHY can be implemented in one or two dimensions. In the technique, an unknown sample (the object) is imaged by an illuminating optical, UV, x-ray, or electron beam. The illuminating probe is translated across the object, and the far-field intensity is measured for each probe position. (The intensities for three positions are sketched here.) A ptychogram is the collection of intensity profiles for all probe positions. The far-field intensity is the square modulus of the Fourier transform of the product of the object and probe. The ptychogram is then used to reconstruct both the probe and the object—the goal of ptychography. For 1D ptychography, the ptychogram is a 2D spectrogram (bottom row), whereas for 2D ptychography, it is a difficult-to-depict 4D entity.

frequency. Similarly, for a 1D object and probe, a 2D ptychogram emerges with both spatial and spatial-frequency axes. The underlying phase, however, is lost in the measurement process.

A reader versed in audio signal processing will notice the connection to the short-time Fourier transform (STFT), which is typically used to create audio spectrograms. For an STFT, an audio signal is multiplied by a sliding temporal window to extract a portion of the signal locally in time. The spectrogram is constructed by computing a Fourier transform for each position of the sliding window.

In a ptychogram, the illumination probe serves as a spatial, rather than temporal, sliding window. The measured far-field signal represents the spatial frequencies that are locally present in the object, albeit convolved with the Fourier transform of the probe. The ptychography reconstruction problem is then mathematically closely related to that of recovering a signal from the magnitude of its STFT.

In 1992 John Rodenburg and Richard Bates formalized the mathematics that connect the ptychography reconstruction in real space to its spatial-frequency description.[3] They showed that a ptychogram is a convolution of the Wigner distributions—space–frequency representations devised to describe quantum states—of the probe and object. They outlined a unique and direct reconstruction method for an arbitrary object, via the well-known procedure of deconvolution. The linear procedure also provided an avenue for further analysis, such as statistical noise propagation.

For a 2D object the ptychogram is a 4D data set. With added dimensions, data processing increases quickly in all aspects: data volume, computational time, and memory. Although the task is manageable today, the barriers were significant when Rodenburg and Bates published their paper. Thus aside from a few impressive proof-of-principle demonstrations, ptychography remained of limited practical application. There was also a sense that generating two 2D images from a large 4D data set was a somewhat wasteful enterprise and that the ptychogram must surely be a highly redundant entity.

Ptychography meets iterative phase retrieval

In his 1982 paper, Hoppe suggested that "tackling of the data in different ways . . . might provide an attractive field for lovers of computers" (reference 2, page 193). Indeed, as early as 1972, electron microscopists Ralph Gerchberg and Owen Saxton had already started exploring iterative phase-retrieval methods that exploited the newly invented fast-Fourier-transform algorithm.[4] Such algorithms start with an estimated initial wave field and use functions to propagate the field back and forth between the object and measurement planes. Constraints can be applied at each step, and the process repeats until it converges on a solution.

James Fienup introduced the hybrid input–output algorithm, an iterative algorithm that could reconstruct an object from the magnitude of its Fourier transform,[5] in 1978. His solution to the phase-retrieval problem used limited *a priori* information about the object to impose constraints in real and reciprocal spaces. It was mainly used with optical telescopes to overcome limits posed by atmospheric turbulence.

Then, in 1999, Fienup's algorithm was applied in the first demonstration of coherent diffractive imaging (CDI) that used x rays to visualize nonperiodic objects.[6] CDI has inherent limitations: The sample must be well isolated and of limited size to satisfy requirements for sampling the diffraction patterns, and the illumination must be uniform across the sample to avoid influencing the object's Fourier spectrum. Yet the method has remained important for imaging with, for instance, x-ray free-electron lasers.

In 2004 Helen Faulkner and Rodenburg showed for the first time that ptychographic reconstructions could be obtained within an iterative phase-retrieval framework, thereby bringing the technique to its modern form.[7] They retained the technique's original experimental procedure: Coherent far-field diffraction patterns are acquired by directing a spatially bound probe at different transverse positions relative to the object. But the researchers analyzed the data in a way similar to that used for CDI, iteratively applying constraints in real and reciprocal spaces until they converged on a solution. The modern version of ptychography can, in fact, be viewed as a scanning version of CDI, but without the requirement that samples be isolated, which means it can be used to image and zoom in on spatially extended samples.

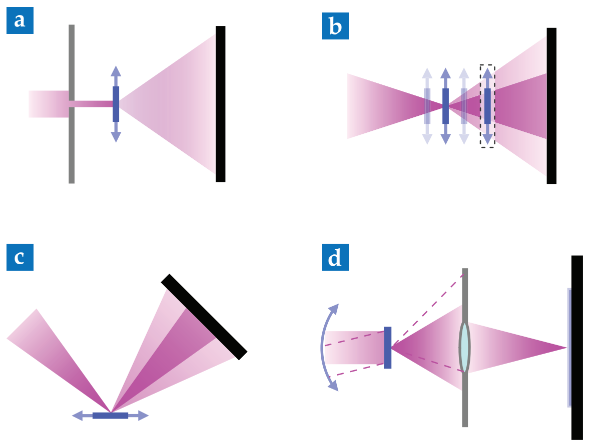

FIGURE 2. DIFFERENT EXPERIMENTAL CONFIGURATIONS enable multiple kinds of ptychography. Arrows indicate scanning motion. The intensity measured at the detector (black) corresponds to a Fourier transform of the exit wave field after the sample (blue). **(a)** In the simplest configuration, an aperture shapes the illuminating beam. **(b)** With a focused beam, the sample can be located at the focus or slightly upstream or downstream. Moving it tunes the size of the illuminating beam. For near-field ptychography, the sample is located significantly downstream of the beam focus (dashed box). **(c)** Reflection ptychography can use either specular or Bragg reflection. **(d)** In Fourier ptychography, a lens forms an image of the sample on the detector. Changing the illumination angle (dashed lines) changes the scattering angles accepted by the lens pupil. Capturing larger angles allows higher-resolution information to pass through the lens.

Unlike CDI, which needs uniform illumination, ptychography requires a probe that has both significant spatial structure and a broad spatial spectrum. Ptychography's phase-retrieval procedure also decouples the contributions of the object and the probe, thereby enabling each to be separately reconstructed. A crucial consequence of introducing iterative phase-retrieval algorithms to ptychography was that the data sets no longer needed the Wigner method's small scanning steps, which had to be at least as small as the resolution sought. Ptychogram sampling in real space can be done with step sizes much larger than the resolution as long as the illuminated regions have sufficient overlap.

The convergence of ptychographic reconstructions benefits from the simultaneous constraints of several diffraction patterns. That improvement, together with the technique's robustness against noise, removes some pesky ambiguities inherent to CDI reconstructions. Enforcing consistency among overlapping illuminated areas during reconstruction provides additional information needed to resolve ambiguities in the solution and aid the phase-retrieval process.

Undoubtedly aware of the value of their ideas, Faulkner and Rodenburg filed a patent in 2004 that claimed wide coverage of iterative methods applied to ptychography. We have observed that the proactive protection of the broad patent by its current owner has influenced the free exchange of algorithmic tools. We deem it likely that the sharing of open-source reconstruction software will continue to remain difficult until existing patent coverage expires, which is expected to happen in 2026.

Demonstrations of the new ptychography approach at third-generation x-ray synchrotron sources, which provide sufficient coherence, quickly followed Faulkner and Rodenburg's demonstration, and the technique rapidly attracted interest from the x-ray imaging community. Researchers developed reconstruction algorithms to tackle a larger number of experimental scenarios, as detailed below. For more comprehensive discussions of x-ray ptychography advances, methods, algorithms, and applications, see references 8–10.

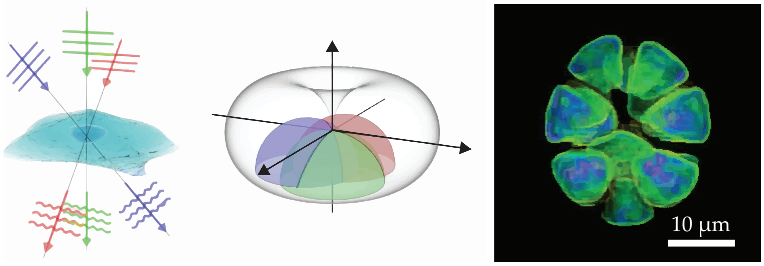

FIGURE 3. OPTICAL 3D IMAGING can be achieved by combining Fourier ptychography with principles of diffraction tomography. Each illumination direction (left) contains information on a hemispherical shell in reciprocal space (center). After an iterative phase-retrieval process, the reconstructed reciprocal-space information can be used to obtain a 3D image (right). (Adapted from C. Zuo et al., *Opt. Lasers Eng.* **128**, 106003, 2020.)

Experimental setups

Variations in the configurations of ptychography experiments emerged in parallel with the algorithmic developments. The new geometries, illustrated in figure 2, accommodate different applications and types of contrast. Early ptychography experiments used apertures to create spatially confined illuminating beams. With a focused beam, however, the sample can be moved away from the focal plane to allow a larger or even tunable beam diameter. The beam can consequently be moved across the sample in larger steps, which, in turn, significantly increases imaging throughput. The idea can be pushed all the way to the near-field regime, in which the distance between the beam focus and the object is increased until the wave-field propagation is best described by a Fresnel transform. Reconstructions for near-field ptychography use the same algorithms as in the far field, but with a suitable adaptation of the object–detector propagation.

Ptychography also has important applications in reflection mode. For x-ray Bragg reflection, a crystalline object is oriented such that the incident probe satisfies the Bragg-reflection condition—that scattered light from the crystal layers interferes constructively. As the object is scanned, minute variations in the crystalline structure can be observed and used to map dislocations and other lattice defects.[11] Specular-reflection ptychography has also been demonstrated in the extreme-UV regime.[12]

Fourier ptychography is, perhaps, the odd member of the family. The basic setup uses a conventional imaging lens between the object and the detector. Normally the NA of the lens limits the imaging resolution. But in Fourier ptychography, changing the direction of the beam incident on the same object region effectively translates the object spectrum in the lens-pupil plane.[13] (With x rays, it is more practical to move the actual lens.[14]) A different part of the spectrum then makes it through the pupil at each angle, and the measured images are treated with ptychography reconstruction algorithms.

For both optical and x-ray wavelengths, Fourier ptychography has the significant advantage in that a high-resolution image can be obtained with low-NA optics, which are easier to manufacture and can have larger fields of view and working distances than the high-NA optics required by other techniques. The technique's underlying process—scanning an optical aperture to synthesize an image with better resolution—is quite similar to synthetic aperture imaging, which has been used for many years with radar and telescopes.

Beyond imaging, ptychography has found applications in the time domain for characterizing ultrashort optical pulses with very high temporal resolution.[15] It has also been used for optical wavefront characterization of free-form optics,[16] an approach showing promise for on-board alignment of space telescope components.

With all those flavors, it is fair to ask, What is ptychography, and what is not? In our view, ptychography is defined by two factors. First, it relies on the encoding of information through the propagation and self-interference of a wave field that originates after the probe interacts with the object. Second, it uses a probe that undergoes a transverse translation to acquire multiple data sets in a way that aids the phase-retrieval process.[17] In other words, ptychography involves some level of stitching. That definition differentiates ptychography from other approaches that rely solely on propagation and interference.

Sampling and information content

The 4D nature of a ptychogram means that sampling constraints apply both in reciprocal space, where the far-field intensity is measured, and in real space through the scanning step size. In the original reconstruction approach using Wigner deconvolution, full sampling in both domains was necessary for a reconstruction: The scanning step size needed to be as small as the sought resolution, and the far-field intensities needed to be Nyquist sampled, meaning the detector's pixel size should be small enough to sample the narrowest oscillations present in the measured intensity pattern. That massive sampling of the phase space led to data sets that were unnecessarily redundant, not to mention difficult to measure and process.

The incorporation of iterative transform algorithms significantly relaxed the step-size re-

BOX 1. ABOUT THE NAME

Ptychography is a cumbersome word. In English, the "p" is silent, as in "psychology," so the word is pronounced tie-KOH-gra-fee. Its etymological roots are from the ancient Greek πτυχή (ptukhḗ, "a fold") and the Greek γράφω (grapho, "to write"). The reasoning behind the name requires a small detour into the German language. As mentioned in the main text, a convolution in reciprocal space is a central aspect of the original technique. In German, convolution is usually referred to as Faltung (folding). From there one can draw a connection between the technique and the ancient Greek word for fold, although the connection is somewhat convoluted. (The authors apologize dearly for the pun.)

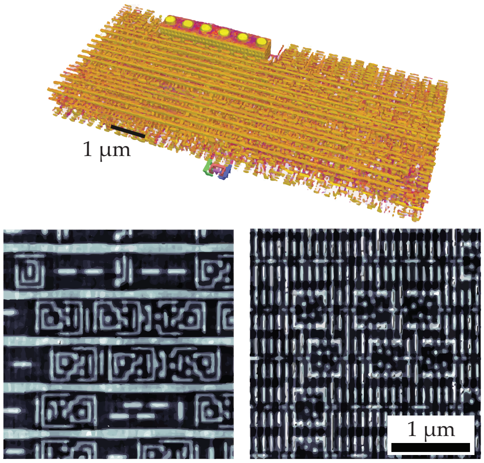

FIGURE 4. X-RAY PTYCHOGRAPHY views with different angular orientations can be combined into a 3D image with nanometer resolution. These images show the metal layers of an integrated circuit. The top image is a 3D rendering with 20 nm resolution. The bottom two images show tomographic virtual cuts in a zoomed-in region of interest. (Adapted from M. Holler et al., *Nat. Electron.* **2**, 464, 2019.)

quirement. As long as the different illuminated regions had some significant overlap, the scanning step could be much larger than the sought real-space resolution. The exact boundaries of what constitutes sufficient sampling of the ptychogram are a subject of current research.

For conventional far-field ptychography, a trade-off exists between sampling in real and reciprocal spaces. For Nyquist-sampled intensities, practitioners have adopted the rule of thumb that all regions of the imaged sample should be illuminated at least twice. An example of the aforementioned trade-off is that a finer step size should be used when the far-field intensities are not Nyquist sampled—when they are measured with a pixel grid too coarse to capture all the oscillations present in the intensity pattern. There appears to be a strong mixing of information in the ptychogram that allows for some freedom in its sparse sampling.

From its origins, ptychography was meant to reconstruct an unknown object illuminated by a known beam. It was of immense practical benefit, then, to discover that it can also recover information about the illumination. In fact, the illuminating beam can be reconstructed with limited prior knowledge, such as its approximate diameter and phase curvature, the latter being determined primarily by the distance between the beam focus and the object.

Without the need for an *a priori* estimate of the probe, the quality of the reconstructions improved tremendously. Ptychography quickly became a valuable beam- and wavefront-characterization technique. Moreover, under certain conditions, errors in the scanning positions can also be recovered and corrected. The self-consistency embedded in the ptychogram can compensate to an impressive extent for experimental unknowns and uncertainties.[17,18]

All the refinements to experimental unknowns have practical capture ranges. For instance, the reconstruction algorithms robustly converge only if the phase curvature and diameter of the illumination are approximately known or, alternatively, if the intensity data are collected in fine steps and with a high signal-to-noise ratio. In practice, it is often beneficial to first characterize the illumination with a fine scanning step; constraints on subsequent measurements can then be relaxed by using that characterization as an initial guess for the probe.

Still more information can be extracted from a ptychogram. For example, one can solve for coherent-mode representations of the object and illumination, which allow for characterization not only of the illuminating wavefront but also of its partially coherent properties. The probe's temporal variations over the course of data collection can also be retrieved, as can multiple-wavelength reconstructions. Other complex interactions between the illumination and the object can be modeled, thereby enabling the retrieval of additional properties, such as the object's polarization and magnetization effects. Even depth-of-field limitations can be surpassed by representing the reconstructed object in multiple slices.

Applications and state of the art

This article would not be complete without mention of current applications. In the interest of brevity—and with the express warning that this is by no means an extensive list—we present three examples that provide a glimpse into optical, x-ray, and electron imaging implementations.

BOX 2. A STRUCTURED-ILLUMINATION TECHNIQUE

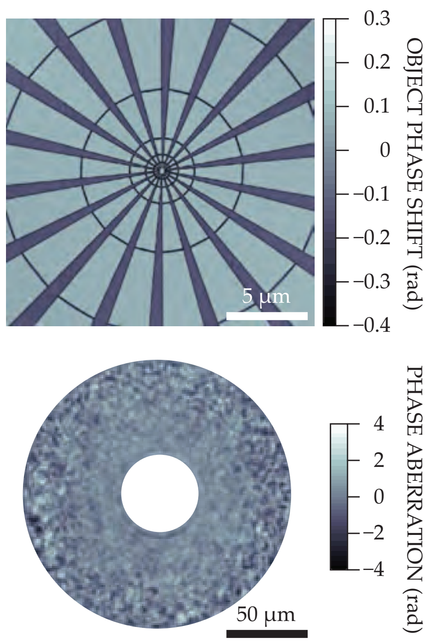

The encoding of information in a ptychogram relies on the spatial structure of the illuminating probe. Without some degree of such structure, transverse shifts of the sample do not create a difference in the measured intensities, and both the ptychogram's dependence on the spatial coordinate and the encoded information disappear.

Several studies in the past few years have found that increasing spatial structure to the illumination is beneficial for ptychographic reconstructions. To that end, methods have been proposed to introduce structure and wavefront aberrations into illuminating beams. The top image here shows a ptychographic reconstruction of a test object. The probe used to make the measurements was created with an x-ray lens that imparted finely controlled wavefront perturbations, which are shown in the bottom image. (For more details, see M. Odstrčil et al., *Opt. Express* **27**, 14981, 2019.)

Such studies were good news for x-ray microscopy because obtaining focused x-ray beams with negligible aberrations is challenging. With ptychography, we can embrace and welcome the ugliness of our beams as long as the illumination is coherent and stable.

Fourier ptychography is well suited to visible-light applications. With the technique, low-magnification objectives with large working ranges and fields of view can generate high-resolution images. The measurements can be made extremely quickly using LED arrays. Fourier ptychography also recovers images with quantitative phase, which is useful in, for example, estimating cellular masses in biological samples.

Three-dimensional imaging using Fourier ptychography principles was first demonstrated by Lei Tian and Laura Waller at the University of California, Berkeley, in 2015. Then, in 2020, Chao Zuo and colleagues at the Nanjing University of Science and Technology pushed the technique beyond proof-of-principle demonstration, obtaining 3D images using wide-field optical micrographs of 1.77 mm^2 at better than 400 nm resolution with 507 nm wavelength illumination.

The basic principle and some of their results are reproduced in figure 3. The researchers achieved a 3D reconstruction of the sample without the need for a through-focus series, also known as a *z*-stack, or any object rotation. At the same time, the researchers increased their lateral resolution in the *xy*-plane. In the demonstration highlighted in figure 3, they recorded 48×10^6 3D resolution elements per second, comparable to what is achievable with *z*-stack microscopy. Fourier ptychography involves no mechanical motion, though, so its speed can, in principle, be much higher. With faster cameras, 3D imaging with gigavoxels-per-second throughput of centimeter-scale areas in cell cultures seems in reach.

In the x-ray regime, far-field ptychography excels at recovering high-resolution images with quantitative contrast. The combination with x-ray spectroscopy and x-ray fluorescence shows great potential for providing structural, chemical, and compositional characterizations. To date, the most widespread application of x-ray ptychography is probably 3D imaging. Figure 4 shows an example in which ptychography was used to acquire nanometer-resolution tomographic projections, which were subsequently assembled into 3D images. The technique leverages the capability of ptychography to deal with extended samples: The researchers first imaged a 500-nm-resolution 3D overview with a 300 μm field of view. They followed up by focusing in on a 40-μm-diameter region of interest, which they imaged with 20 nm resolution.

Hoppe's original dream of using ptychography for electron microscopy took decades to become reality, but electron ptychography now boasts resolutions that surpass electron-lens aberrations and numerical-aperture limitations. It also has the added benefit of providing quantitative phase contrast. In 2018 David Muller's group at Cornell University carried out electron ptychography using a novel pixel-array detector with a high dynamic range and single-electron sensitivity. Shown in figure 5, their results marked a major improvement in contrast and resolution compared with traditional imaging techniques. Muller and his collaborators achieved a resolution of 0.39 Å. Under the same imaging conditions and at the same electron dose, conventional imaging methods could reach only 0.98 Å. The technique has since been improved to the point where its resolution is limited by lattice thermal vibrations.

Capabilities for ptychography continue to be developed, and in the past 10 years the technique has become increasingly available. Electron ptychography is already carried out, or soon will be, in several institutions around the world. X-ray ptychography is slightly ahead of the curve, with many third-generation synchrotron sources enabling ptychography measurements in some form and offering the capability to users across scientific fields. With planned upgrades, fourth-generation synchrotron sources, such as MAX IV in Sweden, Sirius in Brazil, and the upgraded European Synchrotron Radiation Facility in France, will advance ptychography and other coherent imaging techniques. Researchers will be able to exploit their high coherent fluxes to gain improved resolution, throughput, and characterization dimensionality.

Ptychography's applications are expected to grow and broaden, and new ones continue to emerge. Established techniques are already widely used for imaging with light, x rays, and electrons, and ptychography's different geometries and contrast mechanisms are being applied in an increasing number of scientific applications. As sources, scanning technology, and detectors improve, the capabilities and applications of ptychography will continue to expand and diversify.

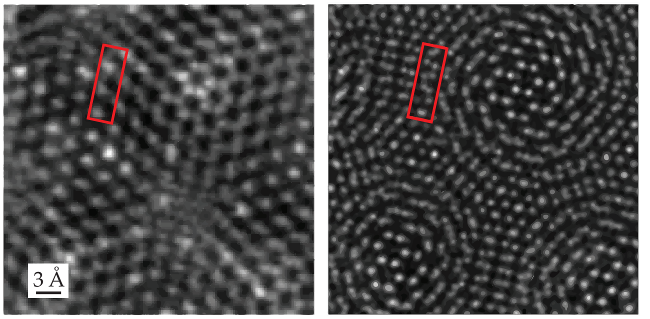

FIGURE 5. ELECTRON MICROGRAPHS of a twisted molybdenum disulfide bilayer show that ptychography (right) produces higher resolution than high-angle annular dark-field microscopy (left), a conventional method for high-resolution imaging. Red boxes highlight the same area in each image. (Courtesy of David Muller.)

Manuel Guizar-Sicairos's research is currently supported by the Swiss National Science Foundation. Pierre Thibault's research is currently supported by the European Research Council under the European Union's Horizon 2020 research and innovation program (grant agreement no. 866026).

REFERENCES

1. W. Hoppe, *Acta Cryst.* **A25**, 495 (1969).
2. W. Hoppe, *Ultramicroscopy* **10,** 187 (1982).
3. J. M. Rodenburg, R. H. T. Bates, *Philos. Trans. R. Soc. London Ser. A* **339**, 521 (1992).
4. R. W. Gerchberg, W. O. Saxton, *Optik* **35**, 237 (1972).
5. J. R. Fienup, *Opt. Lett.* **3**, 27 (1978).
6. J. Miao et al., *Nature* **400**, 342 (1999).
7. H. M. L. Faulkner, J. M. Rodenburg, *Phys. Rev. Lett.* **93**, 023903 (2004).
8. F. Pfeiffer, *Nat. Photonics* **12**, 9 (2018).
9. J. Rodenburg, A. Maiden, in *Springer Handbook of Microscopy*, P. W. Hawkes, J. C. H. Spence, eds., Springer (2019), p. 819.
10. C. Jacobsen, *X-Ray Microscopy*, Cambridge U. Press (2020).
11. P. Godard et al., *Nat. Commun.* **2**, 568 (2011).
12. M. D. Seaberg et al., *Optica* **1**, 39 (2014).
13. G. Zheng, R. Horstmeyer, C. Yang, *Nat. Photonics* **7**, 739 (2013).
14. K. Wakonig et al., *Sci. Adv.* **5**, eaav0282 (2019).
15. D. Spangenberg et al., *Phys. Rev. A* **91**, 021803(R) (2015).
16. A. M. Michalko, J. R. Fienup, *Opt. Eng.* **59**, 064101 (2020).
17. M. Guizar-Sicairos, J. R. Fienup, *Opt. Express* **16**, 7264 (2008).
18. P. Thibault et al., *Science* **321**, 379 (2008).

PT

Hong Kong University of Science and Technology: Innovating Today, Imagining Tomorrow


Photo credit: **Guancong Ma**

The Hong Kong University of Science and Technology (HKUST) is a dynamic, young research university with a diverse international student body and faculty who relentlessly pursue excellence in teaching and research. Situated on a hillside overlooking scenic Clear Water Bay at the eastern edge of Hong Kong and the southeastern coast of China, HKUST has rapidly established itself as a leading institution on the academic world map. Since the university's founding in 1991, the physics department has grown from 9 to 37 faculty members and now has 175 research graduate students. The department's research areas have also expanded to include condensed-matter physics; atomic, molecular, and optical systems and quantum optics; particle physics and cosmology; quantum information; scientific computation; soft-matter and biological physics; and metamaterials.

The physics department promotes the pursuit of cutting-edge research by cultivating a collaborative, supportive, and cohesive environment. For example, the Center for Fundamental Physics focuses on theoretical and experimental research about the origin, fate, and fundamental building blocks of the universe, and it has participated in several global endeavors, including the ATLAS collaboration at CERN. The emphasis of the Center for Metamaterials Research is on the design, fabrication, and characterization of different metamaterials to explore novel wave phenomena and to manipulate light and sound in ways not possible before. The newly established Center for Quantum Technologies brings together a team working across several core areas with focuses on quantum materials and devices, quantum control, and software.

The physics department's research efforts are supported by critical infrastructure, specialized equipment, high-performance computer clusters, and services provided by the university's Central Research Facilities. For example, the Materials Characterization and Preparation Facility offers advanced characterization tools, sample and materials preparation apparatus, and a helium liquefier. The Nanosystem Fabrication Facility has state-of-the-art equipment for developing innovative micro/nano devices and systems.

The department's goals for future growth are to enhance existing core strengths and build up world-class capabilities in rapidly developing areas aligned with university initiatives, such as big data and renewable energy and new energy materials. To achieve these goals, the department will strive to continuously attract outstanding new faculty members at all ranks, and it plans to fill 10 new faculty positions in the next few years. To learn about opportunities as soon as they are posted, interested candidates may visit jobs.physicstoday.org and create an alert for "HKUST."

JIM CAMPBELL/AERO-NEWS NETWORK/PUBLIC DOMAIN

Theoretical physicist Stephen Hawking experiencing near-weightlessness during a 2007 flight that simulated a zero-gravity environment.

Stephen Hawking, human

How should we remember Stephen Hawking? As a cosmologist, a science popularizer, a media darling, or the world's most famous wheelchair user? In *Hawking Hawking: The Selling of a Scientific Celebrity*, an unauthorized biography of the late theorist, science writer Charles Seife shows that the answer is all of the above. His science gave Hawking something to say, and his computer-generated voice let it be heard.

Hawking began exhibiting signs of amyotrophic lateral sclerosis in 1963, at 21, when he was still completing his graduate degree at the University of Cambridge. His prognosis was bleak; at best, he likely had only a few years left. Instead, he lived another half century, during which time he made good use of a series of assistive technologies and adaptive equipment to continue writing, lecturing, and living. A tracheostomy in 1985 saved his life but eliminated his ability to speak without the computer-generated voice that became his trademark.

And that familiar voice may have been legally trademarked: Although Seife acknowledges that he couldn't find evidence to support the claim, he repeats actor Eddie Redmayne's assertion that Hawking owned the copyright to his computer-generated voice and gave the

Hawking Hawking

The Selling of a Scientific Celebrity

Charles Seife

Basic Books, 2021. $30.00

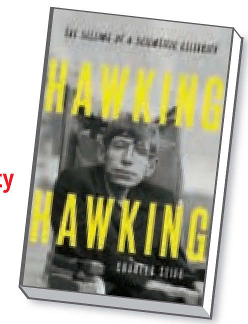

makers of the 2014 film *The Theory of Everything* permission to use it. In any case, after the tracheostomy, Hawking relied on popularization and media appearances to bankroll the extraordinary medical costs associated with his round-the-clock care.

Popular media representations of Hawking, whether in the *Daily Telegraph* or on *The Simpsons*, tended to portray him as a singular genius or a disembodied brain. "He had become," Seife writes, "a symbol to the public, a transcendent mind in a withered body." In rightly rejecting that metaphor, Seife imposes a troubling alternative: Hawking as a black hole. And in truth, Hawking held his own story close. He resisted entreaties from his in-house editor, his personal editor, and his agent to incorporate more of his own story into his career-defining *A Brief History of Time: From the Big Bang to Black Holes* (1988). Nor is his memoir, *My Brief History* (2013), particularly revealing, as it was largely collated from previously published materials, not all of which were even written by Hawking.

Barred from Hawking's archives and frustrated by the scientist's reticence, Seife adopts Hawking's methodological insights to seek deeper biographical truths. Like a black hole, Seife suggests, Hawking is best understood by looking backwards through time. The book is therefore structured in reverse chronological order, using events from Hawking's life as emissions with a diminishing signal.

Because Hawking so frequently outlived the relevance of his theoretical contributions, that narrative approach—challenging under the best of circumstances—means that Seife frequently introduces readers to Hawking's ideas at the moment they were experimentally negated. For example, Hawking's particle-physics contributions from the 1960s and 1970s are discussed in the early 2010s, when the Higgs boson's existence was experimentally confirmed. Hawking had publicly bet that it would never be found.

In Seife's account, Hawking's increasing disability produces a biographical event horizon, beyond which information cannot escape. But how, I wondered, was Hawking's desire to control his own story different from that of any other public figure? Working in the long tradition of unauthorized biographers, Seife relies on a series of less-than-charitable sources, including British tabloids, Hawking's first wife, betrayed grad students, and even Hawking's ex–literary agent, Al Zuckerman, who recounts being "stunned" by his firing in 2015. (Hawking wanted more money.)

Seife uses those tidbits to reestablish Hawking as a man rather than a disembodied brain. The author depicts Hawking as a complicated human being with a chronic illness to be managed and human needs to be fed. Hawking's home life, which at one point included his wife, her lover, his future wife, and her husband, did not meet middle-class expectations. Later there were reports that he was abused by his second wife. When traveling, he routinely asked his hosts to take him to strip clubs. It's all a little tawdry, but then, that's fame.

Hawking Hawking frequently returns to a theme previously explored in philosopher and anthropologist Hélène Mialet's *Hawking Incorporated: Stephen Hawking and the Anthropology of the Knowing Subject* (2012)—namely, the layers of infrastructure that made it possible for Hawking to become singularly famous despite his total dependence on other people. The fact that Hawking used a computer to vocalize his speech, for example, meant that his words could be produced, recorded, and circulated without his participation. During the making of Errol Morris's documentary film *A Brief History of Time* (1991), Hawking provided the director with a duplicate of his speech synthesizer. In 2015 his voice and image toured with the band U2.

For Mialet, the impossibility of separating Hawking, the man, from "Hawking," the product, serves as a source of fascination and an example of how scientists' work is always embedded in their social worlds. For Seife, it's a symbol of Hawking's distance from mainstream scientific practices.

But Stephen Hawking was not a "collapsed star" or a "faint reflection of what he once had been," nor did he stop being a "real human being" when his health declined, as Seife asserts in the introduction. He was not a singularity. He was a cosmologist, a science popularizer, a media darling, and the world's most famous wheelchair user. Recognizing that he was all of that all at once should enrich rather than diminish our understanding of Hawking's life.

Audra J. Wolfe
Philadelphia

Chimera states are named after the fire-breathing beast from Greek mythology, which is composed of parts of a lion, a goat, and a snake. The bronze Chimera of Arezzo, found in the Italian town in 1553, dates from roughly 500–400 BC.

SAILKO/WIKIMEDIA COMMONS/CC BY-SA 3.0

An overview of complex systems

Chimera Patterns in Networks
Interplay between Dynamics, Structure, Noise, and Delay
Anna Zakharova
Springer, 2020. $159.99

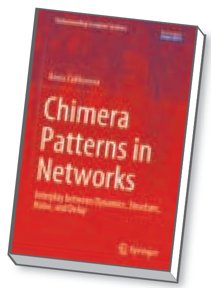

In 2002 Yoshiki Kuramoto and Dorjsuren Battogtokh discovered a novel phenomenon when studying a ring of identical, nonlocally coupled phase oscillators: The oscillators formed spatially distinct but coexisting regions of synchronization and desynchronization. That counterintuitive dynamic state was subsequently generalized to describe any system in which an ensemble of identical elements self-organizes into coexisting coherent and incoherent regions. Daniel Abrams and Steven Strogatz later named the phenomenon a "chimera state," after the hybrid beast from Greek mythology that's composed of parts of a lion, a goat, and a snake.

At that time, interest in complex systems was exploding, so chimera states quickly drew attention from the nonlinear dynamics community. Research into the states draws on principles from that field as well as those of complex networks, self-organization, stochasticity, and time delay. They embody complexity like few other topics and wrap it up in a simple but head-scratchingly satisfying physical phenomenon.

Almost 20 years after Kuramoto and Battogtokh's initial discovery comes *Chimera Patterns in Networks: Interplay between Dynamics, Structure, Noise, and Delay* by Technical University of Berlin physicist Anna Zakharova. Her new book provides the nonlinear dynamics and complex systems communities with a comprehensive account of the rich dynamics exhibited by chimera states. It also elucidates the role that stochasticity, time delays, and network structures play in giving rise to the phenomenon. Zakharova is perfectly positioned to give such an account, as she has spent a decade researching self-organizing systems from both theoretical and experimental perspectives. Her work, much of which is mentioned in the book, has directly contributed to the community's current understanding of the dynamics of chimera states.

Chimera Patterns in Networks is primarily aimed at physicists, applied mathematicians, and engineers at the graduate level or beyond who are interested in chimeras and other synchronization patterns. Given the attention it pays to a blend of rich dynamics and practical considerations, the book will be particularly useful to those readers who are new to the study of complex systems that exhibit chimeras. They will appreciate how Zakharova includes a thorough discussion of topics that tend to puzzle researchers entering the world of chimeras, such as the choice and importance of parameters and initial conditions.

The book comprises four chapters, the first of which is an introduction that briefly summarizes existing literature on chimera-state research. Chapters 2 and 3 dive into amplitude chimeras and coherence-resonance chimeras, both of which are covered in the context of ring networks. Using rings as the narrative thread was a smart decision, because they both are historically important to the field and tend to be the best environment for intuitively visualizing the various important dynamic states. The book contains an especially cogent discussion of amplitude chimeras, which provide a perfect platform for exploring chimera death and investigating the effects of time delays and stochasticity. Control, on the other hand, is primarily discussed in the context of coherence-resonance chimeras.

The book closes with an exploration of novel synchronization patterns and chimera states in more general and realistic network topologies, both traditional and multiplex, rather than rings. Given her focus on limit-cycle oscillator systems, Zakharova does not discuss the analytical treatment of chimera states. Readers interested in analytical methods and the intuition they provide will thus have to go directly to the literature.

Chimera Patterns in Networks aims to highlight the richest possible dynamics exhibited by chimeras and link them to themes at the forefront of complexity—namely, stochasticity, time delay, and network structure. Zakharova is overwhelmingly successful in doing so, and the result is a text that is both practical and inspirational.

Per Sebastian Skardal
Trinity College
Hartford, Connecticut

NEW BOOKS & MEDIA

What's Eating the Universe?

And Other Cosmic Questions

Paul Davies
U. Chicago Press, 2021. $22.50

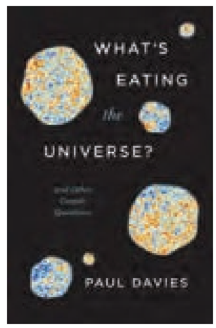

Understanding theoretical physics is a daunting task, but cosmologist Paul Davies's new book *What's Eating the Universe?* is here to guide readers through the field. Davies covers general relativity, antimatter, time travel, the multiverse, and just about any other topic he could fit into the book's 200 pages. Each chapter is short—less than 10 pages—but jargon-free and full of information. Davies uses a conversational tone to draw the reader in as he skims the history, experiments, and significance of each concept. Regardless of the reader's prior physics knowledge, the book provides an accessible introduction to cosmology. —MRB

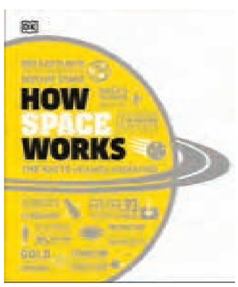

How Space Works

The Facts Visually Explained

DK, 2021. $22.00

How big is the universe? What preceded the Big Bang? Why do stars appear to move across the night sky? Those are just some of the questions addressed by *How Space Works*, an introductory reference book aimed at beginning astronomers, ages 12 and up. Featuring colorful graphics and brief, nontechnical text, the book starts off with a discussion of space from the vantage point of Earth before moving on to explore the solar system, stars, galaxies, and the universe. Among the many topics the book touches on are dark matter, star formation, cosmic rays, and even the search for alien life. The seven-page index should help readers navigate the book's encyclopedic format. —CC

Quantum Technology

Our Sustainable Future

The Quantum Daily/Teralon, 2021

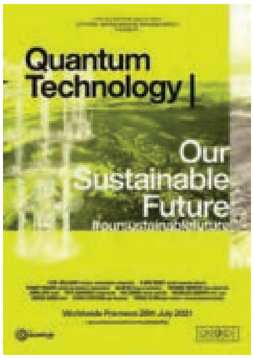

Computation is a notoriously energy-intensive task, and classical computers just won't cut it. They aren't powerful enough to simulate impossibly complex chemical systems—but quantum computing could be. The new minidocumentary *Quantum Technology* argues that the future of quantum computing should be approached with sustainability in mind. The film features interviews with leaders in the quantum world who suggest that a useful quantum computer could need as much energy as the top classical supercomputer. Researchers must find ways to limit energy demands and efficiently cool the superconductors needed for computation. *Quantum Technology* argues that quantum computing must be sustainable if it is to be done ethically. —MRB

Brave New Worlds

Mickey McDonald

Kickstarter, 2020. $65.00

In Brave New Worlds, a board game created by physicist Mickey McDonald, 2–6 players compete to explore our solar system. To do so, they must send satellites, rovers, and astronauts to planets like Mars, moons like Titan, and dwarf planets like Pluto. But they must balance their desire to explore with the fuel considerations necessary to get spacecraft across interplanetary space. Fortunately, just as mission control does in real life, players can send their probes by planets like Jupiter and Saturn to gain gravity assists that enable them to reach distant worlds more quickly. McDonald received a PhD in atomic, molecular, and optical physics from Columbia University and says he created the game to inspire children and adults about the wonders of the solar system. Although the rule book could be streamlined, the game is brisk, fun, and relatively easy to learn. A companion book contains information about the heavenly bodies featured in the game. —RD

Ten Patterns That Explain the Universe

Brian Clegg

MIT Press, 2021. $29.95 (paper)

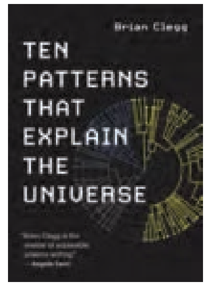

Science writer Brian Clegg presents an introduction to the cosmos through 10 patterns in this new book. Interestingly, Clegg chooses to feature not only patterns that scientists have discovered in nature, such as the cosmic microwave background and Earth's complex weather systems, but also those developed by researchers to explain natural phenomena, like Feynman diagrams and the periodic table. Using beautiful illustrations and illuminating diagrams, the book is a feast for the eyes. The final chapter, on symmetries in nature of all shapes and sizes, is particularly enlightening. Anyone interested in the natural world will enjoy the unique perspective offered in the book. —RD PT

NEW PRODUCTS

Focus on test, measurement, and analytical equipment

The descriptions of the new products listed in this section are based on information supplied to us by the manufacturers. PHYSICS TODAY can assume no responsibility for their accuracy. For more information about a particular product, visit the website at the end of its description. Please send all new product submissions to ptpub@aip.org.

Andreas Mandelis

Optical-spectrum-analyzer software

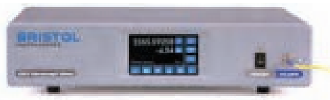

NuView software from Bristol Instruments converts the company's 438 series multiwavelength meter into a high-resolution optical spectrum analyzer. That capability allows the model 438 to analyze optical transceivers and wavelength-division multiplexing (WDM) signals. The meter simultaneously measures the wavelength, power, and optical signal-to-noise ratio of as many as 1000 discrete optical signals. Featuring high accuracy, a measurement rate up to 10 Hz, and a broad operational range of 1000–1680 nm, the model 438 provides precise, efficient, and versatile WDM testing for lasers and systems. For a more detailed analysis, the NuView software generates and displays an optical spectrum with a resolution better than 10 GHz (0.08 nm at 1550 nm). That lets users determine the transceiver side-mode suppression ratio and discriminate between closely spaced WDM channels. ***Bristol Instruments Inc****, 770 Canning Pkwy, Victor, NY 14564, www.bristol-inst.com*

Test solutions for oscilloscopes

Tektronix has brought to market three testing solutions designed to meet the requirements of advanced technologies for large, fast data transfers and low-latency video displays. The USB4, Thunderbolt 4 (TBT4), and DisplayPort 2.0 (DP2.0) automated compliance and debugging solutions easily integrate into test environments and address common test-time, signal-integrity, and device-under-test control challenges. They also offer physical layer electrical testing and characterization, which is crucial for compliance with the next-generation standards over USB-C connectors. The USB4, TBT4, and DP2.0 solutions can be used with DPO 70000SX, MSO 70000SX, DPO 70000DX, and MSO 70000DX oscilloscopes that have 23 GHz bandwidth and above and a sample rate of 100 GS/s. The scope setup can also be used for USB 2.0, USB 3.2, DP 1.2, and DP 1.4 testing. ***Tektronix Inc****, 14150 SW Karl Braun Dr, PO Box 500, Beaverton, OR 97077, www.tek.com*

Handheld microwave analyzer

Keysight has introduced a compact, ruggedized, handheld microwave analyzer to speed installation of 5G, radar, and satellite communications systems. The FieldFox supports an extended frequency and bandwidth range and has measurement integrity comparable to laboratory-based tools. It enables users in the field to install a millimeter-wave infrastructure and to reliably measure the network's key performance indicators. The multipurpose tool has a task-driven user interface and incorporates spectrum and signal-analysis and signal-generation capabilities. It accurately measures signal interference, antenna and cable performance, levels of electromagnetic field exposure, and path loss in communications systems. It also ensures that 5G services in the frequency range 2 can reach full connectivity potential. ***Keysight Technologies Inc****, 1400 Fountaingrove Pkwy, Santa Rosa, CA 95403-1738, www.keysight.com*

System for synchronous sourcing and measuring

The MeasureReady M81-SSM system from Lake Shore provides synchronous DC, AC, and mixed DC and AC sourcing and measuring to 100 kHz for very low-frequency and low-signal-level applications. The convenient system eliminates the complexity of multiple function-specific instrumentation setups and operates in cryogenic, room-temperature, and high-temperature environments. Up to three source and measurement modules can be connected. According to the company, noise and sensitivity are on a par with the best scientific-grade source and measurement instruments. The M81-SSM is suitable for characterizing various test structures, including single- and multilayer atomic structures, MEMS, organic semiconductors, and superconductors. ***Lake Shore Cryotronics Inc****, 575 McCorkle Blvd, Westerville, OH 43082, www.lakeshore.com*

Wide-bandwidth digital oscilloscopes

Rohde & Schwarz has enhanced usability and performance in the latest generation of its R&S RTO6 oscilloscope, available in six bandwidth models from 600 MHz to 6 GHz and with a sample rate of up to 20 GS/s. An updated user interface on a larger, 15.6-inch HD touch screen and straightforward workflows enable users to quickly set up measurements. The digital oscilloscopes feature such state-of-the-art specifications as a 9.4 effective number of bits and an update rate of 1 million waveforms/s. The RTO6 offers excellent signal fidelity, a powerful digital trigger, responsive deep memory, and a comprehensive tool set of analysis functions. The fully integrated test solution for time and frequency domains and the protocol and logic analysis support many applications, including electromagnetic interference debugging, spectrum and serial bus analysis, and power electronics processing. ***Rohde & Schwarz GmbH & Co KG***, *Muehldorfstrasse 15, 81671 Munich, Germany, www.rohde-schwarz.com*

Automated AFM with artificial intelligence

According to Park Systems, its Park FX40 atomic force microscope is the first AFM to autonomously execute all setup and scanning processes. With integrated artificial intelligence and robotics techniques, intelligent learning features, and safety mechanisms, the Park FX40 can perform functions such as probe identification and exchange, beam alignment, sample location, tip approach, and imaging optimization. Built-in intelligence allows the AFM to autonomously image several samples according to user requirements. Environmental sensing self-diagnostics and the head-crash-avoidance system ensure optimum performance. Various key AFM aspects have also been upgraded, including electromechanics for much-reduced mechanical noise, smaller beam spot size, improved optical vision, and multi-snap-in sample chuck. ***Park Systems Inc***, *3040 Olcott St, Santa Clara, CA 95054, https://parksystems.com* PT

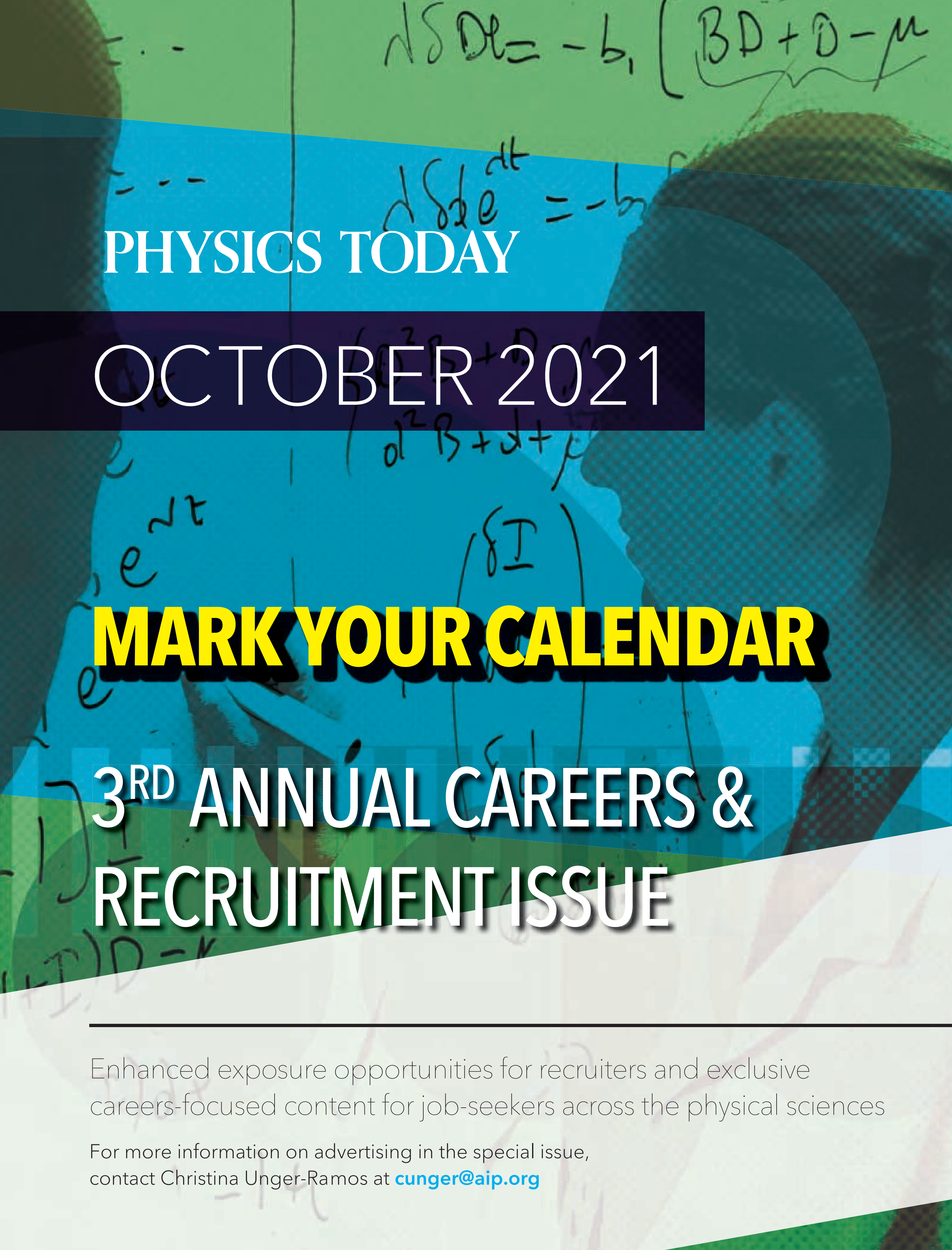
PHYSICS TODAY
OCTOBER 2021
MARK YOUR CALENDAR
3RD ANNUAL CAREERS & RECRUITMENT ISSUE
Enhanced exposure opportunities for recruiters and exclusive careers-focused content for job-seekers across the physical sciences
For more information on advertising in the special issue, contact Christina Unger-Ramos at cunger@aip.org

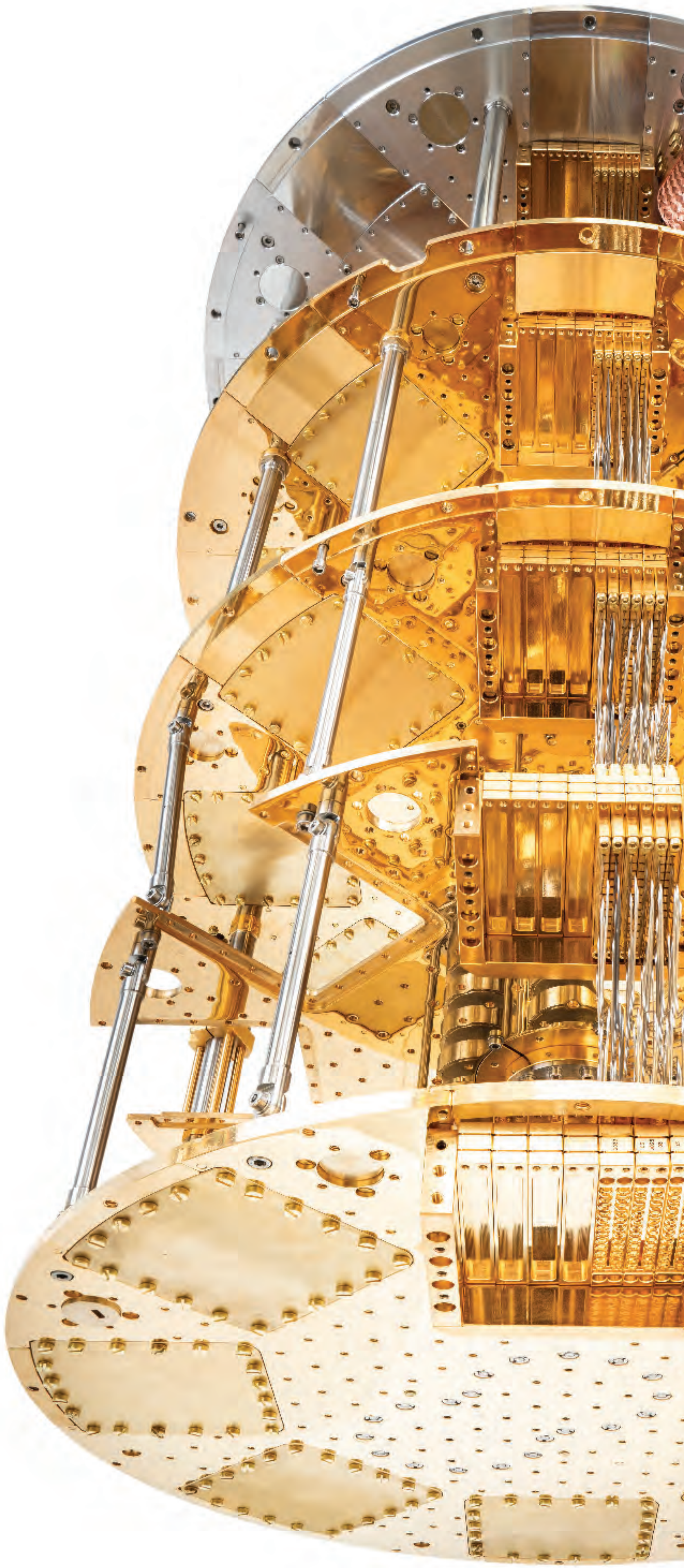

Jack Steinberger

Jack Steinberger, a corecipient of the 1988 Nobel Prize in Physics, died on 12 December 2020 among his family at his home in Geneva.

Jack was born on 25 May 1921 to a Jewish family in Bad Kissingen, Germany. In 1934, the year after the Nazi Party came to power, US Jewish charities helping to relocate German refugee children found separate homes in Chicago for Jack and his older brother. Jack's host eventually was able to bring his parents and younger brother to the US in 1938.

Jack studied chemical engineering at the Armour Institute of Technology (now the Illinois Institute of Technology) for two years and then used a scholarship to attend the University of Chicago, where he received an undergraduate degree in chemistry in 1942. He joined the US Army and worked at MIT in the antenna group. When he left the army not long after World War II ended, he went back to the University of Chicago. For his thesis, suggested by his adviser, Enrico Fermi, Jack conducted an experiment on cosmic-ray muons and found that they exhibit three-body decay, probably an electron and two neutrinos.

At the invitation of J. Robert Oppenheimer, Jack then went to the Institute for Advanced Study in Princeton, New Jersey. There he calculated the decay rate of a neutral pion to two gamma rays via intermediate nucleons. That calculation paved the way for later developments in theory—notably, the triangle anomaly.

In 1949 Jack went to the University of California, Berkeley, to work with theorist Gian Carlo Wick. Because of the many opportunities available, Jack began conducting experiments, including with Berkeley's new electron synchrotron. With Wolfgang Panofsky and Jack Steller, he revealed the existence of neutral pions; with other colleagues, he measured the pion mean life.

After declining to sign an anticommunist loyalty oath, Jack left Berkeley the following year for Columbia University. Using the new 380 MeV cyclotron, Jack determined the spins and parities of charged and neutral pions and studied the scattering of charged pions. In 1954 Jack and three graduate students performed physics experiments with the bubble-chamber technique, developed two years earlier. Their first results uncovered the properties of unstable strange particles at a level unattainable with older techniques. A few months later, the four reported on three events that demonstrated the existence of the sigma-zero hyperon and measured its mass.

Over the next decade, Jack, working with numerous colleagues, made some groundbreaking discoveries. They included revealing parity violation in lambda hyperon decay and measuring the omega and rho meson decay lifetimes.

In 1961 Jack worked with Melvin Schwartz and Leon Lederman, among others, to conduct the first experiment to use a high-energy neutrino beam. The 10-ton detector had just enough mass to detect 51 neutrino-induced events and could discriminate between electrons and muons. They demonstrated that the accelerator neutrinos from pion decay produced muons but not electrons and that the neutrinos emitted in pion decay are distinct from those emitted in beta decay and therefore constitute a second kind of neutrinos. That work earned Steinberger, Schwartz, and Lederman the Nobel.

In 1964 Jack went to CERN on sabbatical. He proposed, with Carlo Rubbia, me, and others, to look for the interference between the long-lived K^0_L and the short-lived K^0_S amplitudes in the time dependence of K^0 decay. The experiment began a decade of successful ones into *CP* violation.

In 1968 Jack joined the staff at CERN, where he continued to study the K^0 decay with a spectrometer that had proportional wire chambers, which Georges Charpak had just developed there. Jack initiated a similar experiment at Brookhaven National Laboratory. Among the discoveries were the small, *CP*-violating charge asymmetry in K^0_L leptonic decay, the time-dependence measurement of that asymmetry, a determination of the regeneration phase, and checks on the superweak model.

From 1976 to 1984, Jack led several groups—from CERN, the Technical University of Dortmund and Heidelberg University in Germany, and the Atomic Energy Commission in Saclay, France—in conducting an experiment on deep inelastic neutrino interactions in iron. The collaboration used CERN's Super Proton Synchrotron to precisely determine the Weinberg angle of weak interactions, demonstrate the existence of right-handed neutral currents, and test quantum chromodynamics through scaling violations in the structure functions of the nucleon, among many other discoveries.

Jack Steinberger

KONRAD KLEINKNECHT

Beginning in 1983, Jack was also instrumental in designing and building the ALEPH detector for the Large Electron–Positron Collider, which started operations in 1989. Among the collider's discoveries were the number of neutrino flavors and the decay modes of the intermediate neutral boson Z^0, in agreement with standard-model predictions.

In addition to his enormous achievements in physics, Jack played the flute, especially works of Johann Sebastian Bach, and held regular chamber-music sessions. Jack enjoyed mountaineering and skiing in the French Alps, and he regularly traveled from his home in Geneva to visit his native city of Bad Kissingen. He was made an honorary citizen, and the local secondary school was renamed after him.

To his students and collaborators, Jack had a great personality, characterized by his being a reliable friend and an exemplar of decency and imagination.

Konrad Kleinknecht
Ludwig-Maximilians University Munich
Garching, Germany

Wolfgang Stodiek

Plasma physicist Wolfgang Stodiek died on 7 March 2021 in Bielefeld, Germany, the town of his birth. Stodiek spent most of his career at the Princeton Plasma Physics Laboratory, where he pioneered much of the research on the biggest fusion devices of the day—the C-Stellarator, the Symmetric Tokamak (ST), and the Princeton Large Torus (PLT). His scientific contributions drove the world's magnetic fusion program for many years.

Stodiek's scientific career did not start auspiciously. Born on 22 May 1925, he was drafted into the German army at age 17 to be an electronics technician. Toward the end of World War II, he fled west across a wrecked bridge over the Elbe River intent on evading the Red Army and being captured by British soldiers, who immediately put Stodiek to work preparing military trucks for civilian use. He subsequently studied physics at Georg-August University in Göttingen, but he never finished his PhD.

Stodiek joined the Max Planck Institute for Physics under Werner Heisenberg, who had formed a small fusion group. In 1958 in Geneva, Stodiek snuck into the International Atomic Energy Agency Conference, where attendees discussed declassified studies of fusion energy. Motivated by his detailed conversations with Project Matterhorn team members from Princeton University, he traveled to its plasma physics laboratory in 1959 for a year's commitment. Instead he stayed until he retired in 1996. He may not have been fluent in English when he arrived, but he learned the language quickly, paying his colleagues a nickel for every new word they taught him.

At Princeton, Stodiek first joined a team working on the B-3 Stellarator. The team members determined that plasmas heated ohmically by an electric current had plasma confinement dependent on Bohm's diffusion—that is, proportional to the ratio of the magnetic field over the temperature of the plasma. In 1961 Stodiek joined the recently completed, larger C-Stellarator, designed by Lyman Spitzer Jr. Working with Donald Grove and others, Stodiek studied plasma energy confinement and many other phenomena over an enormous range of plasmas. They used ohmic heating, electron heating, ion heating, and injection from plasma guns. Stodiek was especially concerned about the losses of energetic ions and by the impact of the magnetic deformations caused by the coils providing the necessary field configuration.

After the Soviet Union demonstrated better performance by its T-3 tokamak, in 1969 Princeton converted its C-Stellarator to the ST. Stodiek planned the conversion and led the engineering team, which completed the project in only four months. The ST demonstrated good plasma performance with better plasma diagnostics than the Soviet Union had available.

While he was managing the ST, Stodiek worked with Harold Furth and others on the specification and initial design of the PLT, which began operation late in 1975. The PLT had twice the linear dimensions of its predecessor.

As head of the PLT operations for many years, Stodiek facilitated the efforts of 10 technical staff, roughly 30 dedicated physicists, and up to 20 visiting scientists. The PLT achieved excellent results from additional heating systems, particularly neutral-beam heating. It reached plasma temperatures of roughly 6×10^7 K, giving the scientific community encouragement for the continued pursuit of fusion.

Stodiek was adroit at overcoming technical difficulties in device operations and thus facilitated the completion of many PLT experiments. He was gifted at finding inexpensive and quick solutions when issues arose with power supplies, coils, cooling systems, or the vacuum vessel. As a result, the PLT team published more than 150 groundbreaking papers on plasma confinement, stability, heating techniques, and plasma–wall interactions.

Although Stodiek should be remembered for his contributions in driving magnetic fusion devices forward, he was also an advocate for and made major contributions to better measurements of high-temperature plasmas. Because the PLT had much higher plasma temperatures than previous tokamaks, making diagnostics of fusion products became more important. Stodiek led the group

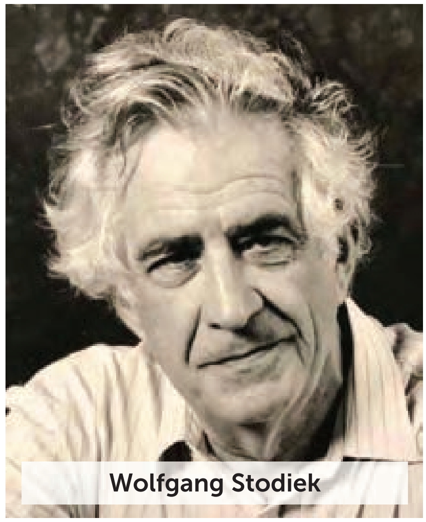

Wolfgang Stodiek

PRINCETON PLASMA PHYSICS LABORATORY

that developed many neutron- and charged-fusion-product-detecting instruments, x-ray imagers, and spectrometers. All those diagnostic instruments are workhorses in understanding present-day fusion plasmas.

After leaving the PLT in 1981, Stodiek worked on various fusion studies and energy issues. In 2007 he and Elsmarie, his wife, returned to Bielefeld, the German town where they both were born.

Stodiek was rigorous and thorough in his scientific pursuits. Colleagues appreciated his realistic assessment of the difficulties to be encountered on the way to achieving practical fusion energy. His ideas and his understanding of the complexity of the engineering necessary for fusion devices influenced, to a considerable extent, the direction of the Princeton laboratory's experimental program. He was effective at demolishing overhasty hypotheses and carelessly done experiments. But he nevertheless continued his dedicated pursuit of fusion energy while encouraging others to do the same. His thinking was not always easily understood, but his solutions could always be trusted. He could often be found assisting the engineers, even going so far as to help balance the generators necessary for storing electrical energy.

Stodiek was an avid photographer who specialized in black-and-white portraits. He was a charming and insightful physicist who is deeply missed by his coworkers.

Kenneth M. Young
Dale M. Meade
James D. Strachan
Princeton Plasma Physics Laboratory
Princeton, New Jersey PT

QUICK STUDY

Joost Daniels is a senior research engineering technician, **Alana Sherman** is an electrical engineering group lead, and **Kakani Katija** is a principal engineer, all at the Monterey Bay Aquarium Research Institute (MBARI) in Moss Landing, California.



Illuminating gelatinous life in the deep sea

Joost Daniels, Alana D. Sherman, and Kakani Katija

Many transparent animals rely for survival on structures built from their own mucus. To study such organisms deep underwater, researchers are using robots outfitted with lasers.

The ocean remains vastly unexplored. Although researchers have completely mapped the surfaces of the Moon and Mars, they have resolved less than 10% of the ocean seafloor. Yet the ocean is the largest habitable space on Earth. The midwater—the vast region between the seafloor and the sunlit, shallower depths—makes up most of that living space and is a particularly difficult place to explore. Far out of reach of scuba divers, the cold, dark, and high-pressure environment requires specialized technology outfitted with cameras and other sensors. GPS does not work underwater, and options for tracking wildlife are much more limited than on the ocean surface or on land. Much of what we know about midwater animals is based on sparse samplings gathered in nets dragged behind ships. However, many species are too fragile to be studied that way: The soft, gelatinous tissues that make up many of their bodies are easily broken, as are the mucus structures some animals create.

One such soft-bodied, deep-sea creature that builds intricate living structures—essentially houses made out of mucus, sometimes called snot palaces—is the giant larvacean (genus *Bathochordaeus*), shown in figure 1. With a translucent, tadpole-like body barely 10 cm long, the animal primarily lives at depths down to 500 meters. The larvacean secretes its house from cells lining its head and then inflates it by beating its tail. The mucus house serves as a protective shield from passing predators and filters small organic particles suspended in the water column. The animal feeds on those particles, known as marine snow. By using its tail to pump water through its mucus filters, the larvacean concentrates the particles it feeds on. Eventually the particles clog the filter and the animal abandons its house, which sinks to the seafloor. The abandoned houses may account for one-third of the carbon transported to the seafloor in Monterey Bay.

Details of that process and the larvacean life cycle remain mysterious, including the way the animals construct their houses, why the houses have such a characteristic shape, how often the animals rebuild their houses, and how much water they filter. More research is needed to understand those critical processes, which are an important part of Earth's carbon cycle.

Robots in the deep

Studying such fragile deep-sea animals requires observing and measuring them noninvasively. With Paul Roberts and Denis Klimov, two other members of our group at the Monterey Bay Aquarium Research Institute, we use tethered underwater robots, known as remotely operated vehicles (ROVs), which are ideal for the job. Shown in figure 2a, each is operated by pilots in a control room on a ship. For deep-sea research, an ROV can be outfitted with a host of cameras, sensors, collection containers, and manipulator arms that can operate equipment and conduct experiments several kilometers deep in the animals' natural environment. Imaging provides views of animals underwater at the spatial and temporal scales needed for studies of their form and function, and careful selection of lighting in an otherwise dark environment reveals a plethora of information.

One specialized imaging and illumination system is the newly developed DeepPIV (particle image velocimetry) instrument, which uses a red laser projected into a 1-mm-thick sheet of light, as shown in figure 2b. A camera captures light scattered by objects in the laser sheet. DeepPIV is used in tandem with an ROV, which allows the pilot to carefully position instru-

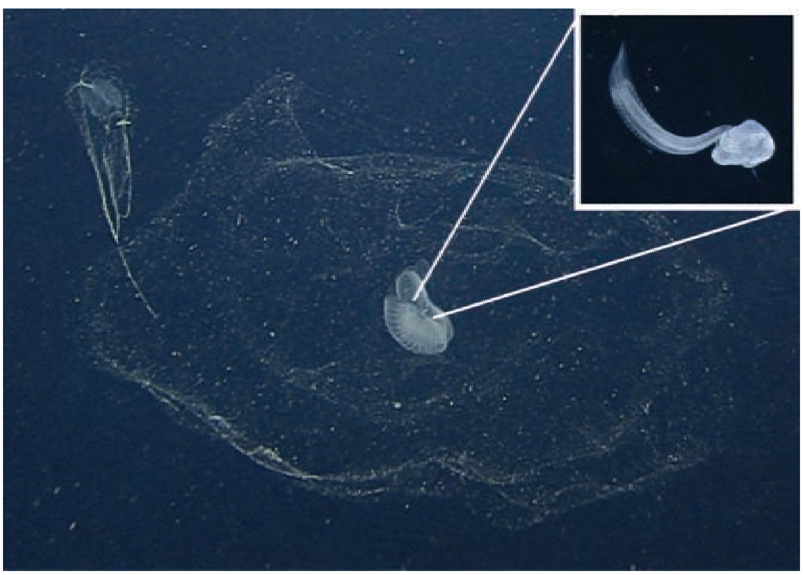

FIGURE 1. A GIANT LARVACEAN inside its mucus house, which consists of a coarse outer filter up to a meter in diameter and a fine, inner filter. The inset shows the tadpole-like animal, whose roughly 10 cm length is dominated by its tail, which beats to pump water and food particles through the house's intricate cavities. The oblong-shaped blob in the upper left is an old, abandoned mucus house that has not yet sunk to the seafloor. (Courtesy of MBARI.)

FIGURE 2. TETHERED to a ship on the ocean surface, **(a)** this remotely operated vehicle (ROV) controls the position of the DeepPIV instrument mounted to its frame. Using the ROV camera and a laser extended by a half-meter rigid arm, the instrument collects video data for particle velocimetry experiments and three-dimensional reconstructions. The laser projects a sheet of light that illuminates the motion of suspended particles and the interior structure of any sea creature nearby. The camera captures the lit objects. **(b)** Extending from the ROV, the laser illuminates air bubbles in a laboratory tank. (Courtesy of MBARI.)

ments around an animal of interest without disturbing it. That's no easy feat: The meters-long vehicle has to be positioned with subcentimeter accuracy, which is complicated by currents that affect both the ROV and the animal. The researchers can then either hold the instrument stationary relative to a target or scan the laser sheet through a volume. The two options yield very different perspectives of an animal.

The DeepPIV laser sheet reveals any objects or suspended particles present in the illuminated slice of water. The laser light even propagates inside the translucent bodies of many midwater animals, so the technique effectively reveals water flow as well as body structures. The image recorded by DeepPIV when the ROV is held stationary relative to an object can be analyzed with either particle tracking or particle image velocimetry—methods commonly used to characterize fluid flow in laboratory environments. Both methods visualize a two-dimensional slice of the animal and the surrounding particle field.

But if the laser sheet is moved through the target of interest while recording, a stack of images is generated that represent different planes in a volume. From that stack, researchers can create a 3D model in a fashion akin to a medical computed tomography (CT) or magnetic resonance imaging scan. Recording the image stack takes only a few seconds but requires moving the ROV with exquisite precision. Different pixel intensity levels distinguish the animal's features in much the same way that a CT scan distinguishes bones and tissues from internal organs (see the article by John Boone and Cynthia McCollough on page 34 of this issue).

A look inside

Imaging results from DeepPIV offer a close look at water flow in and around the larvacean house. By zooming in on specific locations while the moving particles are illuminated by the laser, one can measure water-filtration rates and discern water-transport pathways through the house. A single giant larvacean can filter up to 76 liters of water per hour—an impressive achievement for an animal less than 10 cm long.

In comparison with other, larger animals in Monterey Bay, larvaceans have a profound impact on the movement of organic matter: Collectively, they filter all the water in their depth range every 13 days. Every time a larvacean abandons its house—which may happen as often as once a day—the captured particles and carbon sink to the ocean floor, where they provide nutrients for bottom dwellers or become part of the sediment. Moved far away from surface waters and the atmosphere, the carbon is effectively sequestered in the seafloor.

How is such a small invertebrate able to filter so much water? The answer may lie in the structure of its house. For a closer look, our group used DeepPIV to scan larvaceans inside their mucus structures at depths between 200 and 400 meters. The images and 3D visualizations, coupled with flow data collected by DeepPIV, allowed us to navigate through the house's chambers and flutes to better appreciate how they function. We discovered that water enters the inner house through two inlet channels, and a coarse, mesh-like filter prevents large objects from entering. The larvacean's tail pumps the water through the tail chamber and into the bifurcated inner chamber, and downstream tapered channels help transport food particles to the animal's mouth. Although the 3D models provide an unprecedented view of structure and connectivity inside the mucus house, it's still unclear exactly how the animal filters water at such a high rate.

Significant contributions to our work were made by other engineers, ROV pilots, and ship's crew at MBARI.

Additional resources

- ▶ For a DeepPIV scan of a giant larvacean and a three-dimensional animated flight through its inner cavities, see www.youtube.com/watch?v=J2zJgo1QveU.
- ▶ For an introduction to studying larvaceans, see www.youtube.com/watch?v=0fCnHyxYVMw.

▶ K. Katija et al., "Revealing enigmatic mucus structures in the deep sea using DeepPIV," *Nature* **583**, 78 (2020).
▶ K. Katija et al., "New technology reveals the role of giant larvaceans in oceanic carbon cycling," *Sci. Adv.* **3**, e1602374 (2017). PT

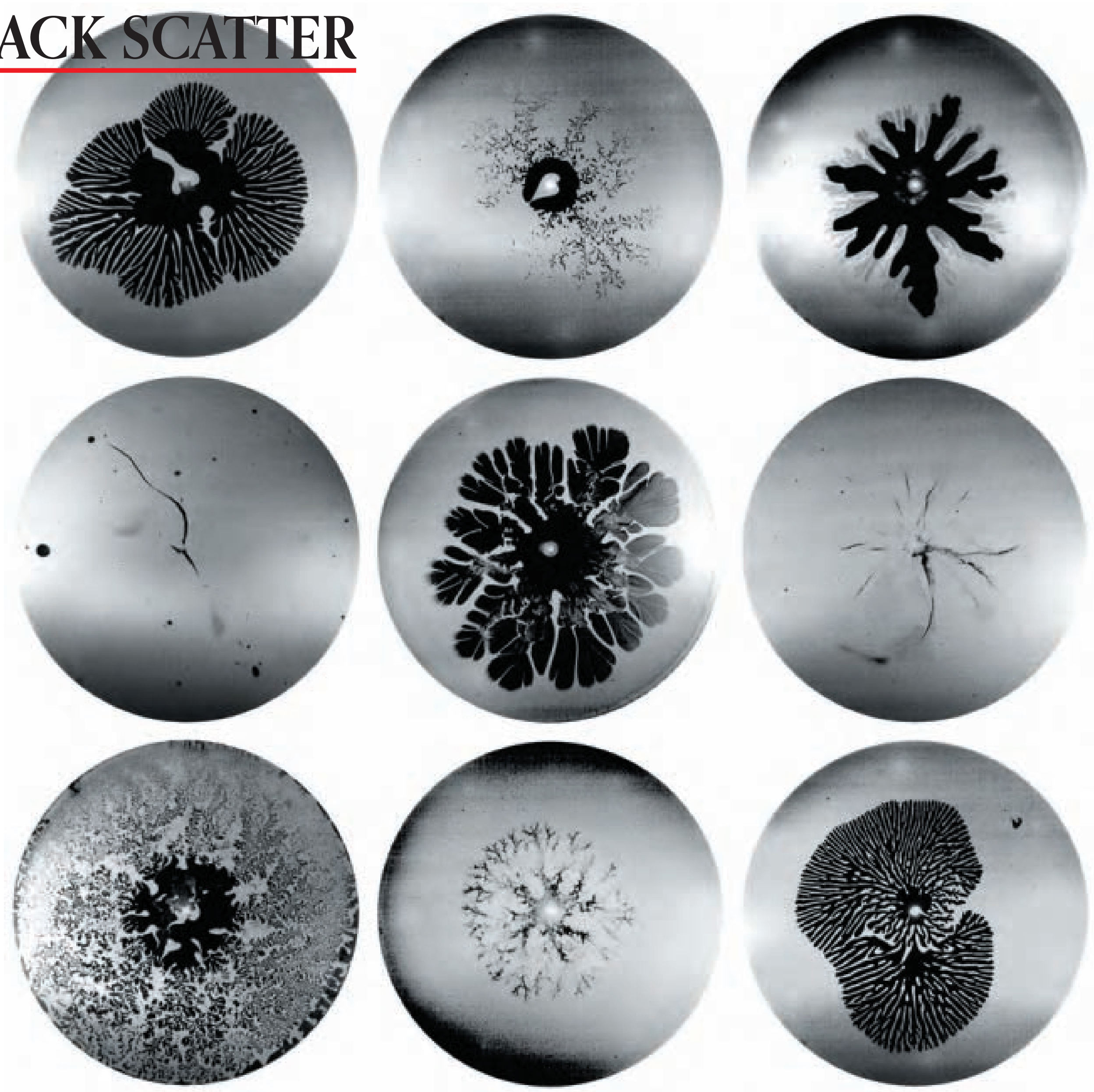

Solid and liquid responses of a non-Newtonian fluid

Oobleck, a muddy mixture of cornstarch and water, is an example of what scientists term a discontinuous shear thickening fluid. Students marvel at its ability to support impulsive loads as if it were a solid. To investigate the counterintuitive substance, Deren Ozturk, Miles Morgan, and Bjørnar Sandnes of Swansea University in the UK shot pressurized air at oobleck sandwiched between two transparent plates 0.2 mm apart. These images show the substance's response at various air pressures and cornstarch concentrations. Black regions are air pockets, and light regions are the cornstarch mixtures. The researchers were the first to use the thin oobleck sandwich to observe three distinct responses: viscous fingering, dendritic fracturing, and large-scale fracturing.

Viscous-fingering features are characterized by rounded edges. They can be seen in the first and third images in the top row, the second image in the middle row, and the third image in the bottom row. Dendritic fracturing produces thinner branches that, unlike viscous-fingering offshoots, can be perpendicular to their parent branch. Such branching is visible in the second image in the top row and the first and second images in the bottom row. Large-scale fracturing doesn't have many offshoots. It is discernible in the first and third images in the middle row. Ozturk and colleagues found that viscous fingering appears at low air pressures and low concentrations, dendritic fracturing happens at intermediate pressures and concentrations, and large-scale fracturing is seen in mixtures with high concentrations and air pressures. Viscous fingering is oobleck's liquid response, whereas both types of fracturing can be understood as the gooey substance's solid-like responses. (D. Ozturk, M. L. Morgan, B. Sandnes, *Commun. Phys.* **3**, 119, 2020; image courtesy of Deren Ozturk and Bjørnar Sandnes.) —MRB

TO SUBMIT CANDIDATE IMAGES FOR BACK SCATTER VISIT https://contact.physicstoday.org.

GradSchoolShopper

The Student Guide to Grad School in Physics, Astronomy, and Related Fields

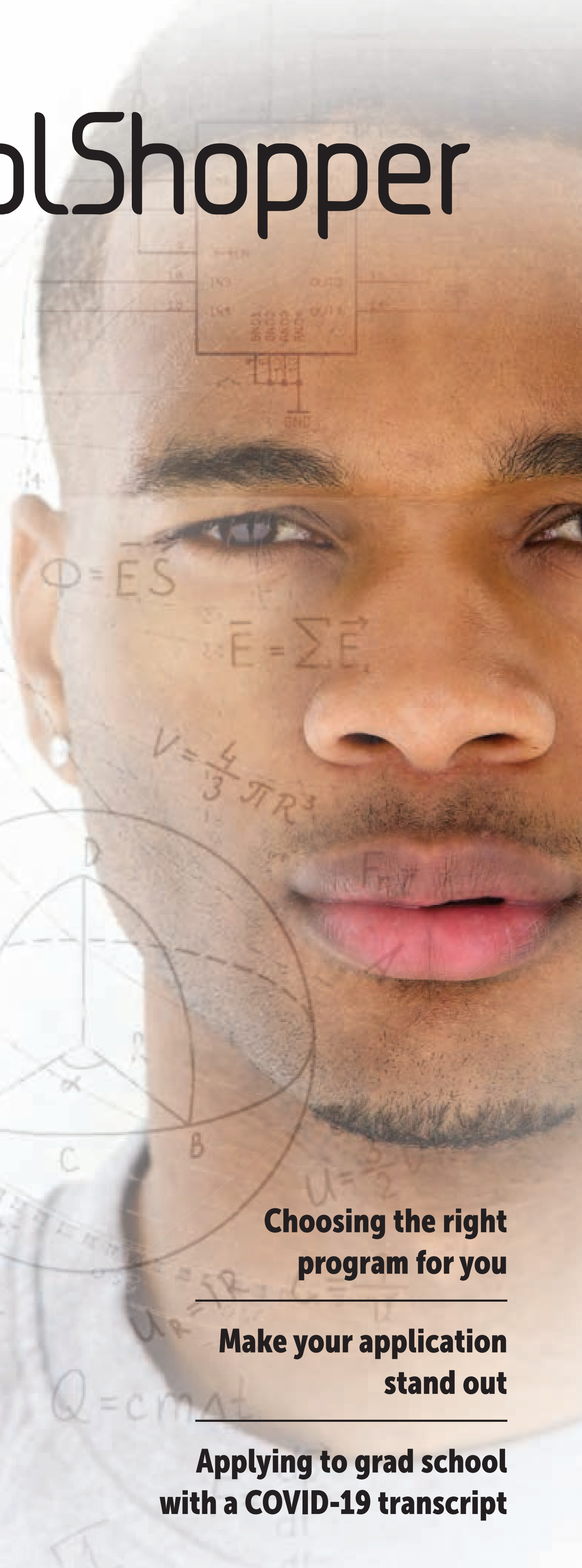

Choosing the right program for you

Make your application stand out

Applying to grad school with a COVID-19 transcript

presented by

AIP | American Institute of Physics

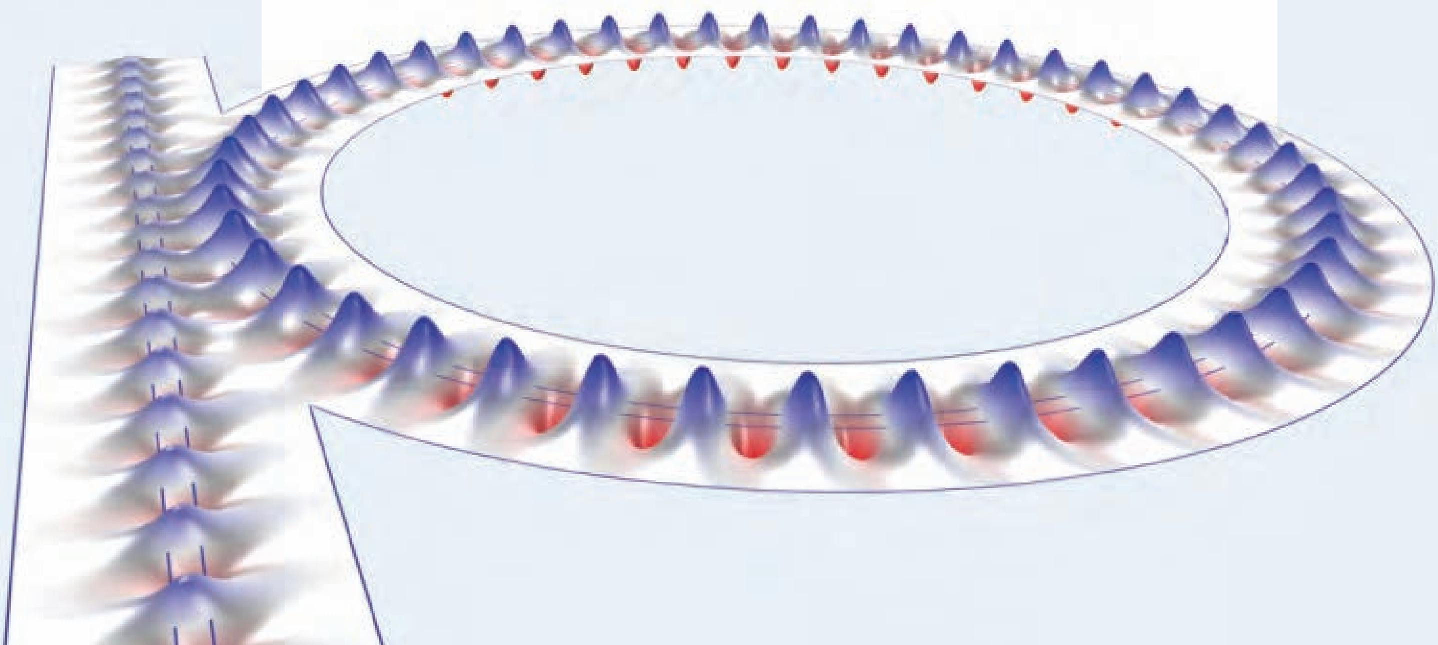


N-Control
Improve UHV system integrity with our highly configured vacuum solutions
Adjustable-gap collimators eliminate undesirable electrons, thus avoiding excessive radiation due to beam loss in sensitive areas, and reducing activation of accelerator components.
Allow Nor-Cal Products' vacuum engineers the opportunity to apply their expertise in the design and manufacturing of your next beamline project. Let's talk.
Nor-Cal Products
NC
by PFEIFFER VACUUM
Full service engineering
Precision manufacturing
Global sales and technical support
Over 6000 standard components
www.n-c.com | 800.824.4166 | ncsales@n-c.com
International Organization of Standardization
ISO
9001:2015
Registered